The Characterization of the Multinucleated Giant Hemocyte, a Novel Player in Innate Immunity

Ph.D. Dissertation

Lilla Brigitta Magyar

Supervisor: Dr. Gyöngyi Ilona Cinege

Biological Research Centre

Institute of Genetics, Innate Immunity Group

University of Szeged, Faculty of Science and Informatics

2024

Szeged

Table of Contents

List of Abbreviations

AMP	antimicrobial peptide
ClyA	Cytolysin A
DEG	differentially expressed gene
Dopa	dihydroxyphenylalanine
FREP	fibrinogen-related protein
GC	giant cell
GCE	giant cell exosome
GO	Gene Ontology
HGT	horizontal gene transfer
HL	Hemolysin E
JNK	Jun N-terminal kinase
mdb	multiform dense body
MGH	multinucleated giant hemocyte
NLR	nucleotide oligomerization domain (NOD)-like receptor
PAMP	pathogen-associated molecular patterns
PGRP	Peptidoglycan recognition protein
PO	Phenoloxidase
PPO	Prophenoloxidase
PRR	pattern recognition receptor
PSC	posterior signaling center
RER	rough endoplasmic reticulum
RIG	retinoic acid-inducible gene
ROS	reactive oxygen species

RNS	reactive nitrogen species
SP	serine protease
TE	transposable element
Tep	thioester-containing protein
TLR	toll-like receptor
VLP	virus-like particle
WGD	whole-genome duplication

I. Introduction

1. An Overview: the Role of the Immune System

The immune system is a network of different cells and proteins, which recognizes and combats pathogens, such as bacteria, fungi, viruses, and parasites, thus defending the organism from infectious diseases. It also plays a role in the response of the organism to other conditions, like tumours and allergies. It is tightly regulated to prevent the attack of the own tissues. The immune system can be divided into two main branches: the innate and the adaptive immune system (Jiravanichpaisal et al., 2006).

Innate immunity represents the first line of defense that is present from birth and does not require prior exposure to pathogens. It is a non-specific and rapid response that relies on germline encoded pattern recognition factors which can detect the evolutionarily well conserved amino acid sequences of pathogen-originated proteins.

The adaptive immune system is a more specialised system that develops over time as it encounters new pathogens. It is the second in line to react as it involves the creation of receptors by somatic gene rearrangement to detect the specific proteins of specific pathogen strains. It thus provides a highly specific response and creates immunological memory that allows the organism to recognize and respond more quickly to future encounters with the same pathogen.

Understanding the immune system is crucial for developing effective treatments and vaccines for infectious diseases, as well as for treating cancer, autoimmune disorders and other conditions that involve immune dysfunctions.

2. The Importance of Innate Immunity in Host Defense

Innate immune reactions are rapid responses to harmful microorganisms, as they occur within minutes to hours after exposure to a pathogen. Innate immunity consists of both cellular and humoral components that work together to detect, respond to, and eliminate pathogens.

In mammals, cellular components of innate immunity involve specialised immune cells, such as phagocytic cells like macrophages, neutrophils and dendritic cells. Other, non-phagocytic immune cells include innate lymphoid cells, mast cells, eosinophils, basophils, and natural killer cells. They patrol the body and are able to detect, capture or even directly kill pathogens. These immune cells are present in various tissues and organs, including the blood, skin, mucosal surfaces, and lymphoid organs.

The humoral components of the innate immune system are antimicrobial peptides (AMPs), cytokines, and other soluble factors that help to eliminate pathogens. AMPs are small, cationic peptides that can directly kill or inhibit the growth of bacteria, fungi, and viruses, while cytokines are signaling molecules that promote inflammation and activate immune cells to target pathogens.

All the above-mentioned innate immune processes are triggered by the recognition of pathogen-associated molecular patterns (PAMPs), which can be found in the cell wall of microbes, but are absent on host cells (Hoffmann et al., 1999; Janeway and Medzhitov, 2002), such as bacterial peptidoglycans, lipopolysaccharides (LPS), or fungal β-1,3 glucans (Lu et al., 2020). Pattern recognition receptors (PRRs) on the surface of immune cells recognize these PAMPs, leading to the activation of signaling pathways that initiate the immune response.

Innate immunity is essential for host defense against a wide range of pathogens and plays a critical role in shaping the adaptive immune response. Defects in innate immune function can lead to increased susceptibility to infections and the development of inflammatory and autoimmune diseases. The study of innate immunity is therefore of great importance for understanding basic mechanisms of host defense and for the development of new therapies to treat infectious and inflammatory diseases. The aforementioned mechanisms can be studied with the help of model organisms.

3. *Drosophila* Innate Immunity

Innate immunity is ancient and evolutionarily conserved, as it is present in all multicellular organisms, from plants to mammals. *Drosophila melanogaster*, the fruit fly, is a widely used model organism to study innate immune responses, because of its short generation time, small size, easy and low-cost maintenance, applicability for ex vivo culturing methods, the lack of legal or ethical restrictions, well-characterized genome, and the evolutionary conservation of transcription factors and signaling pathways (Jiravanichpaisal et al., 2006; Banerjee et al., 2019; Younes et al., 2020; Kúthy-Sutus et al., 2022). Most of the genes involved in *Drosophila* host defense have orthologs in mammals (Hoffmann, 2003). For example, the Toll, Imd, and JAK/STAT signaling pathways, which are crucial for the activation of humoral immune responses in *Drosophila*, fulfil similar functions in mammals. Moreover, the involvement of Toll signaling in immune defense reactions was first demonstrated in the fruit fly.

Like all insects, *Drosophila* lacks an adaptive immune response. However, there seems to be mounting evidence that invertebrates possess an immunological memory-like mechanism, as they demonstrate a more effective immune response upon pathogen re-exposure (Kurtz, 2005; Kvell et al., 2007; Cooper and Eleftherianos, 2017; Melillo et al., 2018). Different mechanisms were suggested through which this memory could be achieved: differentiation and recruitment of hemocytes, long-lasting upregulation of regulatory pathways or involvement of different proteins. Fibrinogen-related proteins (FREPs), which contain regions similar to Ig superfamily members and diversify at an unusually high rate and the Down syndrome cell adhesion molecule 1 (Dscam1), the gene of which possesses several variable and constant exons that can potentially generate 38,000 splice variants, could both be involved in immunological memory creation (Adema et al., 1997; Schmucker et al., 2000; Zhang et al., 2004). The transfer of this memory to offsprings, known as transgenerational immune priming, was also described (Tetreau et al., 2019).

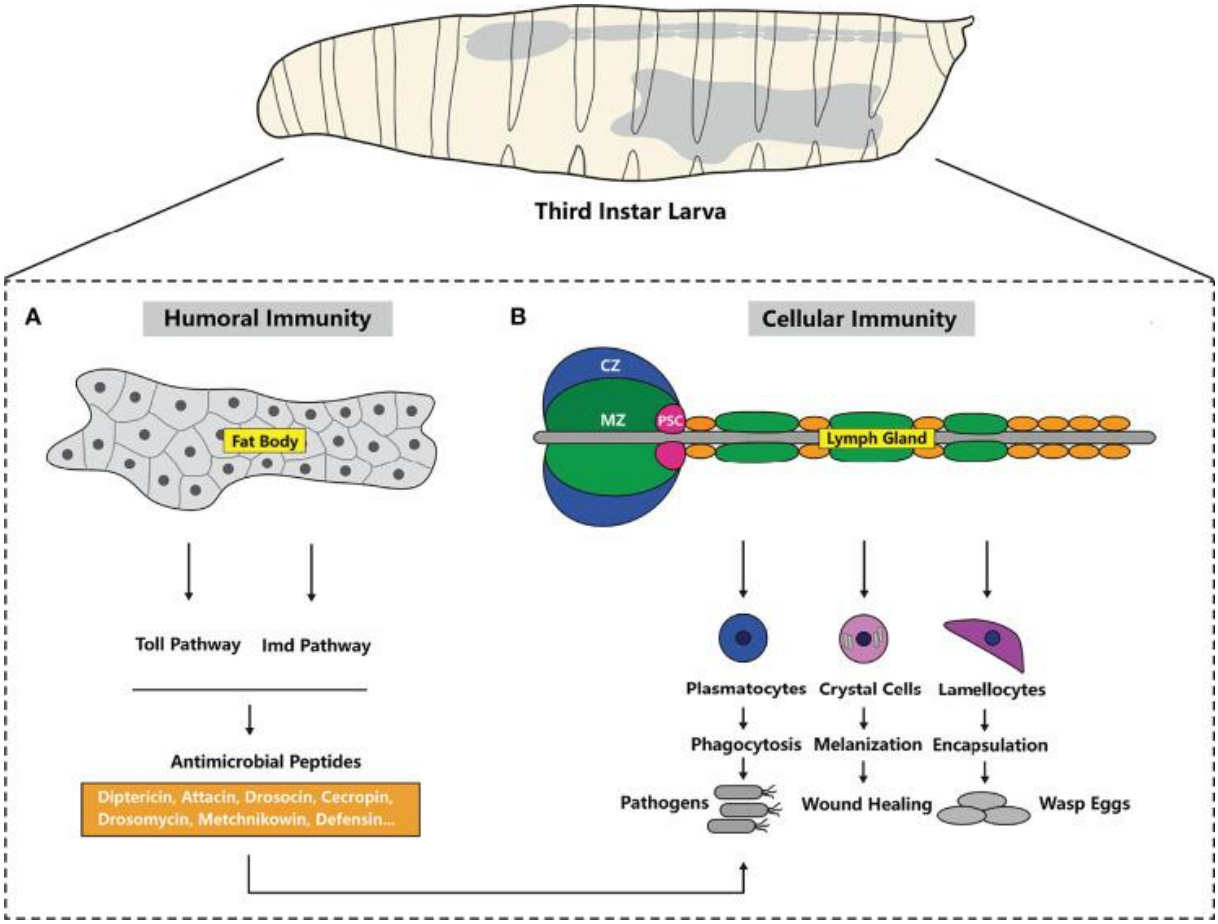

Figure 1. Overview of the *Drosophila* immune system (Yu et al., 2022)

The well-developed innate immunity of *Drosophila*, similarly to mammals, consists of both cellular and humoral components (**Fig. 1.**), which act together to defend against pathogenic invaders (Lavine and Strand, 2002). However, immune response mechanisms cannot be separated clearly to humoral and cellular categories as these two are intertwined. Cellular defense includes hemocyte-mediated processes, such as phagocytosis, encapsulation, melanization, and production of reactive oxygen species (ROS), while humoral defense includes clotting and the production of antimicrobial peptides (AMPs).

In this introduction, I will delve deeper into the mechanisms of drosophilid innate immunity, including the various signaling pathways involved in its activation and the key players of the immune response.

3.1. The Frontline of Defense: Hemolymph Clotting and Wound Healing

The first lines of defense are the physical barriers that are in contact with the environment and thus with external pathogens. These barriers overlap with the natural routes of infection, which in insects include: the exoskeleton with its cuticular coverage and the cuticle lining of the gut wall, tracheae, and reproductive organs (Eleftherianos et al., 2021).

The main body cavity of insects is called the haemocoel, in which, - as blood vessels are absent-, the hemolymph (analogous to vertebrate blood) circulates in direct contact with other organs. The hemolymph is comprised of a fluid plasma in which immune cells called hemocytes (blood cells) are suspended. These circulating hemocytes function as a surveillance system for damaged tissue and are recruited to the wound site by adhesive capture (Babcock et al., 2008).

Upon damage to the epithelial barriers the individual responds with hemolymph coagulation, which is analogous to mammalian blood clotting and prevents hemolymph loss and the spread of infection, by localising the immune activity to the wound site. This rapid reaction involves collaboration between humoral and cellular components as both releases soluble coagulogens: the fat body releases Fondue, Lipophorin, larval serum proteins and Fat body protein 1, while blood cells release Prophenoloxidase, the von Willebrand factor domain-bearing Hemolectin and Eig71Ee (Theopold et al., 2014). During clotting these hemolymph proteins bind to each other to create an insoluble matrix that stops bleeding, while microbes are trapped in the clot matrix.

Clotting occurs in two phases (Bidla et al., 2005). First, a primary soft clot is formed through the interaction of coagulogens, which are cross-linked by Transglutaminase (Tg) in the presence of Ca^{2+}. The phenoloxidase cascade is then activated and the primary clot is

subsequently melanized by phenoloxidases, resulting in a hard clot (Dushay, 2009). The coagulation in insects happens significantly faster than in vertebrates, as within 10-15 min after wounding, the wound site darkens and a clot is formed (Galko and Krasnow, 2004; Loof et al., 2011).

Moreover, hemolymph coagulation also contributes to wound healing, as the clot may serve as a scaffold for the repair of the epithelium and cuticle. The JNK pathway and small GTPases are involved in the melanization of the clot and in wound healing by restoring tissue integrity through the spreading of the damaged epithelium across the wound (Galko and Krasnow, 2004; Dushay, 2009). The damaged epithelial cells fuse with each other to form a syncytium, which has the capacity to phagocytose debris at the wound site.

3.2. Cellular Immunity of *Drosophila*

3.2.1. Cellular Innate Immune Cells of *D. melanogaster*

In insects, the main role of the circulating blood cells is the protection against invading pathogens by detection, phagocytosis, encapsulation, and melanization (Banerjee et al., 2019). They also play a role in blood clotting, wound healing, tumour cell death, extracellular matrix production (Fessler et al., 1994) and even metabolic regulation (Shin et al., 2020). Similarly to mammalian immune cells, insect hemocytes also perform other, non-immune roles in the organism, such as participating in molting, apoptotic cell clearing in the central nervous system and iron transport (Stanley et al., 2023), but these functions are outside of the scope of this dissertation. Blood cell of drosophilid larvae reside in three compartments: the hematopoietic organ, the lymph gland, the circulation, and the sessile tissue, which is comprised of segmentally distributed clusters of hemocytes attached to the integument (Lanot et al., 2001).

The blood cells of *Drosophila* were first classified based on cell morphology, ultrastructure, histochemical and functional characteristics (Rizki, 1953, 1957; Whitten, 1964; Shrestha and Gateff, 1982; Lanot et al., 2001). This was later refined through various monoclonal antibodies specific to different cell types (Kurucz et al., 2007a; Balog et al., 2021). The identification of genetic markers, such as lineage-specific transcription factors and elements of signal pathways involved in hemocyte differentiation (Lebestky et al., 2000; Duvic et al., 2002; Honti et al., 2010) is considered the most accurate method of hemocyte lineage classification.

Under naive conditions, *D. melanogaster* has three main blood cell types: plasmatocytes, crystal cells and prohemocytes (Banerjee et al., 2019). The majority of

hemocytes, around 95%, are spherical cells of 7-12 μm in diameter, called plasmatocytes (Lanot et al., 2001). They are macrophage-like cells that phagocytose apoptotic cells and microbes, and produce AMPs, like Cecropin A1, Drosomycin, and Diptericin (Evans et al., 2003). Plasmatocytes are also involved in the first steps of foreign body encapsulation. These cells possess a well-developed Golgi apparatus and rough endoplasmic reticulum (RER), a high number of pinocytotic vesicles, and numerous phagolysosome-like inclusions (Ribeiro and Brehélin, 2006). As they are motile cells, particularly those isolated from pre-pupae, they often possess lamellipodia and/or filopodia (Sampson and Williams, 2012). In the recent years, single-cell RNA sequencing elucidated that plasmatocytes, similarly to human macrophages, are in fact a heterogeneous population with several subpopulations with supposedly different roles (Cattenoz et al., 2020; Fu et al., 2020; Tattikota et al., 2020). However, it is contested whether these subpopulations represent different stages of plasmatocyte maturation, functional subtypes or a similar process to human macrophage polarization (Murray et al., 2014; Coates et al., 2021).

Crystal cells represent a small fraction of hemocytes (2-5%), and they can be distinguished from plasmatocytes due to the presence of crystalline inclusions of prophenoloxidases (PPOs) in their cytoplasm (Shrestha and Gateff, 1982). The crystal inclusions are up to 10 in number and are never membrane bound (Rizki et al., 1980). Crystal cells are very fragile and upon wounding lyse easily (Ribeiro and Brehélin, 2006). Furthermore, the crystal can dissolve within the cytoplasm, consecutively the cell swells and a strong Brownian movement of intracellular particles can be observed (Rizki, 1957). In other species, like *Drosophila teissieri*, *Drosophila willistoni*, *Drosophila pseudoobscura*, *Drosophila novamexicana*, *Drosophila nebulosa* and *Drosophila yakuba* the inclusions of the crystal cells are rounded and do not look like crystals (Ribeiro and Brehélin, 2006). The ultrastructure of crystal cells can be characterized by few vesicles and ribosomes, and a low number of mitochondria, RER, and Golgi apparatus (Shrestha and Gateff, 1982). Crystal cells facilitate wound healing by their involvement in the melanization reaction, which results in a darkened and hardened tissue and in reactive oxygen species that damage pathogens (Banerjee et al., 2019). They also participate in foreign object melanization during encapsulation.

Prohemocytes represent the smallest hemocyte type with a diameter of 5-7 μm. As stem cells in general, they have high nucleus to cytoplasm ratio. They contain only a few cytoplasmic inclusions, but have a high number of free ribosomes and large lipid droplets (Lanot et al., 2001).

In response to mechanical wounding or oviposition by parasitoid wasps *D. melanogaster* differentiates specialized cells, called lamellocytes (Banerjee et al., 2019). They have role in the encapsulation and therefore isolation of parasitoids, while participating in the melanization of the capsule, too. Lamellocytes have a flat and slightly elongated shape with irregular margins and are about 60–250 μm in diameter. They possess relatively small nuclei, and although these cells are not involved in phagocytosis (Lanot et al., 2001), they contain the highest number of primary lysosomes and phagocytic vacuoles compared to other blood cells (Shrestha and Gateff, 1982). The cortical part of their cytoplasm is organelle-free.

Most drosophilids have other encapsulating hemocyte types instead of the lamellocyte described above, (**Fig. 2.**), such as lamellocyte-like cells, nematocytes, pseudopodocytes and multinucleated giant cells (Hultmark and Andó, 2022). Multinucleated giant cells (MGHs) are the main encapsulating cells in the *ananassae* subgroup and in *Zaprionus indianus* (Márkus et al., 2015; Cinege et al., 2020), and, as being the main topic of this dissertation, they are discussed in detail in part 4 of the Introduction.

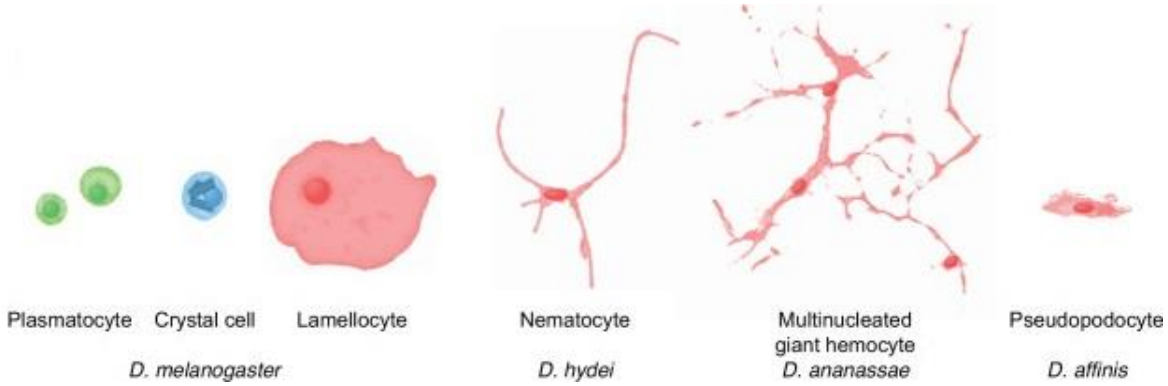

Figure 2. Schematic representation of hemocyte types in drosophilids (Hultmark and Andó, 2022)

3.2.2. Hematopoiesis of *D. melanogaster*

Many signaling pathways influence hematopoiesis in *Drosophila,* such as the Notch, JAK/STAT, Toll and VEGFR pathways (Evans et al., 2003). Several transcription factors are involved in hematopoiesis regulation, which are conserved in *Drosophila* and mammals (Jiravanichpaisal et al., 2006). For example, Serpent (Srp) is required for hematopoiesis in *Drosophila* embryos and has several mammalian orthologs (GATA-1, GATA-2, GATA-3) involved in erythropoiesis, megakaryopoiesis and T cell lymphopoiesis. Lozenge is required for crystal cell differentiation, while its mammalian ortholog, AML1 is involved in blood

cell development (Canon and Banerjee, 2000). The U-shaped (Ush) in *Drosophila* is a negative regulator of crystal cell formation, while FOG-1 is required for erythroid and megakaryocytic cell differentiation in mammals (Gregory et al., 2010).

Drosophila hematopoiesis occurs in two waves: in embryonic and in post-embryonic developmental stages (Banerjee et al., 2019). During embryogenesis, hemocytes arise from the head (procephalic) mesoderm, while in the post-embryonic development, they are generated within the mesodermally derived hematopoietic organ, the lymph gland and from circulating and sessile blood cells.

The hematopoiesis during embryogenesis results in blood cells that later spread throughout the larva and can be found in the circulation and as sessile pools of cells attached to the integument, organized in so-called epidermal–muscular or hematopoietic pockets (**Fig. 3.**) (Márkus et al., 2009; Banerjee et al., 2019). The hematopoietic pockets are positioned in a way that they form a striped pattern. The sessile blood cells tightly co-localize with peripheral neurons, which inhibit the apoptosis and promote the adhesion and proliferation of the hemocytes (Letourneau et al., 2016; Makhijani et al., 2017). Sessile blood cells are released into the circulation in response to stressors and during moulting. There is a dynamic exchange between circulating and sessile blood cells (Makhijani et al., 2011).

The majority of circulating blood cells are plasmatocytes, which are highly plastic cells that can transdifferentiate into crystal cells and during inflammatory conditions into lamellocytes (Anderl et al., 2016; Csordás et al., 2021). A machine learning study showed that upon wounding 5.6% of plasmatocytes are capable of differentiating into lamellocytes (Szkalisity et al., 2021). This transdifferentiation cannot be induced by bacterial challenge, therefore it is not pathogen dependent, but is probably caused by larval cuticle damage (Márkus et al., 2005; Evans et al., 2022).

The lymph gland, the hematopietic organ of the *Drosophila* larva, originates from a small population of cells attached to the sides of the dorsal vessel of the embryo (Evans et al., 2003), which proliferate during early larval development to form three to six lobes (Lanot et al., 2001). The anterior or primary lobes are comprised of three functionally distinct areas: the medullary zone containing prohemocytes, the cortical zone with differentiated blood cells (plasmatocytes, crystal cells and lamellocytes), and the posterior signaling center (PSC), which controls lymph gland homeostasis (**Fig. 3.**) (Banerjee et al., 2019). The PSC is made up of a group of 30-40 cells at the posterior tip of the primary lobes, which regulates hemocyte preservation and differentiation through the release of regulatory factors. The

posterior or secondary lobes are smaller in size and have very low hematopoietic activity. The lobes are separated by pericardial cells.

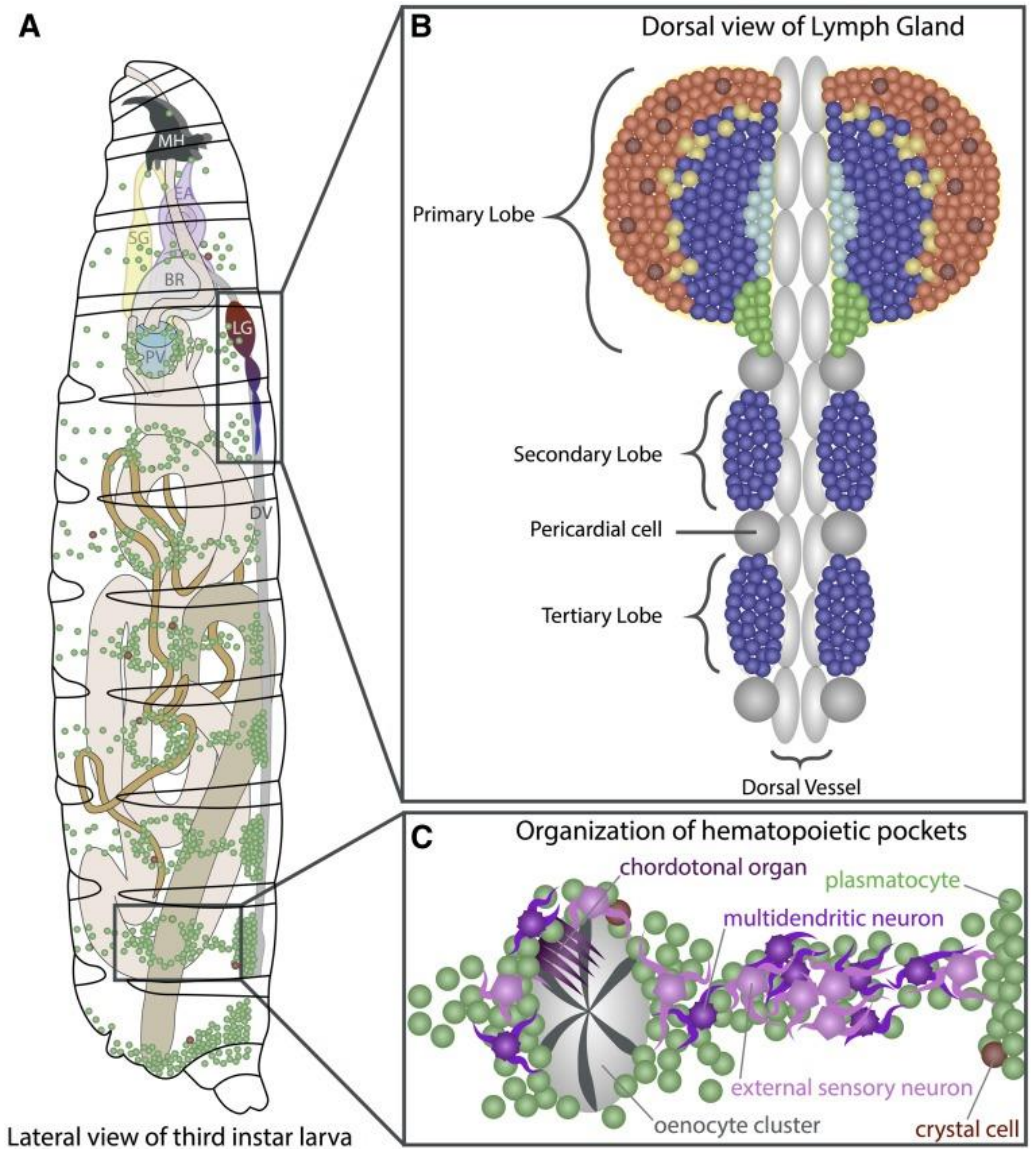

Figure 3. Hematopoietic compartments of the Drosophila larva (Banerjee et al., 2019)

During pupariation, the lymph gland disintegrates and thus releases the hemocytes into circulation (Robertson, 1936). These hemocytes have role in the phagocytosis of dead cells and debris and the remodelling of tissues during moulting. Disintegration of the lymph gland happens in response to parasitoid wasp infection too (Letourneau et al., 2016). Between 48 and 72h post parasitism a massive lamellocyte differentiation takes place here, followed by the disruption of the organ releasing all blood cells into the hemolymph. This

reaction can be triggered by other stressors, like the introduction of a large foreign object into the hemocoel or the disruption of the basement membrane.

In the adult fly the number of hemocytes is low, as there is no hematopoiesis at this stage and the adult blood cells originate from the embryonic head mesoderm or larval lymph gland. Adult flies possess only plasmatocytes and crystal cells, and blood cell mitosis was not detected (Lanot et al., 2001).

3.2.3. Cellular Immune Responses

3.2.3.1. Phagocytosis

Phagocytosis is a complex, evolutionarily conserved process. The dedicated blood cell type for phagocytosis in *Drosophila* is the plasmatocyte, which recognizes, engulfs and degrades infecting microbes. Phagocytosis also plays a role in tissue remodeling and clearance of apoptotic cells (Wood and Martin, 2017). The molecular processes particularly important for phagocytosis are target recognition and binding by PRRs, the cytoskeletal-remodeling required for the engulfment and the vesicle transport and lysosomal degradation leading to pathogen destruction (Melcarne et al., 2019). The PRRs known to be triggering phagocytosis include class C Scavenger receptor I (Sr-CI), class B Scavanger receptors Peste and Croquemort, peptidoglycan recognition protein LC (PGRP-LC), Down syndrome cell adhesion molecule 1 (Dscam1), Nimrod C1, Eater (Kurucz et al., 2007b; Ulvila et al., 2011), and the heterodimer formed by Integrin αPS3 and βv subunits (Nagaosa et al., 2011; Nonaka et al., 2013). Studies show that these receptors are specific to different pathogen groups (Melcarne et al., 2019). The binding of ligands to these receptors elicits signaling pathway activation that initiates the phagocytosis process.

The extracellular detection of pathogens is not the only trigger for immune pathway activation. A study found that bacterial-derived peptidoglycan components can be transported from phagosomes with the help of two SLC15 transporters, Yin and PEPT2 to the cytosol, where they bind to NOD2 receptors and activate the NF-κB pathway, which mediates AMP production (Charrière et al., 2010).

Opsonisation may enhance pathogen recognition and therefore the effectiveness of phagocytosis. Because opsonins are humoral molecules, which enhance the phagocytosis of cells by binding to them and thus tag them for the macrophages, they are discussed in detail in the humoral immunity section (part 3.3. of the Introduction).

Phagocytic uptake is accompanied by cytoskeletal modification, which is mainly driven by actin polymerization and depolymerization. Factors important for the particle

internalization include the nucleation-promoting factors D-SCAR and D-WASp, which activate the Arp2/3 complex responsible for actin-polimerization at the engulfment site (Pearson et al., 2003). Other factors that regulate the actin network include Rho GTPases Cdc42, Rac1, and Rac2, Profilin, and the coat-protein complex I and II (COPI, COPII) (Melcarne et al., 2019). In *Drosophila*, both zippering and macropinocytic phagocytosis types were observed (Pearson et al., 2003).

Maturation of the newly formed phagosomes is achieved through their fusion with endosomes or lysosomes. Small GTPases of the Rab family are regulating this process, including Rab5, Rab7 and Rab14 (Poteryaev et al., 2010; Garg and Wu, 2014). A protein complex named HOPS (Homotypic Fusion and Protein Sorting), composed of six subunits: Vps11, Vps16, Vps18, Vps33, Vps39 and Vps41, are also essential in phagosome maturation (Nickerson et al., 2009). During maturation, the pH in the phagosome reaches 4.5–5, which is optimal for lysosomal enzyme activity. This pH is attained through the activity of the proton pumping vacuolar ATPase (V-ATPase) (Melcarne et al., 2019).

3.2.3.2. Encapsulation

Foreign particles that are too big to be phagocytosed are eliminated through a process called encapsulation, in which blood cells accumulate on the foreign object in a way that they create a coherent layer around it (Meister, 2004). Foreign objects triggering this process could be either eggs laid by parasitoid wasps, a natural immune challenge frequently encountered by *Drosophila* in the wild, or even artificially introduced beads (Lanot et al., 2001).

It is worth to mention that there are around 50 species of hymenopteran parasitoids that can infect *Drosophila* larvae or pupae (Carton et al., 1986). They are called parasitoids as they are not true parasites: successful parazitization always kills the host as the host's entire body is consumed by the developing larva. The adults are free-living. The most investigated are the parasitoid wasps of the *Leptopilina* genus: *Leptopilina boulardi*, *Leptopilina heterotoma* and *Leptopilina victoriae*.

Parasitoid wasps lay their eggs in the hemocoel of second instar fly larvae (**Fig. 4.**). A few hours after oviposition, plasmatocytes detect the foreign object and attach to its surface (Russo et al., 1996). This is followed by intensive lamellocyte differentiation, and the deposition of successive cellular layers on the parasitoids (**Fig. 5.**). The Integrin-β heterodimeric receptor plays an important role in the adhesion process (Xavier and Williams, 2011). Between lamellocytes septate junctions are formed to strengthen the connections

between the cells, hence completely seal and isolate the parasite (Russo et al., 1996). After 24 hours, the hemocytes in the multilayered capsule become drastically flattened and the capsule blackens as a sign of melanization. Both crystal cells and lamellocytes contribute to capsule melanization. Rac GTPases, Rac1 and Rac2 are crucial for encapsulation, as Rac1 promotes hemocyte differentiation, while Rac2 contributes to the flattening of blood cells, cell adhesion and spectate junction formation (Eleftherianos et al., 2021).

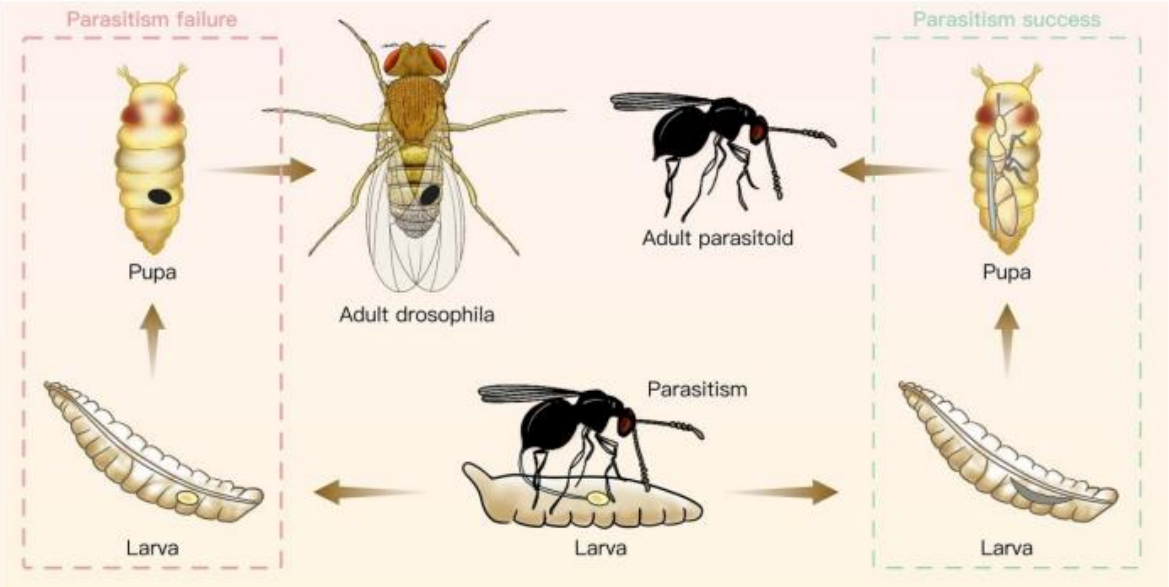

Figure 4. Wasp parasitisation of *Drosophila* larvae (Yang et al., 2021)

Little is known about the PAMPs of parasitoids recognized by plasmatocytes. However, there are two gene candidates for PRRs, which have an elevated expression level after infection: *Tepl* and *Lectin-24A* (Yang et al., 2021). Encapsulation is as well based on the cooperation between cellular and humoral factors. A peptide called Edin (Elevated during infection) is secreted by the fat body within hours after parasitoid infection and is required for the release of sessile hemocytes and the increase of plasmatocyte number in the circulation (Vanha-aho et al., 2015).

Melanization (**Fig. 5.**) is a multistep enzymatic chain reaction which results in the deposition of melanin on the capsule and also releases reactive oxygen species (ROS). It is considered that the main cause of parasite death is asphyxiation and the toxic effect of ROS (Meister, 2004). However, following the encapsulation the parasitoid is not absorbed, as the black capsule is often visible in the body cavity of the adult flies (Lanot et al., 2001).

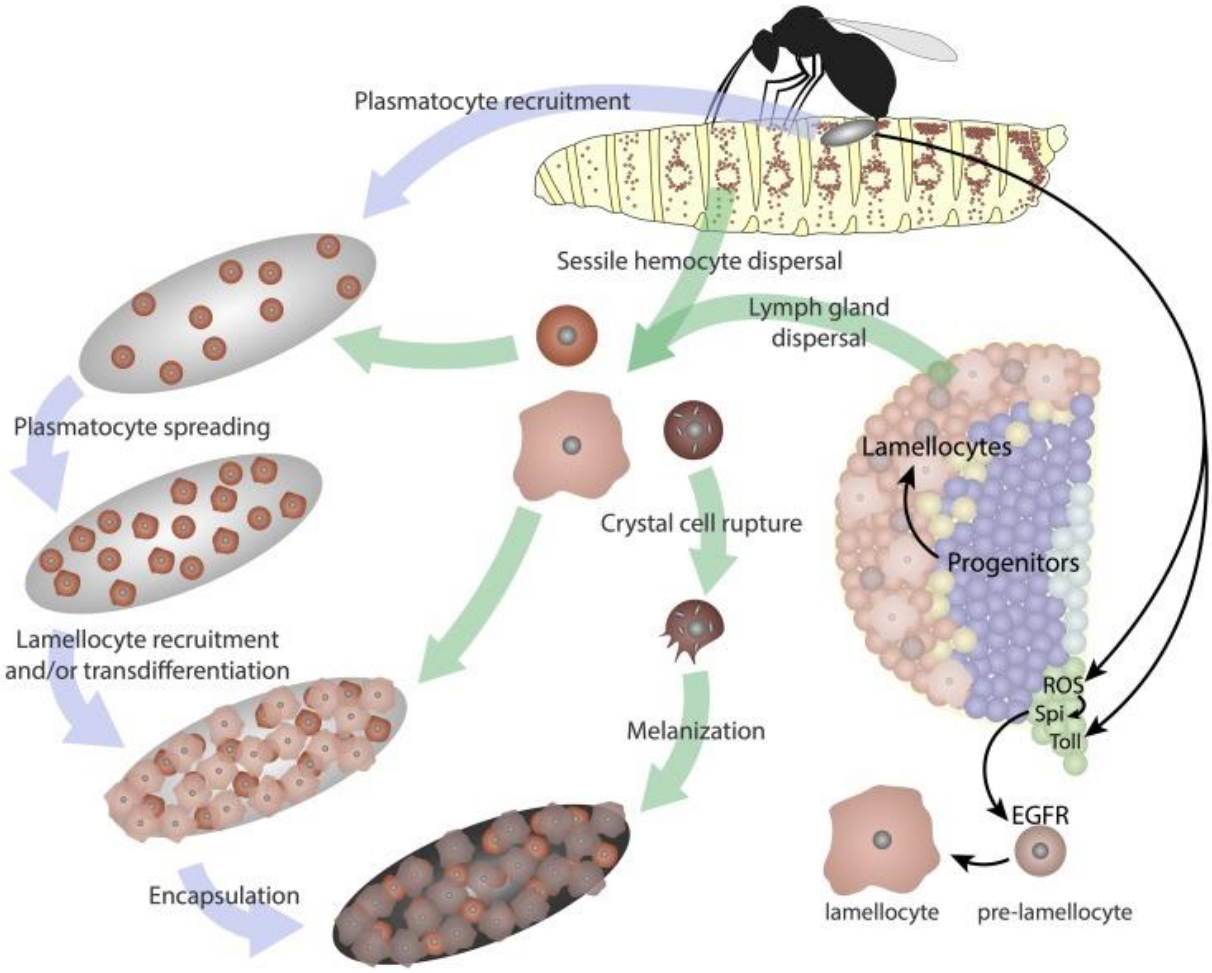

Figure 5. Encapsulation as a response to parasitoid infection (Banerjee et al., 2019)

There are a variety of strategies that parasites use to evade encapsulation, mostly by injecting venom proteins during oviposition. *L. heterotoma* injects virus-like particles (VLPs), which cause the lysis of lamellocytes (Rizki and Rizki, 1990). *L. boulardi* interferes with the lamellocyte morphology and adhesion by inhibiting the Rho GTPases Rac1 and Rac2 (Colinet et al., 2007), and inhibits melanization through a serpin (LbSPNy) and a superoxid dismutase (SOD3) (Colinet et al., 2009, 2011).

3.2.3.3. Melanization and the PPO Cascade

Melanization is a major host defense mechanism in insects, during which tyrosine is converted through several enzymatic steps to a black pigment called melanin (Meister, 2004). As mentioned earlier, this process takes place following wounding or encapsulation, and the resulting melanin deposition hardens the clot or the capsule. Furthermore, reactive oxygen species are created as a byproduct, which are toxic to both microbes and parasitoids (Tang, 2009). The ROS formed are superoxide anion and hydroxyl radicals, which are highly reactive and can form other cytotoxic molecules (Eleftherianos et al., 2021).

The reaction chain is set off by the Phenoloxidase enzyme, which converts tyrosine into dihydroxyphenylalanine (Dopa). Phenoloxidase is synthetized in an inactive form as prophenoloxidase (PPO). *D. melanogaster* carries three such genes on its second chromosome: PPO1, PPO2 and PPO3 (**Fig. 6.**) (Dudzic et al., 2015). The activation of PPO1 and PPO2 is achieved through limited proteolysis via serine proteases (SPs), namely MP1 (Melanization Protease 1), MP2 (Melanization Protease 2) and Hayan (Tang et al., 2006; Nam et al., 2012). Apart from the other PPOs, PPO3 is not activated by SPs, and might be enzymatically active in its native form (Nam et al., 2008).

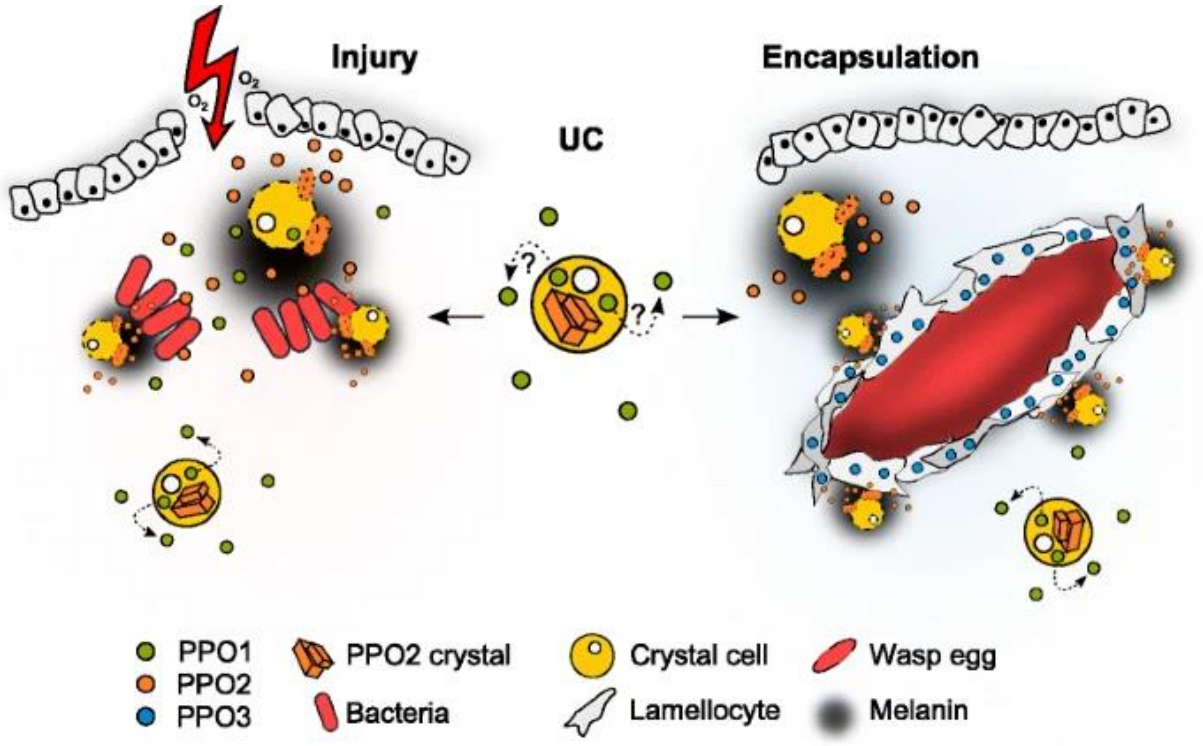

Figure 6. The involvement of PPOs in clotting and encapsulation (Dudzic et al., 2015)

PPO enzymes possess overlapping functions. PPO1 and PPO2 is released into the hemolymph by crystal cells in response to septic or sterile wounding (Fig. 6.). Similarly, during encapsulation, the PPO2 of crystal cells and the PPO3 produced by lamellocytes act together in the melanization of the capsule (Dudzic et al., 2015). Although they are in operation extracellularly, PPOs lack a signal peptide. Their release from crystal cells is attained through a process termed proto-pyroptosis, an ancient form of programmed cell death (Dziedziech and Theopold, 2022).

To avoid autotoxicity, melanization is tightly regulated through the sequential activation of SPs. This is accomplished by SP inhibitors, serpins, such as Spn27A, Spn28D or Spn77Ba (De Gregorio et al., 2002; Tang, 2009). The storage of PPOs as inactive

zymogens also contributes to autotoxicity avoidance and allows the fast activation of the cascade when required.

3.3. Humoral Immunity of *Drosophila*

3.3.1. The Main Humoral Organ, The Fat Body

The fat body is a paired, multifunctional organ that functions as liver-, adipose- and endocrin-like tissue (Arrese and Soulages, 2010). It bears the comprehensive role of regulating the development and behaviour of the whole individual, achieved by the secretion of regulatory molecules (Li et al., 2019). From the point of immunity, the fat body releases a wide variety of immune factors into the hemolymph in large quantities, including clotting factors, PRRs, AMPs, opsonins, and the SPs that activate the melanization cascade.

The fat body originates from clusters of cells of the inner embryonic mesoderm (Zheng et al., 2016). In the larva it is arranged in thin lobes of around 2200 cells, which during development undergo 256 cycles of endoreplications, resulting in a polytene tissue (Nordman et al., 2011). Although being composed of a single cell type, fat cells, or adipocytes, a single-cell RNA-sequencing study showed that the fat body is not homogenous, but consists of several distinct cell subpopulations (Gupta et al., 2022).

The fat body stores energy in the form of glycogen and triglycerides in cytoplasmic lipid droplets (Meschi and Delanoue, 2021). The glucose originating from dietary carbohydrates are converted by the fat body cells through several enzymatic steps to glycogen or trehalose, the main insect blood sugar. As immune responses are energetically expensive processes, a trade-off between immunity and growth is necessary (McKean et al., 2008). The deployment of immune responses promotes insulin resistance, thus impeding nutrient storage and the growth of the animal (DiAngelo et al., 2009; Roth et al., 2018). If nutrients are scarce, energy is relocated to development at the expense of immunity. In this case the fat body secretes a molecule called NimrodB5, which reduces the hemocytes in circulation by promoting sessility and inhibiting proliferation (Ramond et al., 2020).

A study suggest that fat body cells are highly plastic and can have cellular immune functions, too. In pupae, they are actively migrating to wound sites, where they assist plasmatocytes with debris phagocytosis, seal the wound and secrete AMPs that act locally thus preventing infections (Franz et al., 2018). The fat body also secretes stress-induced humoral factors encoded by the Turandot (Tot) gene family, consisting of eight genes, which can be induced by heat stress, oxidative stress, UV irradiation and bacterial infection (Ekengren and Hultmark, 2001). Their roles include protecting against heat stress (Ekengren

et al., 2001; Amstrup et al., 2022), protection against sexually transmitted fungal infections (Zhong et al., 2013) and inhibition of tumour growth (Kinoshita et al., 2023). The AMPs and putative lectins secreted by the fat body are discussed below.

3.3.2. Antimicrobial Peptides

The activation of Toll and Imd signaling pathways result in the production of AMPs, small, cationic peptides that kill microbes. So far, 20 AMP genes have been identified in *Drosophila*, which are classified in 7 families (Hanson and Lemaitre, 2020). Drosomycin and Metchnikowin AMPs act against fungi, Defensins against Gram-positive bacteria and Diptericin, Attacin, Drosocin, and Cecropin against Gram-negative bacteria. AMPs are mainly secreted by fat body cells, but some are also expressed by barrier tissues or by plasmatocytes (Govind, 2008).

AMPs being positively charged molecules, embed into the negatively charged membrane of pathogens, which ultimately results in the destabilisation and neutralisation of the target organism (Hanson and Lemaitre, 2020). Studies show that AMPs are also involved in intestinal microbiota control, antitumor activity and brain function regulation. However, there is no evidence for AMPs participating in parasitoid killing and has been no humoral antiparasitoid agent identified in *Drosophila* so far (Yang et al., 2021).

3.3.3. Opsonins

Opsonization was first described in 1903 and named after the Greek "opsono" meaning "I prepare victuals for" (Wright and Douglas, 1903). The name is fitting as opsonization means the preparation of pathogens for phagocytosis or encapsulation by tagging them with opsonins, small humoral molecules, which ease recognition and adhesion. The opsonin molecules usually recognize the PAMPs on target cells. Compared to other insect species, there is not much research regarding *Drosophila* opsonins, nonetheless, several candidates have been identified, including thioester-containing proteins (Teps), C-type lectins and Dscam1.

Thioester-containing proteins (TEPs) are conserved molecules that contribute to immunity in both insects and mammals (Dostálová et al., 2017). The *Drosophila* genome encodes 6 Tep family genes, however only four of them are immune inducible, possess signal peptide, and are secreted by the fat body, hemocytes and epithelial cells. The Teps are acting in the recognition and phagocytosis of fungi (Dostálová et al., 2017), Gram-positive (Stroschein-Stevenson et al., 2005; Dostálová et al., 2017) and Gram- negative bacteria (Stroschein-Stevenson et al., 2005; Haller et al., 2018).

C-type lectins belong to a superfamily of calcium-dependent carbohydrate binding proteins (Xia et al., 2018). They generally possess signal peptides, as they are secreted molecules. In *D. melanogaster*, there are more than 30 genes with C-type lectin domains (Lu et al., 2020), however, very few studies address them. The galactose-specific *Drosophila* lectins 1, 2 and 3 (DL1, DL2, DL3) are expressed in the fat body and hemocytes, among other tissues. Studies suggest that they act as PRRs. Recombinant DL1 was found to bind specifically to *Escherichia coli* and *Erwinia chrysanthemi*, but not to other investigated microbial strains (Tanji et al., 2006). Recombinant DL2 and DL3 also bound to *E.coli* in a calcium-dependent way (Ao et al., 2007). Agarose (a polymer composed of galactose monomers) beads coated with recombinant lectins had enhanced encapsulation, suggesting that *Drosophila* lectins assist encapsulation too.

Down syndrome cell adhesion molecule 1 (Dscam1) is an immunoglobulin-superfamily receptor, and similarly to other such receptors in higher animals, is able to generate a copious amount of isoforms, but through alternative splicing and not somatic rearrangements (Watson et al., 2005). Dscam1 is expressed in the fat body, by the hemocytes and in the brain. It can possibly function as both phagocytic receptor and opsonin (Li, 2021).

3.4. The Immune Signaling Pathways of *Drosophila*

There are four main immune signaling pathways in *Drosophila*, as the Toll, the Imd, the JAK/STAT, and the JNK pathways. Among these, two are NF-κB-related, being involved in AMP production (De Gregorio et al., 2002). The Imd pathway is mostly activated by Gram-negative bacteria, while the Toll pathway by Gram-positive bacteria and fungi (Govind, 2008). Imd pathway is analogous with the mammalian TNFR, the Toll pathway with the mammalian TLR signaling. The PRRs that activate these pathways recognize peptidoglycan, a polysaccharide that can be found in the cell wall of both Gram-positive and Gram-negative bacteria (Royet et al., 2005). Thus, these receptors are called Peptidoglycan recognition proteins (PGRPs). PGRPs represent an evolutionarily conserved gene family, with 13 members in *D. melanogaster*, and can be classified according to transcript size in two forms: short (S) and long (L). They are expressed in the fat body and by hemocytes. Secreted PGRPs (PGRP-SA and PGRP-SD) activate the Toll pathway, while the intracellular and membrane-bound receptors (PGRP-LC and PGRP-LE) activate the Imd pathway (Govind, 2008). Gram-negative binding protein (GNBP1, GNBP3) recognition factors also leads to Toll pathway activation.

The JAK/STAT pathway is involved in wound healing, stem cell regulation, tumour response and mechanical stress response (Yu et al., 2022). Its activation in the fat body also elicits the secretion of Tep opsonins and Turandot A (TotA). Activation of the pathway requires the production of Unpaired (Upd) family cytokines by circulating hemocytes, tumours, or gut enterocytes (Agaisse et al., 2003; Pastor-Pareja et al., 2008; Nászai et al., 2015). Production of the Upd2 and Upd3 cytokines in hemocytes leads to JAK/STAT activation in skeletal muscles, which is required for the efficient encapsulation of parasitoids (Yang and Hultmark, 2016).

The JNK pathwayis triggered by ROS, DNA damage, UV exposure, bacterial infection, wounding and has role in stress responses (Yu et al., 2022). It cooperates with the Imd pathway to generate AMPs. It also contributes to epithelial cell migration and fusion during wound healing.

It is evident that immune signaling is complex in *Drosophila*, and different pathways act in concert to elicit an immune response. The Toll, Imd and JAK/STAT immune pathways act in host resistance against parasitoid wasps, as mutation in pathway component led to decreased encapsulation and resistance (Yang et al., 2021). The Toll and JAK/STAT pathways are known to be involved in hemocyte proliferation, lamellocyte differentiation (Zettervall et al., 2004), and in antiviral response (Govind, 2008).

3.4.1. The Toll Pathway

The *D. melanogaster* genome encodes 9 Toll receptors (Valanne et al., 2022), all of which have leucine-rich repeats and cystein-rich flanking motifs. Toll receptors do not recognize microbes directly, like mammalian Toll-like receptors, but instead functions as cytokine receptors and are activated by a protein called Spätzle (Valanne et al., 2011). The signals from the PRRs that recognize Gram-positive bacteria or fungi are integrated by the SP ModSP (Buchon et al., 2009). ModSP triggers a protease cascade, in which the SPs Grass, Spirit, Spheroide, Sphinx1 and Sphinx2 are involved (Kambris et al., 2006), leading ultimately to the cleavage and activation of Spätzle.

Following Toll activation, the receptor binds to the MyD88 adaptor protein (Valanne et al., 2011). The adaptor recruits two other proteins, called Tube and Pelle, and they form a heterotrimeric complex (**Fig. 7.**), which results in the phosphorylation and degradation of

Cactus, an IκB factor that is in complex with Dorsal/Dif. As a result, Dorsal/Dif is released and after nuclear translocation activates several genes.

Figure 7. Components of the Imd and Toll pathways (Harnish et al., 2021)

3.4.2. The Imd Pathway

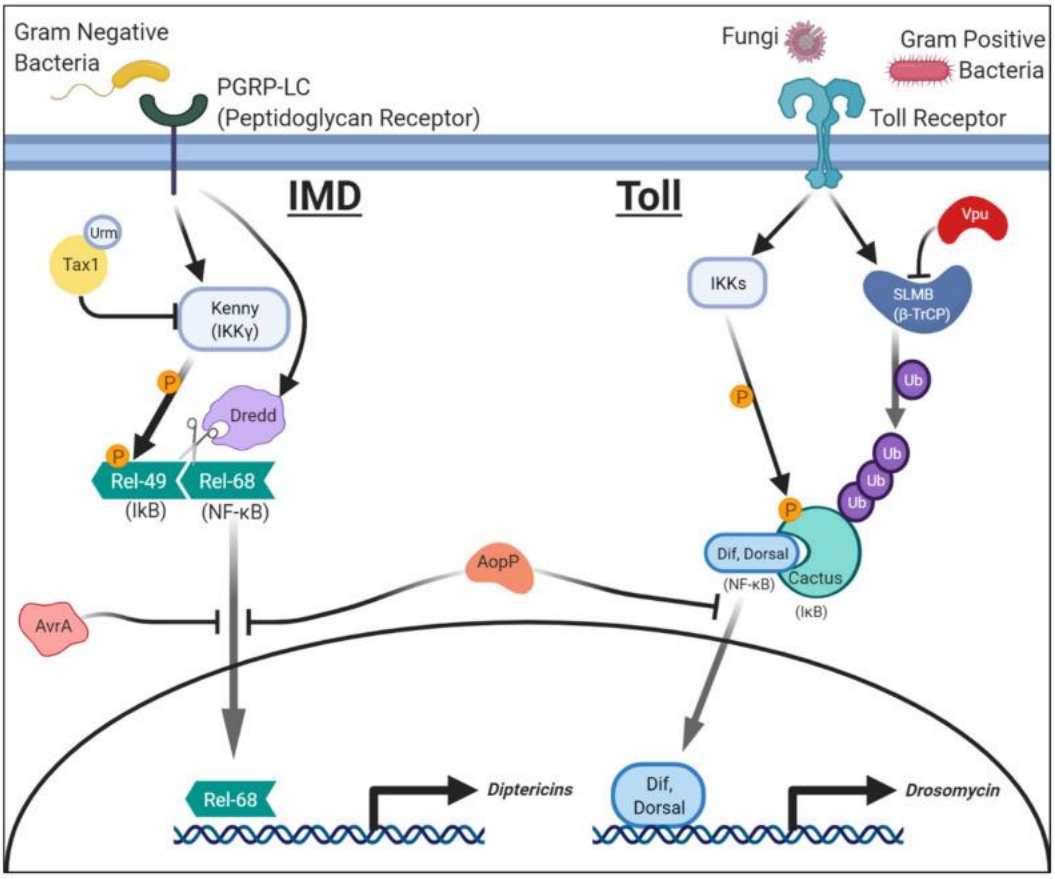

Imd pathway activation also relies on PRRs to recognize the peptidoglycan of pathogens, PGRP-LC being the main activator by binding to Imd, death domain-containing protein (Kaneko and Silverman, 2005). After its activation, Imd forms a complex with Fadd and Dredd (**Fig. 7.**) (Yu et al., 2022). The E3 ubiquitin ligase Diap2 ubiquitinilates Dredd, thus activating it. The active Dredd cleaves Imd, allowing Diap2 to K63-ubiquitinate Imd, which induces the recruitment of TAK1/Tab2 complex. TAK1/Tab2 phosphorylates the Ird5/Kenny complex, which in turn phosphorylates the Relish NF-κB protein N-terminally (Kleino et al., 2005). For the nuclear translocation of Relish the C-terminal cleavage is also needed, which is performed by the caspase Dredd (Stöven et al., 2003). The Relish transcription factor then activates genes involved in humoral immune responses.

3.4.3. The JAK/STAT Pathway

Cytokines of the Upd family are triggering the JAK/STAT (JAnus Kinase protein and the Signal Transducer and Activator of Transcription) pathway (**Fig. 8.**). *D. melanogaster* has three such ligands: Upd1, Upd2 and Upd3, which bind to the Domeless (Dome) receptor (Brown et al., 2001), causing its dimerization. A JAK tyrosine kinase named Hopscotch (Hop) is associated to the receptor, which upon activation phosphorylates both itself and Dome (Binari and Perrimon, 1994). This allows STAT92E protein to dock to the complex, where it is phosphorylated by Hop (Bina and Zeidler, 2013). This results in the dimerization and nuclear translocation of STAT92E. There it binds to a palindromic response element, thus inducing gene expression. The pathway is negatively regulated by SOCS36E, Ken and Barbie, and PTP61F.

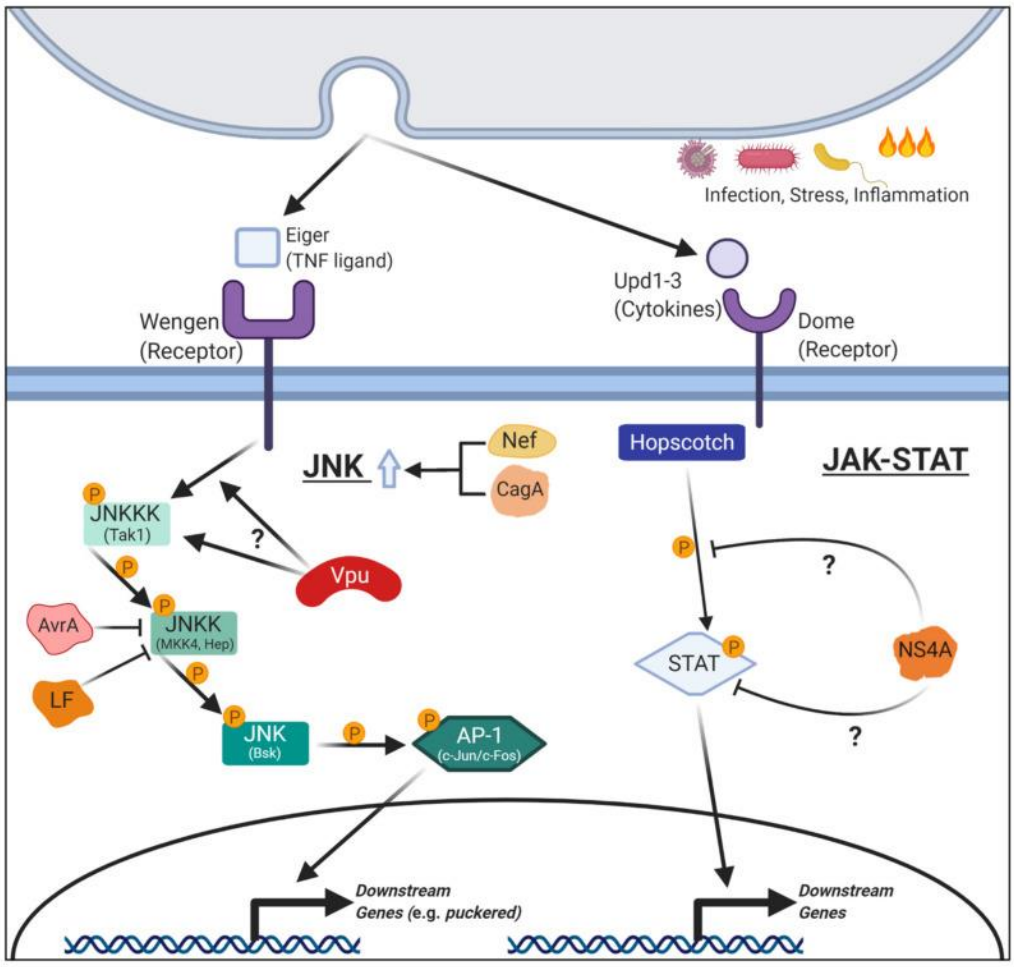

Figure 8. Components of the JNK and JAK/STAT pathways (Harnish et al., 2021)

3.4.4. The JNK Pathway

The c-Jun N-terminal kinase (JNK) pathway is a MAPK (Mitogen-Activated Protein Kinase) cascade (Harnish et al., 2021). The cascade is activated through the binding of the

TNF ligand Eiger (Egr), secreted by the fat body, to either the Wengen (Wgn) or Grindelwald (Grnd) receptors (**Fig. 8.**) (Herrera and Bach, 2021). The components of the kinase cascade are: Msn (JNKKKK), TAK1 (JNKKK), Hep (JNKK) and Bsk (JNK), which pass on the signal through each other by phosphorylation (Yu et al., 2022). Bsk, the final kinase phosphorylates and activates Jra (c-Jun) and Kay (c-Fos), which then form a transcription factor heterodimer: AP-1. AP-1 causes the transcriptional upregulation of target genes.

4. A Novel Encapsulating Cell Type, the Multinucleated Giant Hemocyte

4.1. The Species Differentiating Multinucleated Giant Hemocytes

Although *D. melanogaster* is the most studied among drosophilids, the evolutionary strategy to employ lamellocytes and melanization in response to parasites is not the default (**Fig. 9.**). In fact, lamellocyte differentiation is restricted to the melanogaster subgroup (Hultmark and Andó, 2022). Another widespread encapsulating hemocyte type is the multinucleated giant hemocyte (MGH), which we identified in the *ananassae* subgroup of *Drosophilidae,* including *D. ananassae, D. pallidosa, D. atripex, D. pseudoanassae, D. bipectinata, D. malerkotliana* and *D. parabipecinata* (Márkus et al., 2015), and in *Zaprionus indianus* (Cinege et al., 2020). It was also described to be present in *Drosophila falleni*, *Drosophila phalerata* and *Drosophila grimshawi* (Bozler et al., 2017). These species differentiate MGHs instead of lamellocytes and the melanization of the capsule cannot always be observed. The lack of melanization can be attributed to the lack of the PPO3 enzyme in these species (Hultmark and Andó, 2022), suggesting an immune strategy distinct from that of *D. melanogaster*.

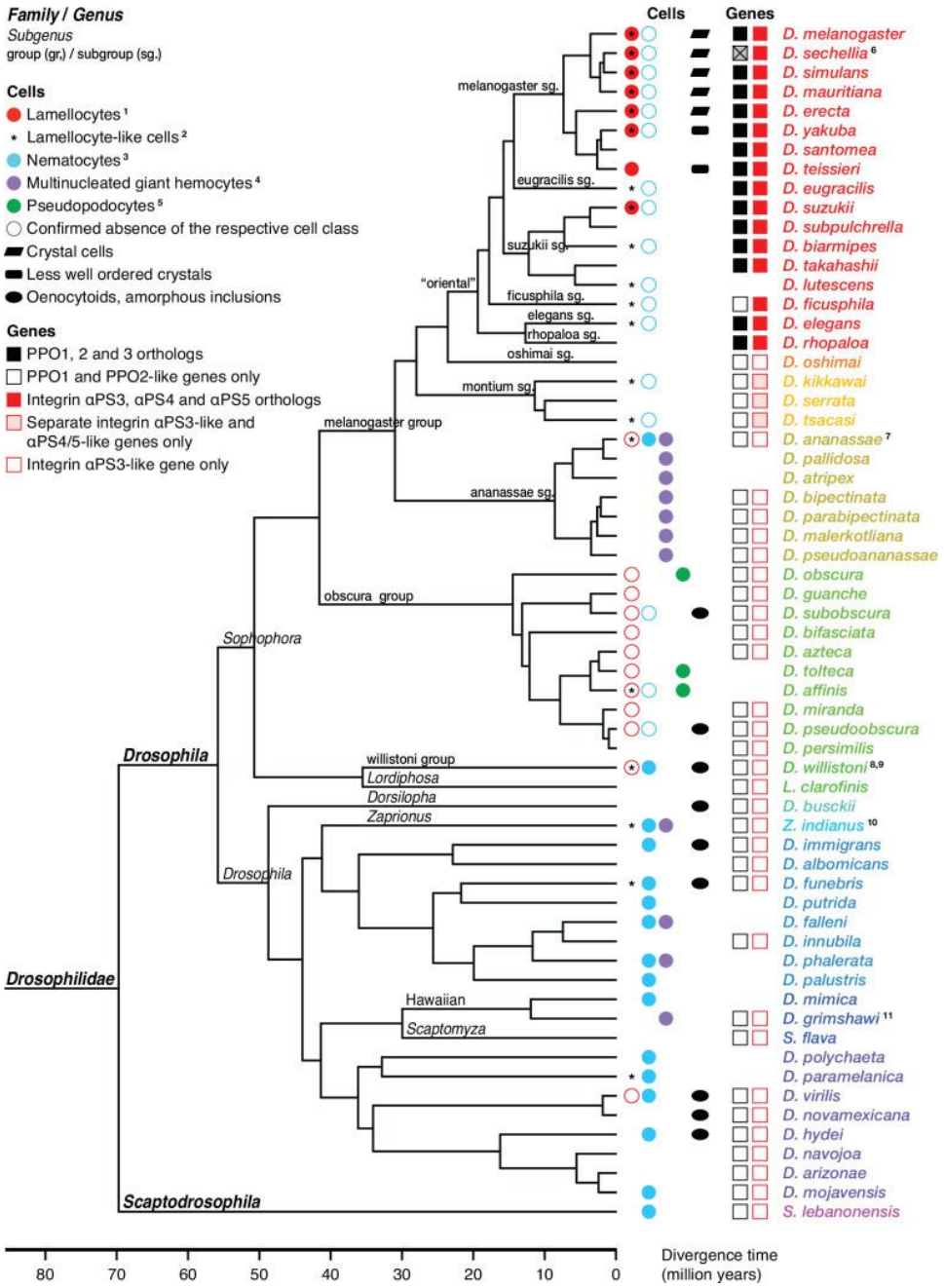

Figure 9. Encapsulating cell types of drosophilids in correlation with PPO3 and Integrin genes (Hultmark and Andó, 2022)

Drosophila ananassae has several remarkable genetic features, such as the high rate of spontaneous genetic mosaics and male recombination, a large number of pericentric inversions and translocations which are unusual for drosophilids (Singh, 2000, 2020). It also exhibits high levels of chromosomal polymorphism in natural populations (Singh and Singh, 2008). Moreover, the entire genome of a *Wolbachia* endosymbiont was found to be horizontally transferred to the chromosomes 2L (Dunning Hotopp et al., 2007) and 4 (Klasson et al., 2014) of some *D. ananassae* strains, and it even duplicated (Choi et al.,

2015). *Wolbachia pipientis* infection is widespread among insects. The bacteria are maternally inherited and present in the germline, where the prokaryotic genes can be transmitted and integrated into the eukaryote genome. This species seems highly susceptible to horizontal gene transfer (HGT) as two toxin encoding bacterial genes were also captured by its genome: *cytolethal distending toxin subunit B* (*cdtB*) and *apoptosis-inducing protein of 56 kDa* (*aip56*) (Verster et al., 2019). We have shown that these acquired genes have integrated into the immune system of the flies and play an important role in the antiparasitoid response (Verster et al., 2023).

Zaprionus indianus, or the African fig fly is an invasive species, which within the EU was detected so far in Cyprus, Malta, Portugal, Spain and France (Bragard et al., 2022). It is classified as a pest as it oviposits on healthy, undamaged fruits thus causing major agricultural damages. Morphologically, *Z. indianus* adults can be recognized by their longitudinal stripes (Fig. 10.). Genetically, this species is not as unique as *D. ananassae*, but it, too, is involved in HGT, albeit between drosophilids, as *Z. indianus* acquired transposon genes from the *melanogaster* subgroup (Deprá et al., 2010; Carareto, 2011).

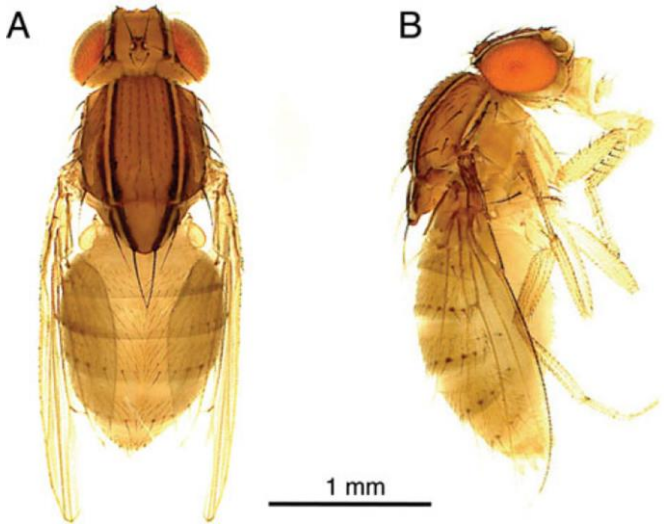

Figure 10. *Z. indianus* adult female fly (Kacsoh et al., 2014)

Studies suggest that the species that differentiate MGHs show a higher resistance to parasitoid wasps than *D. melanogaster* (Kacsoh and Schlenke, 2012; Kacsoh et al., 2014; Márkus et al., 2015).

4.2. What We Know So Far

MGHs are cells with a size between 40 and several hundred μm that possess an irregular shape (Márkus et al., 2015; Cinege et al., 2020). They exhibit high motility, fast shape change and spread vigorously on glass surfaces thanks to their elaborate actin microfilament and microtubule networks. As their name implies, they may contain even more than 30 nuclei in their cytoplasm (**Fig. 11.**).

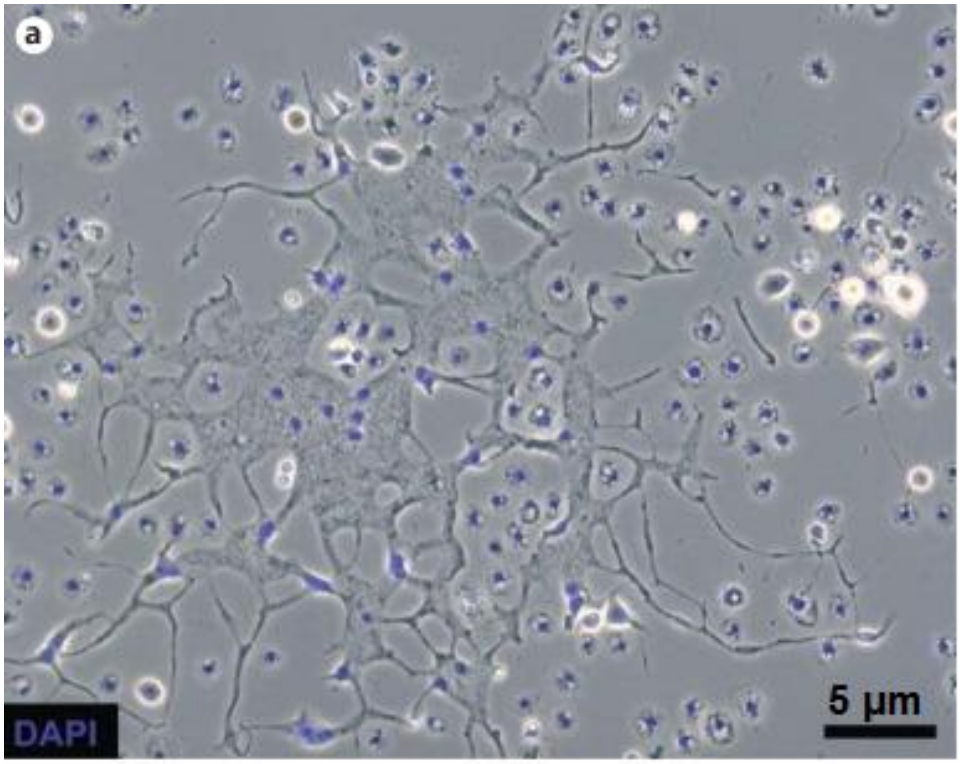

Figure 11. Multinucleated giant hemocyte of *D. ananassae* (Márkus et al., 2015)

MGHs are not present in *D. ananassae* under naive condition, but differentiate after parasitoid infection (Márkus et al., 2015). They do not phagocytose bacteria, instead participate in encapsulation, similarly to *D. melanogaster* lamellocytes (**Fig. 12.**). However, in this species the capsules are not melanized. The lack of melanization is probably caused by the absence of PPO3 encoding gene from the *D. ananassae* genome (Hultmark and Andó, 2022). As PPO1 and PPO2 are encoded by its genome, mechanical wounding of the larval cuticle induces melanisation (Márkus et al., 2015).

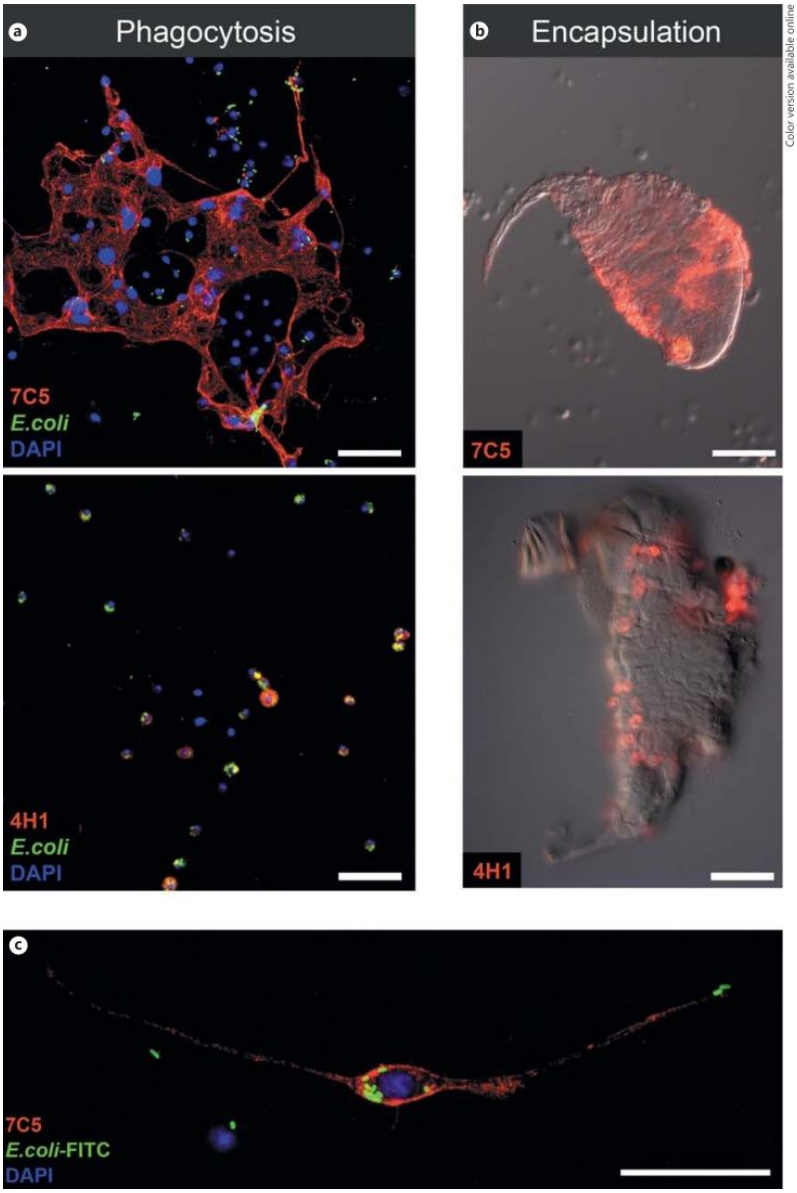

Figure 12. MGHs are not involved in phagocytosis (a), but participate in encapsulation (b). Elongated cells with a single nucleus constitute an intermediary cell in MGH differentiation (c). (Márkus et al., 2015)

In *Z. indianus*, MGHs belong to a group of cells named giant hemocytes, which in addition to multinucleated cells also include elongated cells with single nucleus (dubbed nematocytes in a previous study (Kacsoh et al., 2014)) and anucleated structures, as all are stained by the 4G7 monoclonal antibody (**Fig. 12.**) (Cinege et al., 2020). In this species, MGH formation does not require immune induction, as these cells are constitutively present in the circulation. Compared to *D. ananassae*, another difference is that, while also lacking the PPO3 enzyme, *Z. indianus* employs both melanotic and non-melanotic encapsulation against parasitoids (Kacsoh et al., 2014).

4.2.1. MGH Differentiation

The hemocytes of *D. ananassae* can be detected and traced by monoclonal antibodies. The 7C5 antibody reacts specifically with *D. ananassae* MGHs and was used to characterize MGH differentiation (Márkus et al., 2015). MGHs originate from the circulation and sessile compartment, but not from the lymph gland. In fact, the lymph gland does not disintegrate after parasitization, as in *D. melanogaster*. Twenty-four hours following parasitization 7C5 positive bipolar, spindle-like, mononuclear precursor cells were observed in circulation. At 48h post infection, 7C5 positive multinucleated cells appeared in the circulation and sessile tissue. The number and size of MGHs peaked at 72h. However, parasitization by *L. victoriae* and *L. heterotoma* wasps reduces MGH levels, compared to *L. boulardi* parasitization.

Absence of the phospho-histone H3 mitosis marker showed that division does not play a role in MGH formation. While ex vivo mixing of the blood cells of BrdU labeled and unlabeled individuals showed that MGHs are fusogenic cells. However, this fusion did not take place with plasmatocytes isolated from naive larvae, meaning that blood cell activation is necessary for this process (Márkus et al., 2015).

In *Z. indianus*, all immune compartments: the circulation, the sessile hemocytes and the lymph gland participate in MGH differentiation (Cinege et al., 2020). While 4G7 positive cells (including the MGHs) are present in naive larvae too, parasitoid infection causes change in the size and number of MGHs, and nuclei of the 4G7 positive cells enlarge, indicating genome duplication. Twenty-four hours after wasp infection the phospho-histone H3 marker showed mitotic activity in the 4G7 positive cells of the lymph gland. The organ got swollen and following 72h hours it disintegrated, and the 4G7 positive cells entered in the circulation. We showed that cell fusion plays a role in MGH formation in *Z. indianus* too, which means that in this species both cell fusion and endomitosis participates in MGH differentiation, thus multiplicating the genome in two ways within one cell.

There is evidence that NO, a small gaseous signal molecule produced from L-arginine by nitric oxide synthase (Kraaijeveld et al., 2011), regulates MGH differentiation (Lerner, 2020, PhD diss.). Supplementing *D. ananassae* larvae with L-arginine resulted in augmented MGH differentiation and an increase in successful encapsulation and parasitoid death, while treatment with the nitric oxide synthase inhibitor, L-NAME had the opposite effect and suppressed MGH formation.

4.2.2. MGH Ultrastructure

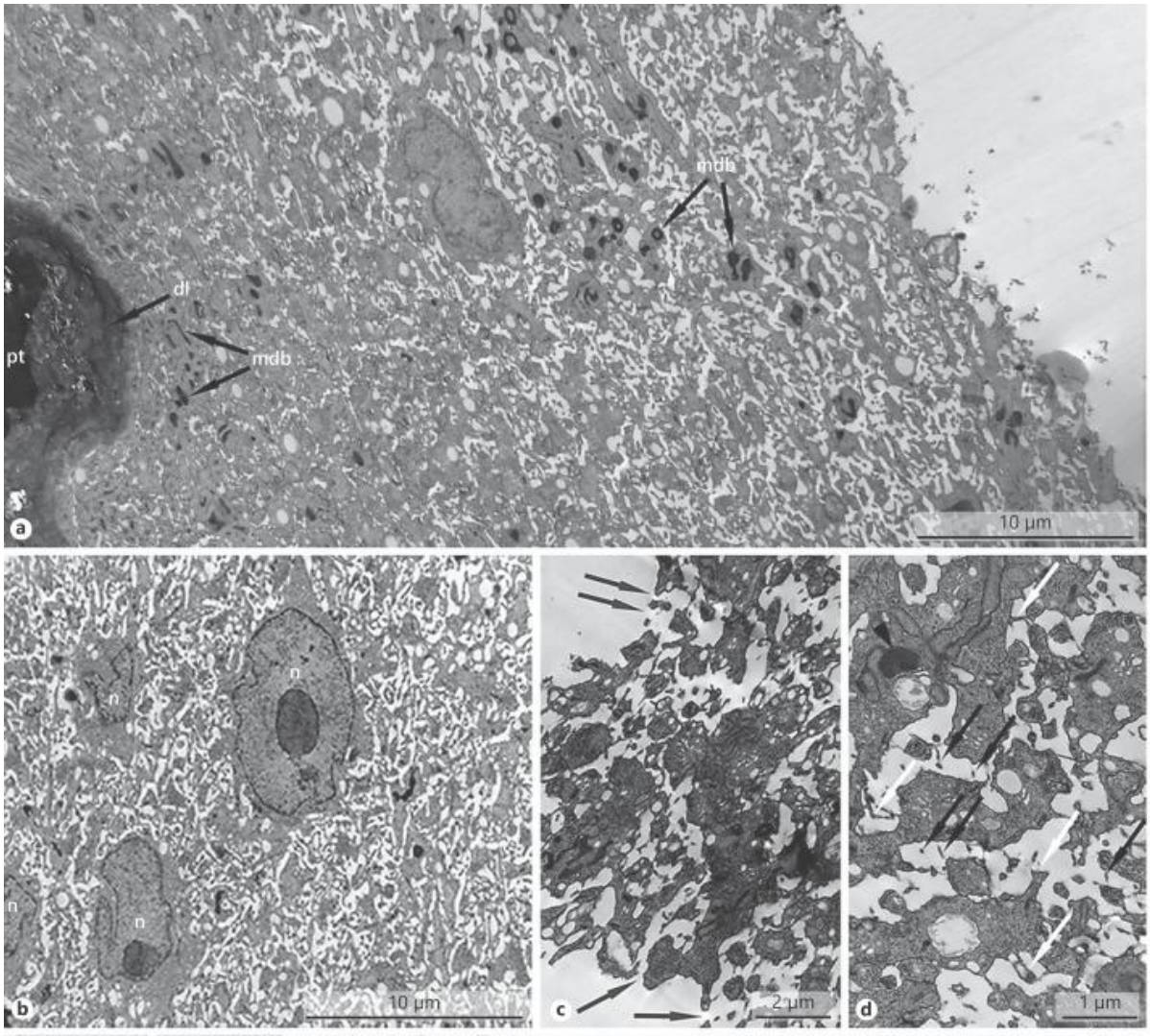

Figure 13. Electron micrographs of *Z. indianus* MGHs. a. The black areas are multiform dense bodies (mdb). An electron-dense layer (dl) is formed around the parasitoid (pt). b. Nuclei are not divided by membrane. c. The canalicular system has openings to the MGH surface (arrows) d. Large number of lamellae (white arrows) and thin microvilli (black arrows) protrude into the canals (Cinege et al., 2020)

Electron microscopic analysis revealed that in both species, *D. ananassae* and *Z. indianus*, the ultrastructure of MGHs has characteristics distinct from plasmatocytes. The cytoplasm of MGHs possess a sponge-like ultrastructure due to an elaborate system of canals and sinuses, which communicate with the hemolymph through openings on the cellular surface, hence providing a large contact area for the cell with the environment (**Fig.13. c**). The nuclei are randomly localized and are not separated by a plasma membrane (**Fig.13. b**). The cytoplasm is scattered with multiform dense bodies with variable shape and size (**Fig.13.**

a). It also contains a high number of free ribosomes, possibly for synthetizing large amounts of effector molecules.

4.3. The Role of Whole-Genome Duplication in Immunity

Whole-genome duplication (WGD) or polyploidy is the result of either cell fusion or endoreplication (premature cell cycle exit) (Anatskaya and Vinogradov, 2022). Depending at what point does the cell cycle stop, the resulting cell can possess multiple nuclei, a multilobed nucleus or an ordinary-looking nucleus containing polytene chromosomes (Orr-Weaver, 2015).

The presence of polyploid cells was described in all multicellular organisms (Anatskaya and Vinogradov, 2022). It can be pathologic, an adaptation to stress or a normal part of development. WGD is a universal mechanism that allows the generation and maintenance of large cells, while also facilitating elongated cell shapes (Peterson and Fox, 2021). In adult *Drosophila*, polyploid mononucleated and fused epithelial cells participate in wound closure, and these giant cells are critical for wound healing (Losick et al., 2013). This provides a faster wound closure and thus healing mechanism than the generation of new replacement cells by mitosis.

In insects, secretory tissues are polytene, as the increased genetic material provides the ability to mass produce molecules. Such tissues include the larval salivary gland and the fat body. The variety of immune factors secreted by the fat body were discussed in part 3.3.1. The salivary gland secretes large quantities of digestive enzymes and an adhesive mucoprotein needed during pupariation (Babišová et al., 2023).

In case of MGHs, the giant size and net-like shape, granted by several occasionally enlarged nuclei, allows these cells increased contact surface with parasitoids during encapsulation, thus making the process more efficient. As cell fusion contributes to their formation, it allows the rapid employment of MGHs when needed. While it might also grant the mass production of immune molecules against parasitoids, like toxins or opsonins, in high amounts. As WGD also contributes to stress tolerance (Schoenfelder and Fox, 2015), MGHs might be less susceptible to the substances (venom molecules, VLPs) used by the parasitoids against the host.

4.4. Multinucleated Giant Cells in Mammals

Mammalian macrophages are considered analogous to *Drosophila* plasmatocytes in terms of function. They are phagocytic innate immune cells that originate from the myeloid cell lineage. There is a lesser-known phenomena in the mammalian immune system, namely

that the intrinsically fusogenic macrophages are able to merge with each other under certain conditions and give rise to multinucleated giant cells, also known as giant cells (GCs) (Brodbeck and Anderson, 2009). The fusion of macrophages was described in 1977 (Chambers, 1977), but GCs were first observed much earlier, more than 150 years ago (Langhans, 1868). Depending on the molecular environment and surrounding cytokines, the fusion of monocytes or macrophage precursors can result in different types of GCs (Quinn and Schepetkin, 2009), including Touton GCs, Langhans GCs, foreign-body GCs and osteoclasts (**Fig. 14.**).

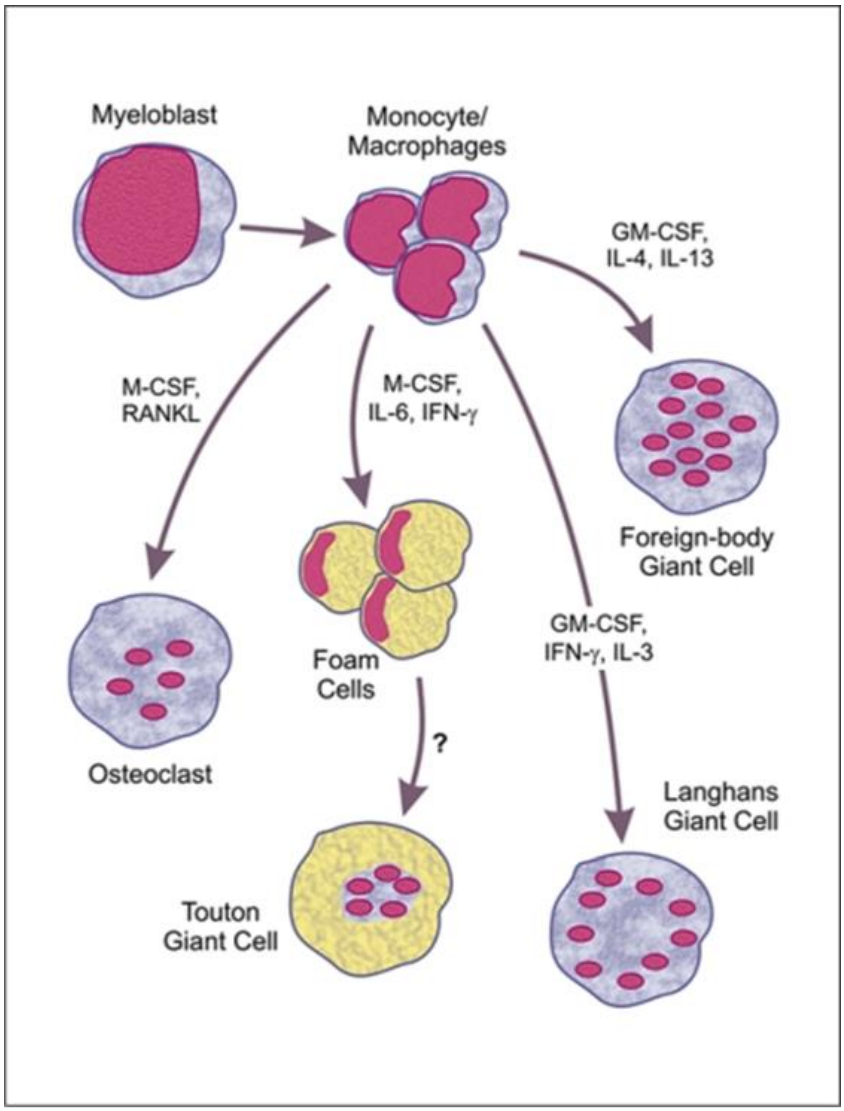

Figure 14. Formation of different types of GCs in mammals (Quinn and Schepetkin, 2009)

The formation of giant cells enables the engulfment of large particles that are too big for macrophage phagocytosis (**Fig. 15.**). Alternatively, these particles can also be degraded

extracellularly with lysosomal enzymes. Evidence suggests that ROS plays regulatory roles in macrophage fusion and multinucleation, while GCs themselves also demonstrate high ROS production (Quinn and Schepetkin, 2009).

The osteoclast is the only GC present under physiological conditions, as it has role in bone resorption by the external degradation of bone tissue (Brodbeck and Anderson, 2009). This is achieved through the creation of an extracellular lysosome with the help of its podosomes, while lowering the pH with vacuolar (V)-ATPase proton pumps (Ahmadzadeh et al., 2022). The bone tissue is degraded by lysosomal enzymes, such as proteases like cathepsin K. Osteoclasts are then able to internalize bone remnants by clathrin-mediated endocytosis and degrade them further intracellularly. It was reported that they can phagocytose foreign materials, such as latex, polymethylmethacrylate, and titanium. Osteoclasts also participate in promoting bone formation by the release of different soluble factors named clastokines, and by direct cell contact with osteoblasts (McDonald et al., 2021). Other roles include angiogenesis stimulation and immunomodulation, including antigen presentation and T cell activation.

Formation of other GC types are restricted to pathological conditions. Foreign body GCs possess irregular shape and up to 200 nuclei. They participate in immune reactions against foreign materials, chronic inflammations generated after host tissue injury and different blood-foreign material interactions (Quinn and Schepetkin, 2009). The first step in their formation, is the creation of a thrombus on the surface of the foreign material, called the provisional matrix, which contains different cytokines, chemokines and mitogens (Ahmadzadeh et al., 2022). These create an optimal environment for the recruited macrophages to fuse and form foreign body GCs. The resulting large cell size enables the elimination of threats bigger than 10-20 μm, as it has been demonstrated that they are able to engulf particles too big for a single macrophage to eliminate. It is believed foreign body GCs participate in both phagocytosis followed by internal degradation and in the extracellular degradation of foreign particles (**Fig. 15.**) (Sheikh et al., 2015).

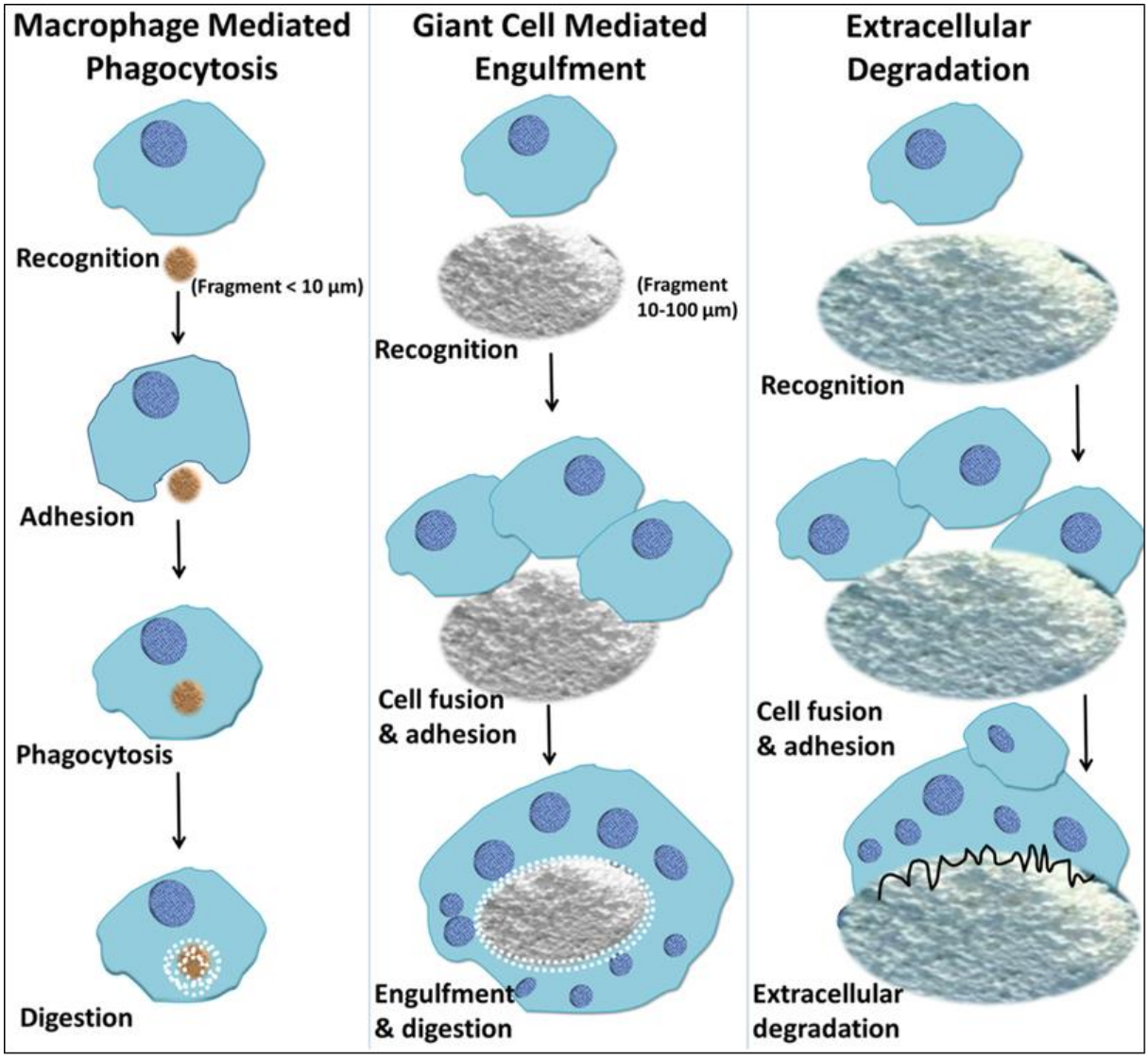

Figure 15. Macrophage and GC response to foreign bodies (Sheikh et al., 2015)

Langhans GCs are associated with granulomas in persistent infectious and non-infectious diseases. They have a typical appearance as their nuclei (less than 20) can be found at the periphery of the cell (Ahmadzadeh et al., 2022). They were described to form a barrier during *Mycobacterium tuberculosis* infection and limit the spread and growth of the bacteria. Langhans GCs also participate in the inflammatory reaction, by secreting cytokines, such as TNF-α and IL-1α. Regarding non-infectious diseases, it was reported they have a role in the clearance of cancer cells (Wang et al., 2021).

Touton GCs are formed in lesions when cell fusion is accompanied by lipid uptake, such as in fat necrosis and xanthogranuloma (Gupta et al., 2014). They contain multiple nuclei that are clustered together and are surrounded by foamy cytoplasm, which is the result of large amount of phagocytozed lipid material (Dayan et al., 1989).

Megakaryocytes are large polyploid cells of different origin, from the megakaryoblast lineage, that can also be considered GCs. Instead of fusion, these cells differentiate through endomitotic cycles. These repeated incomplete mitosis events lack both nuclear (karyokinesis) and cytoplasmic division (cytokinesis) and result in a large cell with a polyploid multilobulated nucleus (Machlus and Italiano, 2013). The megakaryocytes have a different role than 'classical' GCs, as they give rise to the blood platelets. The poliploidy of megakaryocytes provides high transcriptional output that results in large quantities of mRNA, needed for platelets to rely on in lack of a nucleus (Li et al., 2017).

GCs, with exception to osteoclasts and megakaryocytes, have not been extensively studied and represent an uncharted area of mammalian innate immunity (Ahmadzadeh et al., 2022). Studying *Drosophila* MGHs could help elucidate the mechanisms of formation, general action and role of genome multiplication in these types of cells with a more manageable and cost-effective approach.

II. Aims

The aims of my studies were to discover the molecular mechanisms behind the highly effective immune response of MGHs, and to gain insights into their role in two representative species: in *D. ananassae* and in *Z. indianus*. More specifically:

- compare the parasitoid resistance of MGH differentiating *D. ananassae* and *Z. indianus*, and lamellocyte differentiating *D. melanogaster*,
- determine the factors that induce MGH differentiation,
- discover and characterise the structural components of MGHs,
- gain insights into the genetic background of MGHs, including immune pathways,
- identify and characterise toxins encoded by putative horizontally transferred genes that might participate in the effective immune defense.

III. Materials and Methods

1. Insect Stocks and Culturing Conditions

D. ananassae wild type (14024-0371.13) had been obtained from UC San Diego Drosophila Species Stock Center. *Z. indianus* strain strain #3 had been kindly provided by Bálint Z. Kacsoh (University of Pennsylvania, USA). *D. melanogaster* wild type (Oregon-R) was ordered from Bloomington Drosophila Stock Center. Flies were kept at 25°C on standard yeast-cornmeal food. The wasp strains *Leptopilina boulardi* G486, *Leptopilina heterotoma* 14 and *Leptopilina victoriae* LvUNK were a gift from Prof. Todd Schlenke (University of Arizona, USA). Wasps were maintained on *D. melanogaster* Oregon R flies.

2. Parasitisation of the Larvae

In order to infect *Drosophila* with parasitoids, 60 early second instar larvae were selected and transferred to standard yeast-cornmeal food containing vials to be exposed to 15 gravid female wasps for 6 hours at 25 °C. We selected larvae for further experiments based on the presence of melanized spots on the cuticle confirming the site of oviposition.

3. Survival Assay Following Parasitisation

For eclosion analysis, 48 h after the wasp infection, from each vial 10, randomly selected larvae were dissected and scored for the presence of parasitoid eggs or larvae. If each of the 10 tested larvae carried parasitoids, we considered the respective vial 100% infected. Following the pupariation, the eclosed fly and wasp adults were counted and their proportion was determined. The differences among means were analyzed with one-way ANOVA, while the Tukey's HSD (honestly significant difference) test was used for pairwise significance determination.

4. Microbead Injection, Sterile and Septic Injury

Second instar larvae were washed in Drosophila Ringer solution and placed on a sterile Petri dish for treatment. Injury or microbead injection was carried out on the dorsal part of the 5th segment, using 100 μm diameter minutien pins or glass capillary. Microbead injection was done using a glass capillary with a volume of 0.1 μl, 15 μm diameter FluoSpheres polystyrene microbeads (Invitrogen) suspended in sterile Drosophila Ringer solution. As a negative control sterile Drosophila Ringer solution was injected in a similar fashion. For septic injury, prior to wounding the minutien pins were dipped in a 1:1 mixture of Gram-positive (*Bacillus subtilis,* SzMC 0209) and Gram-negative (*Escherichia coli,* SzMC 0582) bacteria (obtained from the Szeged Microbial Collection, University of Szeged,

Hungary) or a 50% suspension of *Beuveria bassiana* entomopathogenic fungus spores (Kwizda Agro, Artis Pro) in sterile phosphate-buffered saline (PBS). After injury or injection, larvae were carefully transferred into vials with standard yeast-cornmeal food, and 48 h after treatment were used for blood cell differentiation assays and sample preparation for qRT-PCR.

5. Indirect Immunofluorescence and Image Analysis

Larvae were dissected in CSM and the blood cells were left to adhere to the glass microscopic slides for 1 h. After the dissection of larvae, the hemocytes were fixed with acetone for 6 min, air dried, and blocked with 0.1% BSA in PBS for 20 min. Fat bodies and parasitoids were removed and fixed with 2% paraformaldehyde for 10 min, washed three times in PBS (5 min each), and blocked with 0.1% BSA in PBS supplemented with 0.1% Triton X-100. For each sample incubation with the primary antibodies was applied for 1 h. The 7C5, L1, 4G7 or a negative control monoclonal antibody T2/48 were used in the form of undiluted hybridoma supernatants, and the anti HL6, anti HL16 polyclonal serum, or as negative control normal mouse serum were used in 1:500 dilution in blocking solution. Samples were washed for 5 min 3 times with PBS, then incubated with the secondary antibody (anti-mouse Alexa Fluor 488 goat antibody (Invitrogen) in 1:1,000 dilution) and DAPI (Sigma; at a concentration of 2.5 μg/ml) for 45 min, washed 3 times with PBS for 5 min and covered with Fluoromount G medium and coverslip. The samples were analyzed with an epifluorescence microscope (Zeiss Axioscope 2 MOT) or with an Olympus FV1000 confocal LSM microscope.

6. Electron Microscopy

Blood cells were isolated and fixed for 48h in a solution of 0.5% glutaraldehyde (EM Grade, Polysciences), 4% formaldehyde (Polysciences), 2 mM CaCl2, and 1% sucrose in 0.1 mol/L Na cacodylate buffer (Polysciences). Then the samples were embedded in 4% agar, washed in 0.1 mol/L Na cacodylate 3 times for 10 min each, stained with 1% OsO4 (Polysciences) in 0.1 mol/L Na cacodylate for 1 h, rinsed with 10% acetone twice, and stained with 2% uranyl acetate (EM, TAAB Laboratory, and Microscopy) in distilled water for 2 h. Staining was followed by dehydration in a graded series of ethanol, and then in propylene oxide (Sigma) for 15 min. Infiltration was done in propylene oxide:Durcupan ACM (Sigma) epoxy resin, 2:1 overnight, in propylene oxide:Durcupan 1:2, and in full Durcupan ACM for 2 h. Polymerization was carried out for 48 h at 60°C. For sample observation sections were created by a Reichert Ultracut ultramicrotome, and their staining

took place in Reynolds lead citrate. Sections were viewed in a JEM-1011 JEOL transmission electron microscope and the pictures were taken with a Morada, Olympus camera, and iTEM software (Olympus).

7. Vesicle Acidity Assay Using LysoTracker Dye

Seventy-two hours after *L. boulardi* infection, *D. ananassae* larvae were dissected in Schneider's medium (Lonza) supplemented with 5% fetal bovine serum (GIBCO) and 0.01% 1-phenyl 2-thiourea (Sigma) (CSM) on microscope slides. The encapsulated parasitoids were separately isolated in CSM and the blood cells were left to adhere to the glass slides for 1 h. Then the medium was discarded and the cells and capsules were washed in PBS. Samples were incubated for 3 min in DND-99 (Invitrogen, 1:1,000 dilution in PBS), a cell-permeable red fluorescent dye that stains acidic compartments. The staining was followed by two washes in PBS, then covered with Fluoromount G medium and coverslip. Samples were analyzed straight away with an epifluorescence microscope (Zeiss Axioscope 2 MOT) or with an Olympus FV1000 confocal LSM microscope.

8. Transcriptome Analysis of *D. ananassae* Hemocytes

8.1. Collection of Samples

D. ananassae larvae 72 h following *L. boulardi* infection were washed in Drosophila Ringer solution. Larvae were bled in Schneider's medium (Lonza) supplemented with 5% fetal bovine serum (GIBCO) on microscope slides. The cytosol of a single blood cell that was adhered to a microscopic slide, was aspired with a glass pipette, which contained 1.5 μL RNase-free sterile Drosophila Ringer solution, using a micromanipulator. Then the pipette holder was removed from the micromanipulator, and by applying positive pressure, the collected sample was expelled to a microtube containing 1 μL lysis buffer with an RNase inhibitor from the TAKARA Clontech SMART-Seq v4 Ultra Low Input RNA Kit for Sequencing (Cat. No. 634889). The tubes were briefly centrifuged and snap-frozen on dry ice. The cytosols of 5 plasmatocytes or 5 MGHs were pooled in 1 microtube. In total, 5 pools were collected of each cell type. Samples were stored at −80°C until further processing according to the manufacturer's protocol. As uninduced blood cells are a heterogeneous population of mostly plasmatocytes, the mRNA was isolated from 5 independent naive blood cell pools, each from 50 age-matched third instar larvae. RNA was isolated with the RNeasy micro kit (Qiagen).

8.2. cDNA Library Preparation and Next-Generation RNA Sequencing

From the RNA originating from MGH and activated plasmatocyte samples, the synthesis of cDNA was performed with the Clontech's SMARTer Ultra Low RNA Input v4 kit. The resulting cDNA was analyzed with a Fragment Analyzer (Advanced Analytical) for quality control. Library preparation was done using an Illumina FC-131-1024-Nextera XT DNA SMP Prep Kit (Cat. No. 1293799) according to the manufacturer's protocol. The samples were sequenced using a NextSeq 150 high-output kit (Cat. No. 20024907) in an Illumina NextSeq 500 System with 2 × 75 paired-end reads. The cDNA synthesis from the naive hematocyte RNA was carried out with the Clontech-Takara SMARTer cDNA synthesis kit. A quality check was done with a Fragment Analyzer (Advanced Analytical), and the concentration-adjusted samples were processed further with a SMART-Seq v4 Ultra Low Input RNA kit, continued from the tagmentation step. Library preparation was carried out using a Nextera XT DNA Sample Preparation Kit (Illumina). Samples were then pooled and sequenced using a NextSeq 300 high-output kit in an Illumina NextSeq 500 System with 2 × 150 paired-end reads.

8.3. Processing of RNA Sequencing Data

Following sequencing, raw reads were de-multiplexed and preprocessed using Trimmomatic and Flexbar. Raw sequencing reads were aligned to the Ensembl Drosophila ananassae genome (release 37), using a STAR aligner with the following parameters: trimLeft = 10, minTailQuality = 15, minAverageQuality = 20, and minReadLength = 30. Gene counts were calculated using HTSeq.

8.4. The Bioinformatic Analysis of RNA Sequencing Data

To assess differential expression, we analyzed the RNA sequencing data with th DESeq2 package. To account for technical dropouts, we first used zingeR to zeroWeightsLS function to weigh gene expression against dropouts. We used DESeq2 to normalize cell gene expressions and then run a differential gene expression analysis.

8.5. Bioinformatic Analysis of the *D. ananassae* Comparative Transcriptome Data

As there is no available information concerning the genes and proteins of *D. ananassae*, we used the Flybase database to gather data about their *D. melanogaster* orthologs. The Gene Ontology (GO) enrichment analysis was carried out using GO: TermFinder open-source software (Boyle et al., 2004). The enrichment analysis was performed against the background of all the annotated *D. melanogaster* genes of the Flybase database. Results were summarized and visualized with REVIGO (Supek et al., 2011).

Physical interaction networks were constructed with Cytoscape (Shannon et al., 2003), using the physical interactions listed on Flybase.

9. Transcriptome Analysis of *Z. indianus* Blood Cells

9.1. Sample Preparation

For sample collection 100 age-matched naive and 100 *L. victoriae* infected (72 hours after parasitisation) *Z. indianus* larvae were dissected and their hemolymph harvested. RNA was isolated with an RNeasy mini kit (Qiagen). Three biological replicates were used for each group. The quantity and integrity of the RNA samples were determined by capillary gel electrophoresis using a 2100 Bioanalyzer instrument (Agilent) with an Agilent RNA 6000 Nano Kit. The mRNA was isolated from 220 ng total RNA per sample with a NEBNext Poly(A) mRNA Magnetic Isolation Module (New England Biolabs).

9.2. cDNA Library Preparation and RNA Sequencing

Library generation was done with a NEBNext Ultra II Directional RNA Library Prep Kit for Illumina (New England Biolab) with NEBNext Multiplex Oligos for Illumina (New England Biolab) following the manufacturer's protocol. After the validation and quantification of the indexed sequencing libraries with an Agilent DNA 1000 kit in a 2100 Bioanalyzer instrument, they were pooled in equimolar ratios. The library pools underwent denaturation and were diluted to 15-pM concentration and sequenced in a MiSeq DNA sequencer (Illumina) using a MiSeq Reagent Kit v3 (150-cycle) producing 2 × 75 bp paired-end reads.

9.3. Data Processing

Base calling and generation of FASTQ sequence files were performed using BaseSpace Sequence Hub algorithms. FASTQ files were quality trimmed using the TrimGalore software and then aligned to the Z. indianus reference genome (Comeault et al., 2020) using HISAT2. To determine the number of sequence reads mapped to each gene, the reference transcriptome was imported into R using the GenomicFeatures package, and then read counts were calculated with the GenomicAlignments package.

9.4. The Bioinformatical Analysis of RNA Sequencing Data

DESeq2 was used for data normalization and differential gene expression analysis. Genes with a read count <10 were excluded from the analysis. A gene was considered to be expressed in a given sample if its Fragments per kilobase of exon model per million reads mapped (FPKM) value was >1. Those genes were considered significantly differentially

expressed in either naive or *L. victoriae* induced *Z. indianus* blood cells, which had an Benjamini–Hochberg adjusted p-value <0.05 and an absolute log2FoldChange ≥1. Regarding orthology relations, a protein was considered ortholog if in pairwise comparison, the coverage reached 20%, the identity was higher than 40%, and the E-value representing the quality of the alignment was lower than 0.0001. Orthology searches were performed in the National Center for Biotechnology Information (NCBI) database. Because of the lack of available information regarding *Z. indianus* genes and proteins, data from their *D. melanogaster* orthologs were used. Functional data regarding the *D. melanogaster* orthologs were acquired from Flybase, while those of mammalian orthologs were acquired with Ingenuity Pathways Analysis (IPA). Gene ontology (GO) enrichment analysis for the differentially expressed genes was carried out with the R software, with the clusterProfiler package.

10. The Analysis of *hemolysin E*-like Genes

10.1. General Bioinformatic Analysis of *hemolysin E-like* Genes

To map out *hl* genes in the *D. ananassae* genome and find all homologs the NCBI Basic Local Alignment Search Tool (BLAST) was used, with the hl genes discovered through the transcriptome as query sequences. The assembly ASM1763931v2 was used. Signal peptides were predicted with SignalP (Teufel et al., 2022). Protein size was predicted with the Sequence Manipulation Suite (Stothard, 2000). Most of the 3D structure predictions were retrieved from the Alphafold Protein Structure Database. The AlphaFold algorithm predicts protein structures with high accuracy via a deep learning approach solely from their amino acid sequence (Jumper et al., 2021). The HL proteins not available in the database were predicted with the AlphaFold Colab (v2.1.0). Multiple sequence alignment was performed with the T-Coffee web server (Di Tommaso et al., 2011), and visualized with Jalview 2.11.3.2.

10.2. Phylogenetic Analysis of Hemolysin-E Molecules

The analysis was done in collaboration with Rebecca L. Tarnopol at the Department of Plant and Microbial Biology, University of California, Berkeley, USA. Hemolysin E homologs were found by conducting TBLASTN (Altschul et al., 1997) searches using the amino acid sequence for the Hemolysin E domain of all paralogs found in the D. ananassae genome as queries. A subsequent phmmer v 3.1b2 search was run on the Refseq protein database (accessed on 19 August 2022) to find more divergent prokaryotic Hemolysin E homologs. Hits from both searches were pared down to retain only hits with E-values <0.01.

To eliminate redundant sequences from the alignment, CD-HIT version 4.8.1 (Li and Godzik, 2006) was used with a 97% similarity cutoff. Sequences were aligned using Muscle v 5.1 (Edgar, 2004). The alignment was visually inspected and remaining redundant, short, or poorly aligned sequences were removed. Additionally, hits from eukaryotic taxa that were on short contigs without any bona fide eukaryotic genes were removed from the alignment. The N-terminal signal peptide was manually trimmed and sequences were realigned with Muscle. This alignment was then trimmed using the ClipKIT smartgap algorithm (Steenwyk et al., 2020). Following quality control, there were 254 sites and 134 sequences, 17 of which were of prokaryotic origin. The best tree inference model was selected using IQTree (Nguyen et al., 2015) as implemented on the CIPRES server. Maximum likelihood gene trees were constructed using RAxML (Stamatakis, 2014) using the JTT+gamma model as implemented on the CIPRES server (Miller et al., 2010). One representative sequence of each bacterial taxon was selected as the outgroup in each tree estimation to determine whether outgroup choice affected topology. All bacterial sequences tested as outgroup resulted in similar topologies with equal log likelihoods. Nodes with <50% bootstrap support were collapsed using the di2multi package form ape v 5.6.2 (Paradis and Schliep, 2019). Phylogenies were visualized using the ggtree package (Yu et al., 2017).

10.3. Sample Collection for Quantitative RT-PCR

Parasitized (see part III. 2.), sterile and septic injured (see part III. 4.) and naive third stage whole larvae were used to test expression of *D. ananassae hemolysin E*-like genes. For tissue expression analysis fat body, hemolymph and rest of body samples were collected from parasitoid infected third stadium larvae directly into the lysis buffer of the RNeasy mini kit (Qiagen).

10.4. Quantitative RT-PCR

RNA samples were prepared with RNeasy mini kit (Qiagen) according to the manufacturer's instructions. One µg of RNA was used to synthetize 25 µl cDNA with the RevertAid First Strand cDNA Synthesis Kit (Thermo Scientific) and Oligo(dT)18 Primer. For the Quantitative RT-PCR reaction, 2 µl of 10 times diluted cDNA was used with PerfeCTa SYBER Green SuperMix (Quanta bio) in a Rotor-Gene Q (Qiagen) qPCR platform. Primers were designed with NCBI Primer-BLAST to ensure specific binding to the individual *hl* genes and are listed in Suppl. Table S1. Reaction conditions were the following: 95°C 2 min, 45 cycles at 95°C for 10 sec, 57°C for 45 sec and 72°C for 15 sec. Two biological replicates were used, with two or three technical replicates in each qRT-PCR

reaction. For data analysis the Rotor-Gene Q Series Software was used. To interpret gene expression levels, the ΔΔCt method was used. The obtained cycle threshold (ct) values were normalized to those of the housekeeping GF23239 gene (LOC6505882). One-way ANOVA and Tukey's HSD tests were used for further statistical analysis between samples.

10.5. DNA Constructs for Recombinant Protein Expression

Coding DNA sequences (CDS) of *D. ananassae* Hemolysin-like 6 (HL6) (Dana\GF22667) and Hemolysin-like 16 (excluding the predicted N-terminal signal peptide) (Dana\GF21479) proteins were PCR amplified using gene-specific oligonucleotide primers listed in Suppl. Table S1. Bacterial Hemolysin E /Cytolysin A (ClyA) (Q68S90_ECOLX) encoding sequence was PCR-amplified from genomic DNA of the wild type *Escherichia coli* (SzMC 0582) (Szeged Microbial Collection, University of Szeged, Hungary) using gene-specific oligonucleotide primers listed in Suppl. Table S1. PCR products were digested with restriction enzymes (hl6: EcoRI-SalI; hl16: BamHI-HindIII; clyA: BamHI-HindIII) and cloned into the pETDuet-1 (#71146-3, Merck Millipore, Burlington, MA, USA) plasmid for bacterial expression.

For the expression of C-terminally 3×Flag-tagged HL6, HL16 (including the predicted N-terminal signal peptide) or ClyA proteins in D.Mel-2 insect cells, the CDSs were PCR amplified using gene-specific oligonucleotide primers listed in Suppl. Table S1. The PCR products were inserted into the pDONR221 Gateway entry vector (#12536017, Thermo Fisher Scientific, Waltham, MA, USA) by BP reaction and subsequently cloned into the pMT-CoHygro-DEST-3×Flag destination expression plasmid (made in house, see the map and sequence in Suppl. Fig S1). This plasmid provides a copper-inducible promoter (pMT) and a C-terminal 3×FLAG tag. All constructs were validated by DNA sequencing.

10.6. Recombinant Protein Expression and Purification

Recombinant HL6, HL16, and ClyA proteins were expressed in SixPack *E. coli* strain (Lipinszki et al., 2018) as follows: cells were cultured in 500 ml standard Luria-Bertani broth supplemented with 100 μg/mL Carbenicillin. Protein expression was induced when the cell density reached 0.6 at OD 600nm, using 0.5 mM IPTG for 20 hours at 16 °C. Proteins were refolded and purified from inclusion bodies using a single freezing-thawing method (Qi et al., 2015). In brief, cells were harvested and lysed by sonication in phosphate-buffered saline (pH=8.0) followed by high-speed centrifugation at 4 C, 30 min, 21,000 xg. Inclusion bodies were completely resuspended (washing) in 20 ml buffer containing 20 mM Tris (pH 8.0), 300 mM NaCl, 1 mM EDTA, 1% Triton X-100, and 1M urea, and centrifuged at 4 C, 20

min, 12,000 xg. Washing was repeated twice. Finally, inclusion bodies were resuspended in PBS supplemented with 2M urea and stored at -20 C for 24h. The frozen samples were thawed slowly at room temperature and centrifuged at 4 C, 20 min, 12,000 xg. Supernatants containing the resolubilized recombinant proteins were collected and dialyzed over PBS supplemented with 0.65M urea at 4 C for 24h, followed by a second dialysis in PBS at 4 C for 16h. After centrifugation at 4 C, 10 min, 5,000 xg, supernatants were collected, filter-sterilized and proteins were concentrated using an Amicon Ultra centrifugal device with 10 kDa MWCO (# UFC9010, Merck Millipore, Burlington, MA, USA) at 4 C, 60 min, 4,000 xg. Proteins were collected, flash-frozen in liquid nitrogen and stored at -80 C before use for immunization. Concentration and integrity were assessed by SDS-PAGE analysis.

3×Flag-tagged HL6, HL16 and ClyA proteins were expressed in stably transfected Schneider's Drosophila Line 2 (D. Mel-2, ATCC CRL-1963, Manassas, VA, USA) cell lines. Cells were maintained in Insectagro DS2 Serum-Free medium (#13-402-CV, Corning, Corning, NY, USA) supplemented with 2 mM stable L-glutamine (#XC-T1755, Biosera, Nuaille, France) and 1× PenStrep (#XC-A4122, Biosera, Nuaille, France) at 25 °C. Cells were transfected with the appropriate plasmid DNA using ExpiFectamine Sf transfection reagent (#A38915, Thermo Fisher Scientific, Waltham, MA, USA) according to the manufacturer, and selected in the presence of 300 µg/mL hygromycin B (#25965.03, Serva, Heidelberg, Germany). Stably transfected cell lines were grown in T175 tissue culture flasks and the expression of Flag-tagged HL6, HL16 or ClyA were induced by CuSO4 treatment (0.5 mM final concentration) for 24 h before harvesting. Cells were lysed in EB buffer containing 50 mM HEPES pH 7.6, 150 mM NaCl, 0.5 mM EGTA, 2 mM MgCl2, 0.1% NP40, 5% glycerol, 0.5 mM DTT, 1 mM PMSF, 1× EDTA-free protease inhibitor cocktail (#11873580001, Roche, Basel, Switzerland), 0.1 µL/mL benzonase nuclease (#70746-3, Merck Millipore, Burlington, MA, USA) using Ultra-Turrax T8 homogenizer (IKA-Werke, Staufen im Breisgau, Germany). Cell lysates were clarified by centrifugation (4 C, 20 min, 12,000 xg) and supernatants were subjected to immunoprecipitation using anti-FLAG-M2 magnetic beads (#M8823, Merck Millipore, Burlington, MA, USA) for 2 h at 4 °C. HL16 harbors an endogenous signal peptide, therefore, the cell culture supernatant containing the secreted protein was also collected and used for protein purification. After binding, matrices were washed with EB, followed by extensive washing with Tris-buffered saline (TBS: 10 mM Tris-HCl pH8.0, 150 mM NaCl). Bound proteins were eluted in TBS supplemented with 150 ng/µL 3×Flag peptide (#F4799, Sigma Aldrich, St. Louis, MO, USA). Eluted proteins were concentrated and tested by SDS-PAGE, flash-frozen and stored at - 80 °C before use.

Protein expression was done by Zoltán Lipinszki and Edit Ábrahám at the MTA SZBK Lendület Laboratory of Cell Cycle Regulation, Institute of Biochemistry, HUN-REN Biological Research Centre, Szeged.

10.7. Generation of Antibodies Specific for HL6 and HL16 Proteins

BALB/C mice were injected subcutaneously with 1 μg purified recombinant HL6 or HL16 proteins produced in *E. coli*, in Complete Freund Adjuvant (DIFCO). Immunization was repeated twice at three-week intervals. Antisera were prepared and screening was done by standard enzyme-linked immunosorbent assay (ELISA). Plates (Corning) were coated with 100 ng/ml recombinant proteins. Sheep anti-Mouse immunoglobulin G (IgG), Horseradish peroxidase-linked whole antibody (GE Healthcare, UK) (1:10,000), and o-Phenylenediamine (Sigma-Aldrich) were used for detection. The polyclonal sera were further characterized by WB analysis on crude protein extracts of *L. boulardi* infected *D. ananassae* samples. Antibodies were used for indirect immunfluorescence assay (as described in part III.5.), on blood, fat body, and isolated parasitoid larvae samples. It was also used for Western blot analysis. As control normal mouse serum was used.

10.8. Western Blot Analysis

Crude protein extracts were prepared in sample buffer (250 mM Tris pH = 6.8, 35% glycerol, 0.75 mg/mL Bromophenol blue, 9.2% SDS, 5mM 2-Mercaptoethanol), using a homogenizer, and then centrifuged at 18,000 x g for 5 min. Protein concentrations were determined by Amido Black assay. One hundred μg protein was loaded per line and run on 12% SDS PAGE, blotted to polyvinylidene difluoride (PVDF) membrane (Millipore), blocked with 5% non-fat milk in Tris-buffered saline (TBS) (10 mM Tris pH 7.5, 150 mM NaCl), and incubated with primary antibodies (polyclonal serum in the following dilutions: 1:10000 for aHL6 and 1:6000 for aHL16) for 1 h. Membranes were washed three times (10 min each) with TBS containing 0.1% Tween 20, incubated with Polyclonal Goat Anti-Mouse Immunoglobulins/horseradish peroxidase (HRP) (Dako) (1:10,000 diluted in TBS containing 0.1% Tween 20 and 1% bovine serum albumin (BSA)), and washed three times. Reactions were visualized with Immobilon Western Chemiluminescent HRP Substrate (Merck).

10.9. Toxicity Assay of HL Proteins

The U937 pro-monocytic cell line was used in toxicity tests. One hundred microliter of $5x10^4$ U937 cells were plated and 3 μg/ml purified HL6, HL16 and ClyA recombinant

proteins were added to the cells. LDH Cytotoxicity Assay Kit (ab65393) was used according to the manufacturer's instructions for the fast and sensitive detection of LDH released from damaged cells. Toxicity was measured after 2, 4, 6 and 24h with a colorimetric microplate reader.

11. Wound Healing Assay in *Z. indianus*

Early third instar naive or *L. victoriae* infected *Z. indianus* larvae were wounded with a sterile 100 μm diameter minutien pin on the dorsal part of the 5th segment. Following 2 h incubation time, cuticle samples were prepared, fixed with 2% paraformaldehyde for 10 min, and blocked with 0.1% BSA in PBS supplemented with 0.01% Triton X-100. Then indirect immunofluorescence followed with 4G7 as primary antibody.

12. Video Microscopy of *Z. indianus* Blood Cells

Two larvae were dissected in 100 μL CSM, 72 h after *L. victoriae* wasp infection. Photographs of the live hemocytes were taken with a Nikon D5300 DSLR camera through an Alpha XDS-1T inverse microscope at room temperature. Shooting duration was 120 min with 9 sec intervals (Suppl. Movie). The images were cropped, and the movie was produced with FIJI.

IV. Results

1. Species Differentiating MGHs Are Highly Resistant to Parasitoids

We compared the fly and wasp emergence rates following parasitization of *D. melanogaster*, D. *ananassae* and *Z. indianus* with two generalist wasp species, *L. heterotoma* and *L. victoriae*. The eclosion of both parasitoid wasp species was significantly lower in *D. ananassae* and *Z. indianus*, species differentiating MGHs, as compared to *D. melanogaster* (**Fig. 16.**). Fly survival rates were generally higher in the MGH differentiating species. Therefore both *D. ananassae* and *Z. indianus* show higher parasitoid resistance than *D. melanogaster*. There was no significant difference between the different species in naive fly emergence (over 70%).

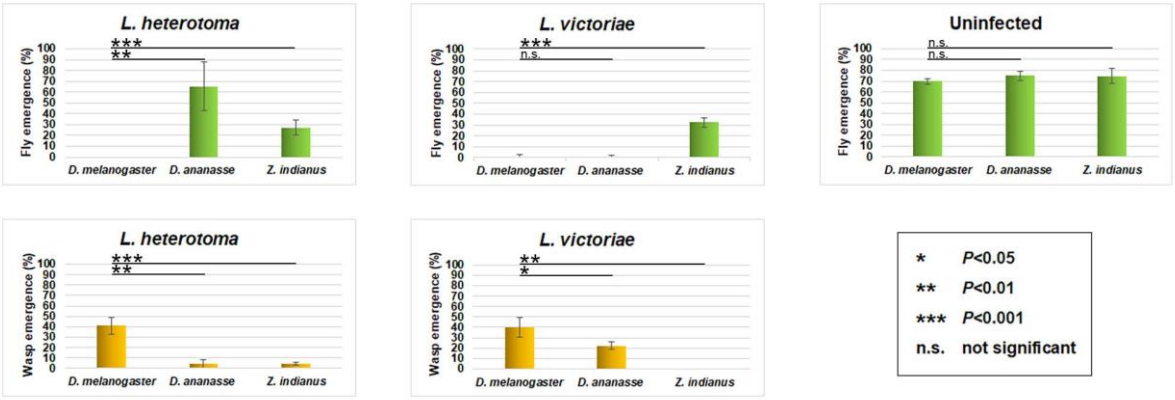

Figure 16. Eclosion success of drosophilid species after parasitoid wasp infection. *D. ananassae*, *Z. indianus*, and *D.melanogaster* larvae were infected with *L.heterotoma* and *L. victoriae* parasitoid wasps. The data of four independent experiments were cropped, with 50 larvae in each. The error bars indicate the standard deviation**.**

2. Parasitoid Wasp Infection Is Required for Normal MGH Development

We have investigated factors that could potentially induce MGHs differentiation in *D. ananassae*, besides parasitoid infection. In *D. melanogaster* the introduction of a foreign object into the larvae, or even the wounding of the cuticle is sufficient trigger for lamellocyte differentiation (Meister, 2004). The assay included naive, sterile wounded and *L. boulardi* parasitoid infected *D. melanogaster* (OregonR) and *D. ananassae* larvae. Because only a fraction of the sterile wounded *D. ananassae* differentiated MGHs, which were relatively small, in this species we injected FluoSphere beads into the larvae, to test whether non-phagocytosable, large foreign objects could trigger MGH differentiation. To analyse the encapsulating blood cells individual larvae were dissected, hemocytes were isolated and

indirect immunofluorescence assays were carried out using lamellocyte- (Atilla) or MGH-specific (7C5) monoclonal antibodies. The average lamellocyte or MGH number per larva is illustrated (**Fig. 17.a**).

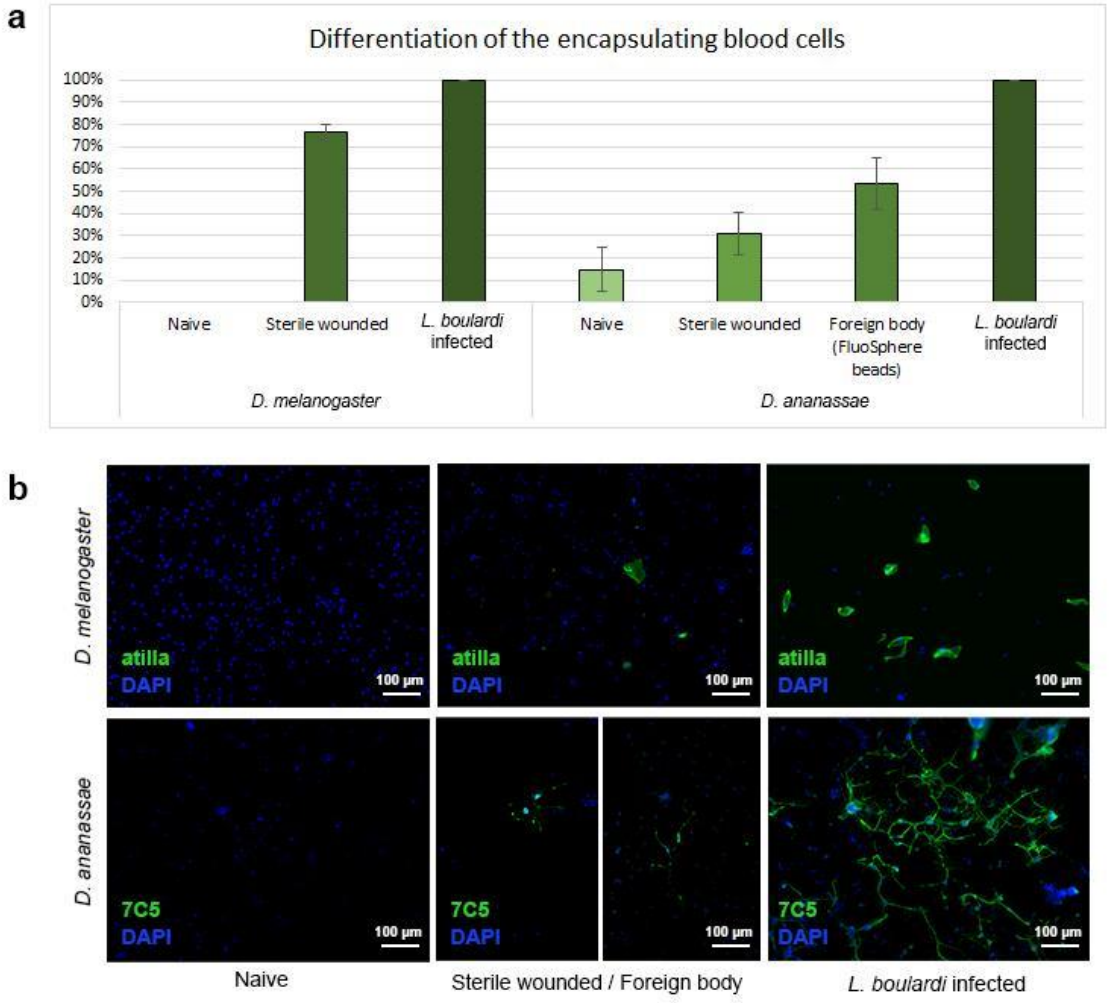

Figure 17. The effect of different factors on the development of encapsulating blood cells. a. Parasitoid wasp infection is required for the appropriate development of MGHs. The average number of encapsulating cells of parasitoid infected animals were considered 100%. The error bars indicate standard deviation. b. Morphology of lamellocytes and MGHs depends on the factors triggering their differentiation.

There were variations between individuals in naive *D. ananassae*. While most samples were totally devoid of MGH-like structures, in a few animals (<10%) the presence of small, nematocyte-like 7C5 positive nucleated structures could be detected. Similar cells were present in both sterile injured and microbead injected individuals (**Fig 17. b**). The nematocyte-like cellular structures, which we supposed to be partially differentiated MGHs, were present in variating numbers. However, their levels were subpar in wounded samples,

and samples injected with foreign body reached only about half the number detected in the parasitized group (**Fig. 17. a**).

Note that while in *D. melanogaster* the sterile wounding resulted in lamellocyte differentiation with a similar degree as in parasitoid-infected individuals (**Fig. 17. a**), these lamellocytes had noticeably different morphology, as they were generally smaller and less flattened in sterile wounded than in parasitized individuals (**Fig. 17. b**).

3. Ultrastructural Characteristics of MGHs

To gain insights in the biological processes that take place in the MGHs, we first investigated their ultrastructure. During MGH development in *D. ananassae*, the cytoplasm becomes gradually saturated with vesicles (**Fig. 18. a**). First, light vesicles appeared, followed by the acquisition of electrondense vesicles. Both types of vesicles were associated with the Golgi apparatus. Dense vesicles were often localized in proximity to microtubules (**Fig. 18. b**), suggesting their possible transport along the microtubules. When electrondense vesicles fuse with each other, they form multiform dense bodies (mdb), which accumulate in the cytoplasm closed to the cellular surface attached to the parasitoid (**Fig. 19.**).

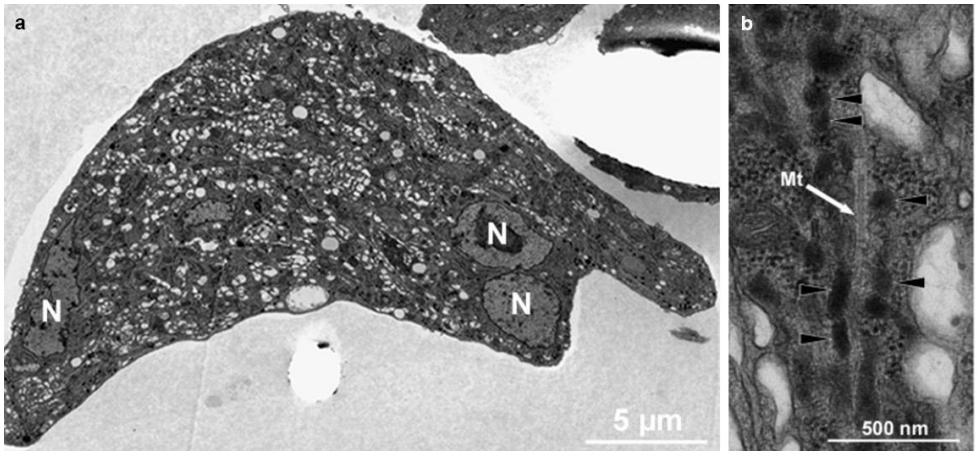

Figure 18. a. MGHs exhibit a large number of light and dense vesicles in their cytoplasm. b. Dense vesicles can often be found aligned with microtubules.

During encapsulation, MGHs demonstrate distinct characteristics. After adhesion to the parasitoid, the ultrastructure of MGHs becomes polarized. The apical region, distant to the parasitoid, contains the nuclei, lipid droplets, and several openings to the hemolymph. At the basal region, proximal to the parasitoid, several cytoplasmic extensions that infiltrated the intersegmental grooves of the parasitoid could be observed. Light vesicles were found to develop into large cysternae filled with a fluffy precipitate, which accumulated under the parasitoid chorion. Furthermore, the basal region contained an abundance of mdbs, which

fused to create a coherent layer (**Fig. 19. a**). This continuous electrondense layer adjacent to the parasitoid surface had varying thickness and lamellar structure (**Fig. 19. b**).

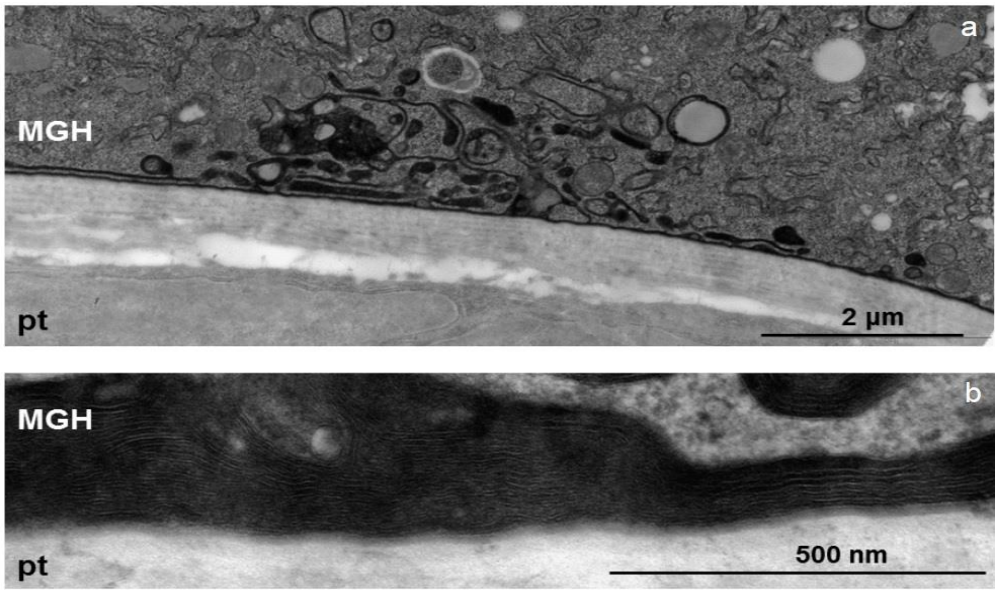

Figure 19. a. Mdbs at the basal region of MGHs. b. The continuous electrondense layer formed on the surface of the parasitoid (pt) possessed lamellar ultrastructure.

We observed that MGHs often give rise by budding to microvesicles, which are released to the hemolymph (**Fig. 20. a**). Moreover, the surface of the apical areas of MGHs often generate a loose network of cytoplasmic extensions (microfilaments) where a high number of small vesicles are released, which we termed as giant cell exosomes (GCEs)(**Fig. 20. b**). The GCEs are generated from the cell surface by detachment from the tip of the microfilaments. Multivesicular bodies could also be detected, and their contents were seen to be released into the hemolymph by fusion with the plasma membrane (**Fig. 20. c**).

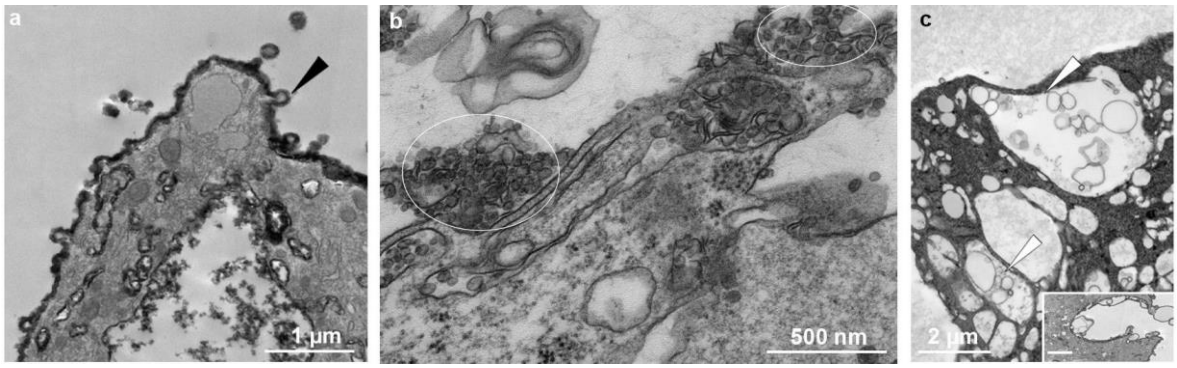

Figure 20. Different vesicular structures released by MGHs into the hemolymph.
Microvesicles (black arrowhead on a) and GCEs (circled on b) are generated from the cell surface with budding. Multivesicular bodies release their content (white arrowheads on c) into the hemolymph (insert).

We could observe a few instances of plasmatocyte internalization within the cytoplasm of MGHs (**Fig. 21.**). During this phenomenon, both cells remain viable and intact. This event slightly differs from mammalian emperipolesis, as it elicits areas with no membrane and with the direct contact of the two cytoplasms.

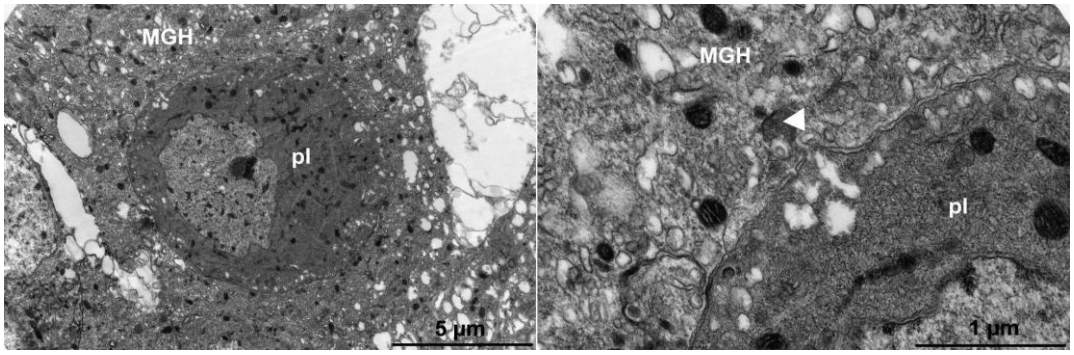

Figure 21. Electron micrograph depicting a plasmatocyte inside the cytoplasm of a MGH

3.1. The Acidic Vesicles of MGHs Participate in the Encapsulation Process

To further characterize the vesicles of MGHs, we used LysoTracker Red dye, which labels acidic organelles. The blood cell staining showed that both MGHs and plasmatocytes carry acidic compartments. However, the LysoTracker staining faded quicker (in 1-2 minutes) from MGHs, suggesting lower dye retention (**Fig. 22.**). The signal in plasmatocytes represents the lysosomes and phagolysosomes associated with their phagocytic nature. As MGHs are not involved in phagocytosis, the role of acidic organelles in these cells were not clear.

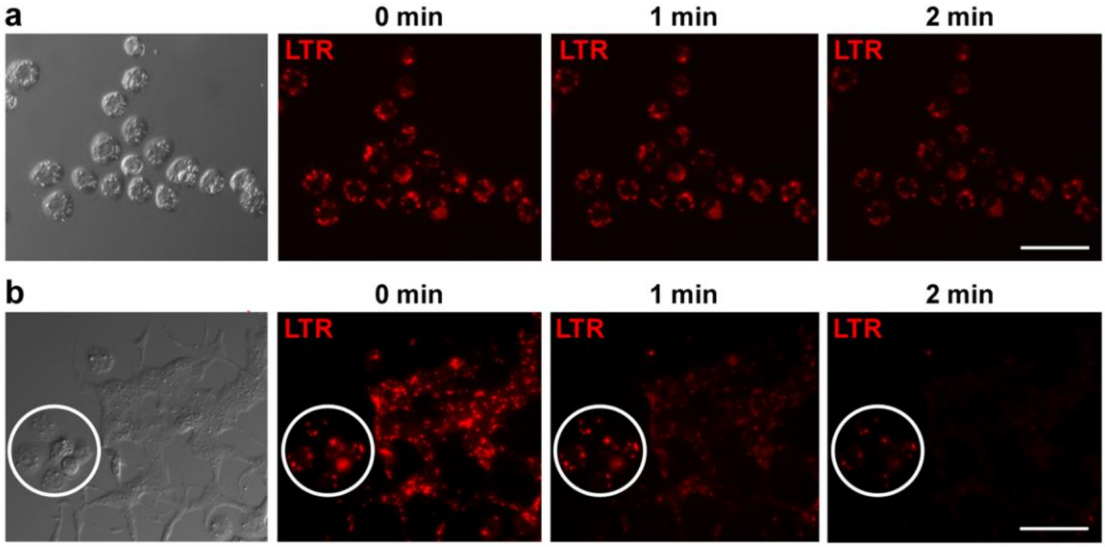

Figure 22. Time lapse analysis of LysoTracker Red dye fading from the acidic vesicles of plasmatocytes (a and circled in b) and MGHs (b)

To assess the role of the acidic vesicles of MGHs in the encapsulation reaction, we isolated *L. boulardi* larvae from *D. ananassae,* and stained them with LysoTracker Red. We observed that in the capsule, these acidic vesicles aggregated at the region close to the parasitoid surface, and they formed a continuous acidic layer on the surface of the wasp (**Fig. 23.**), similarly to the mdbs seen in the TEM images. LysoTracker positive structures were also visible densely scattered all over the capsule. Arrangement of the acidic vesicles highly resemble that of the mdbs seen in the TEM images (**Fig. 19.**), suggesting that mdbs and acidic organelles are overlapping structures.

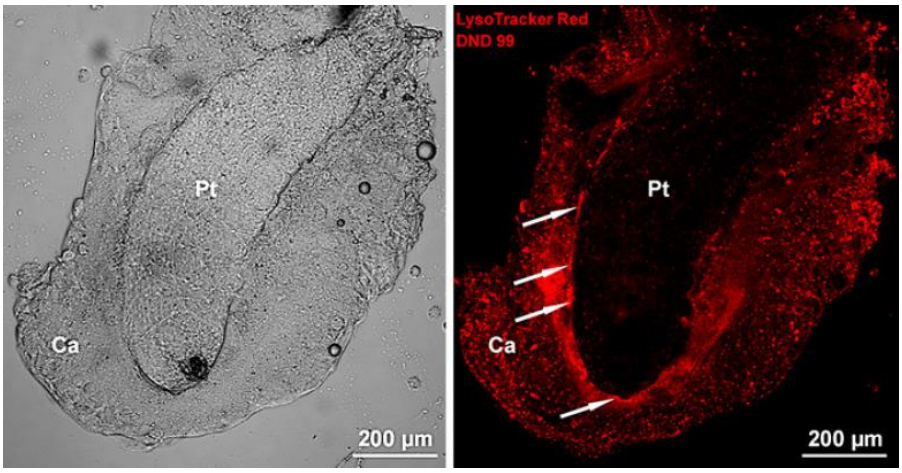

Figure 23. Acidic structures in the MGHs forming the capsule (Ca) around the parasitoid (Pt). A LysoTracker positive, acidic layer (white arrows) is formed along the attachment site with the parasitoid. Images were immediately visualized with an Olympus FV1000 confocal LSM microscope.

4. Transcriptome Analysis of *D. ananassae* Blood Cells

To gain insights into the transcriptional processes of *D. ananassae* blood cells, and elucidate the molecular background settled behind the features and function of the MGHs, we have performed a single-cell-based transcription assay of MGHs and activated plasmatocytes, complemented with uninduced blood cell pool samples. In total, the transcripts of 9,106 genes were detected. After normalization, the differentially expressed genes (DEGs) were determined (**Suppl. Table S2-S4.**) (**Fig. 24.**).

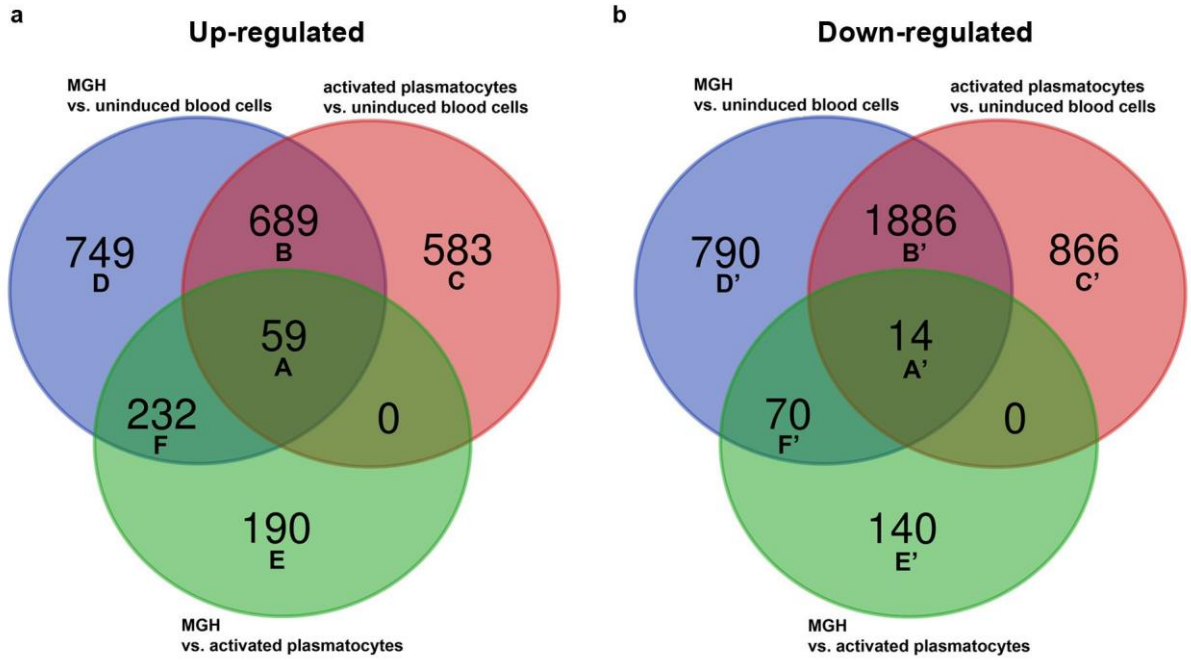

Figure 24. Venn diagram presents cross-comparison of the up- (a) and downregulated (b) DEGs between the three samples

Between MGHs and plasmatocytes there were 705 DEGs in total, with 481 expressed at a significantly higher, and 224 at a significantly lower level in MGHs (**Suppl. Table S2**). These included 200 genes exclusively expressed in MGHs, and 8 exclusively expressed in plasmatocytes. Between MGHs and uninduced blood cells the DEG number was higher with a total of 4,489, of which 1,729 were significantly higher and 2,760 significantly lower expressed in MGHs compared to uninduced blood cells (**Suppl. Table S3**). Among these, 24 genes exhibited exclusive expression in MGHs, and 1,495 genes were exclusively expressed in uninduced blood cells. DEGs between MGHs and plasmatocytes reveal the structural and functional differences between these hemocyte types, while DEGs between MGHs and uninduced blood cells hint at immune response mechanisms against parasitoids.

The 748 genes (A+B set) upregulated in either MGHs or activated plasmatocytes compared to uninduced blood cells (**Fig. 24.**) are the genes commonly activated by parasitoid infection. Out of these, 59 genes (set A) were further enriched in MGHs compared to plasmatocytes, suggesting differences in the function of these genes depending on the type of the hemocyte. Furthermore, sets D and C represent the transcriptomic responses to infection characteristic of each cell type. The genes expressed significantly higher in MGHs compared to either plasmatocytes or uninduced blood cells likely create the unique transcriptomic makeup of MGHs. Similarly, the downregulation of genes can also contribute to the immune responses mediated by MGHs and plasmatocytes. Several genes were

downregulated in both hemocyte types compared to uninduced blood cells, suggesting that in response to parasitoid infection, gene products which are not involved in parasitoid elimination, but in other baseline functions are tuned down as a trade-off.

4.1. Genes Significantly Upregulated in MGHs

The DEGs were further analysed in silico, however, because of the lack of data on *D. ananassae* genes and protein functions, information regarding their *D. melanogaster* orthologs were used. Gene Ontology (GO) enrichment analysis was carried out to assess gene functions. In the "cellular component" category, there was an enrichment in membrane, vesicle, vacuole, lysosome, SNARE complex localised gene products in MGHs, while a relative decrease in almost every other cell organelle was detected, when compared to gene products of activated plasmatocytes (**Suppl. Fig S2.**). The "biological process" category genes enriched in MGHs were related to signaling, membrane docking, vesicle-mediated transport, membrane and vesicle fusion and exocytosis, hinting to the specialised role of these cells in which vesicles are key factors. Functions related to metabolic processes, biosynthesis and regulation of reactive oxygen species were downregulated in MGHs, compared to activated plasmatocytes (**Suppl. Fig S3.**), suggesting that MGHs have minimalised their metabolic processes.

The GO analysis between the DEGs of MGHs and uninduced blood cells resulted in a similar outcome. In the "cellular component" category gene products enriched in MGHs localize to membranes, vesicles, lysosomes, endosomes, autophagosomes, multivesicular bodies, SNARE complexes, vacuolar-type ATPase complexes, endosomal sorting complex required for transport, cytoskeleton, Golgi apparatus, mitochondrion and extracellular space (**Suppl. Fig S4**). The gene products enriched in MGHs compared to uninduced blood cells belonged to the following "biological processes": vesicular and endosomal processes, cellular secretion, exocytosis, endocytosis, microtubule-based transport, ATP synthesis, cell-cell communication, and autophagy (**Suppl. Fig S5**). Uninduced blood cells expressed more gene products related to basic cellular processes, such as carbohydrate-, lipid-, and protein-metabolism, catabolism, and various developmental processes.

The genes overexpressed in MGHs compared to either activated plasmatocytes or uninduced blood cells categorized based on the structures and processes seen in the electron microscopic analysis are listed in **Table 1**.

Table 1. Predicted function of the *D. ananassae* gene products overexpressed in MGHs. *D. melanogaster* orthologs are listed.

Vesicle-related
14-3-3zeta, Ack, alc, alphaSnap, AnxB9, AP-2mu, AP-2sigma, Appl, Arf102F, Arf51F, Arf79F, Arl1, Arl2, Arl4, Arl5, Arl8, Atet, Atg6, ATP6AP2, awd, bchs, Bet1, Bet3, Bet5, BicD, Blos1, boca, BORCS5, CanB2, car, CASK, Ccz1, Cdc42, CG10103, CG10435, CG13531, CG15012, CG16865, CG18659, CG30423, CG32069, CG32576, CG33635, CG43322, CG4645, CG5021, CG5104, CG5510, CG7956, CG8134, CG8155, CG9067, Chc, Chmp1, CHMP2B, Clc, cni, comm, Dab, DCTN2-p50, Dlc90F, epsilonCOP, Esyt2, Exo70, Exo84, fab1, Flo1, Flo2, fwe, gammaSnap1, Gdi, Gga, gish, Gos28, Gp150, ldlCp, Lerp, lsn, lt, Madm, Membrin, milt, Mon1, Muted, nudE, or, PAPLA1, Past1, Pi3K59F, Pldn, poe, Ppt1, ps, Rab1, Rab11, Rab18, Rab19, Rab2, Rab21, Rab35, Rab39, Rab40, Rab5, Rab7, Rab8, RabX1, RabX6, Rac2, Rap1, Ras64B, Rep, Rho1, Rich, Rint1, Rop, Sec10, Sec15, Sec5, Sec6, shi, shrb, sing, Snap24, Snap29, Snx16, spir, spri, stac, stmA, strat, Syb, Synd, Syngr, Syt1, Syx13, Syx16, Syx17, Syx1A, Syx4, Syx5, Syx7, Syx8, Thor, Tomosyn, Trs20, Trs23, Trs31, Trs33, TSG101, unc-104, Use1, Uvrag, Vamp7, Vap33, Vha16-1, VhaAC45, Vps11, Vps15, Vps16A, Vps2, Vps20, Vps24, Vps25, Vps28, Vps36, Vps37B, Vps39, Vps60, Vta1, Vti1b, WASp, yki, Ykt6, zetaCOP
Lysosome-related
Akap200, Arf79F, Arl8, asrij, Atg8a, ATP6AP2, bchs, Blos1, Blos2, Blos3, Blos4, BORCS5, BORCS6, car, Ccz1, cd, cer, CG10681, CG14184, CG14977, CG32225, CG32590, CG4080, CG4847, CG6707, CG7523, CHMP2B, ClC-b, comm, Cp1, CREG, CtsF, ema, fab1, FIG4, GILT2, Iml1, Lamtor5, Lerp, LManII, lt, Mon1, Muted, Nprl3, Nup44A, or, Pldn, Ppt1, Ppt2, prd1, Psn, Rab2, Rab7, RagA-B, RagC-D, Rilpl, Sap-r, Snx16, stac, Syx16, Syx17, Syx1A, Trpml, Vamp7, Vha13, Vha16-1, Vps11, Vps16A, Vps16B, Vps25, Vps36, Vps60, wash, yki
Lipid metabolism

ABCA, Ack, alpha-Est7, AnxB10, AnxB11, AnxB9, Aps, Arf79F, Arfip, Atg12, Atg7, Atg8a, awd, bchs, beta4GalNAcTB, brn, Cerk, CG11975, CG14883, CG15629, CG17544, CG1941, CG1946, CG31460, CG31683, CG31717, CG31935, CG3246, CG33116, CG33774, CG9743, Dad1, Dgat2, Dgkepsilon, disp, Eato, egh, Esyt2, fab1, FER, fh, firl, ghi, gny, Hex-A, Hsl, iPLA2-VIA, kud, lace, lace, Ldsdh1, LPCAT, Npc2a, ORMDL, Pgi, Pi3K59F, PIG-V, PTPMT1, Rab18, Rac2, Rheb, RhoGAP92B, Sap-r, scramb1, smt3, SNF4Agamma, St1, Start1, subdued, sws, Synd, Syt1, TMS1, Treh, Ubc2, Vha16-1, vib, Vps36, zetaCOP
Cytoskeletal organization, motility
14-3-3epsilon, 14-3-3zeta, Ack, Act42A, Akap200, ALiX, alpha-Cat, aPKC, Arf51F, Arfip, Arl2, Arp1, Arp10, Arp2, Arp3, Arpc1, Arpc2, Arpc3A, Arpc3B, Arpc4, Arpc5, awd, bchs, betaTub56D, BicD, BORCS5, BRWD3, Bsg, Calx, Cam, CASK, CCDC53, Cdc42, Cdk9, Ced-12, CG10984, CG13366, CG15701, CG18190, CG1890, CG31715, CG32264, CG32590, CG43867, CG4537, CG6891, CG7497, CG8134, CG9288, Chc, chic, cib, cindr, cnn, cpa, cpb, Crk, dah, DCTN2-p50, DCTN3-p24, DCTN4-p62, DCTN5-p25, DCTN6-p27, Dhc16F, Diap1, Dlc90F, Dlic, Doa, drk, egh, egl, Ehbp1, FER, flr, form3, FRG1, Ggamma1, gish, GMF, grk, gukh, Hem, HSPC300, insc, jub, Jupiter, Kap3, Klc, Klp64D, lds, mad2, mago, Mer, mgr, milt, Mlc-c, Mob4, moody, msn, mtm, nod, nudE, Nup44A, par-1, parvin, pigs, PIP4K, pnut, pod1, Psn, Pvr, Rab1, Rab11, Rab21, Rab35, Rac2, Rbp, Rcd5, ReepA, rhea, Rho1, RhoGAP18B, RhoGAP71E, RhoGAP92B, RhoGAP93B, RhoGEF2, RhoL, rl, robl, Rtnl1, SCAR, Sep2, shi, spir, sprt, sqh, Ssrp, stai, svr, Synd, tacc, Tes, trio, tsr, tsu, Ubc10, unc-104, Vap33, Vav, vib, Vps16A, Vrp1, wac, wash, WASp
Golgi-related
CG31145, Syx17, sll, pns, BicD, PAPLA1, Syx4, CG9773, IPIP, Trs33, Snap29, cni, Bet1, CG3662, CG5447, Bet5, Vti1b, Gga, Vps29, Arf51F, CG30423, LPCAT, CG11753, Rab8, CG9067, CG32069, Exo84, Trs31, Trs20, CG10344, Cam, Arl2, Rab39, CG15168, CG43322, Lerp, Clc, Gos28, Dab, comm, brn, Tomosyn, CG5934, zetaCOP, Arf102F, CG33116, Fer1HCH, Rab2, Trs23, CG7536, CG16865, ATP6AP2, Ykt6, vib, Nhe1, Sec10, Syx16, Doa, ksh, CG15099, Fer2LCH, Snx1, Zip99C, Rab11, Ccm3, CG5021, COX4, Efr, pod1, Rab1, Sec6, park, Bet3, CG5382, boca, Tango5, Rint1, prd1, Snx3, Rab19, CG5196,

Fur2, Use1, strat, CG14511, wash, CG33635, Tango14, Golgin104, beta4GalNAcTB, Sec15, CG1116, c11.1, Sec5, FucTB, CG32485, Syx5, CG8314, RhoGAP1A, Snap24, ema, CG5510, ldlCp, PHGPx, CG14232, Arl5, asrij, Yip1d1, Arfip, Membrin, Madm, CG4645, Arl1, Chc, Rab18, Rich, GPHR, alphaSnap, epsilonCOP, Arf79F
Exocytosis
Arf102F, Arf51F, Arf79F, Arl1, Arl2, Atet, BicD, car, CCDC53, CG31935, Chc, comm, Dab, disp, Esyt2, Exo70, Exo84, fwe, pck, Rab11, Rab35, Rab7, Rab8, Rap1, Rop, Rrp47, Sec10, Sec15, Sec5, Sec6, shi, shrb, Snap24, Snap29, stac, stmA, Syngr, Syt1, Syx17, Syx1A, Syx5, Thor, Tomosyn, TSG101, Vamp7, Vap33, Vps11, Vps20, Vps24, Vps60, WASp
Adhesion
Fas3, sd, CASK, rhea, NijA, Arpc4, Sema2b, Ggamma1, CCDC53, CG34325, NijB, RhoL, Itgbn, parvin, brn, alpha-Cat, Sap-r, cold, tx, eff, CG17278, Bsg, Arpc1, pyr, Flo2, cindr, Hem, Rap1, FER, wash, trio, shi, Flo1, Psn, muskelin, egh, SCAR
Autophagy
Arl8, Atg12, Atg3, Atg4a, Atg6, Atg7, Atg8a, Atg9, bchs, BI-1, Blos1, Blos2, BRWD3, Buffy, Cam, car, Ccz1, CG11781, CG11975, CG12163, CG32039, CG42554, CG5445, CG5676, CG6878, CG8155, CG8270, Chc, CHMP2B, crq, CycC, Doa, DOR, Dronc, ema, fab1, Fis1, Fkbp39, Iml1, Lerp, lt, MED24, Nprl3, Nup44A, park, Pi3K59F, Rab1, Rab11, Rab19, Rab2, Rab21, RagA-B, RagC-D, Ras85D, Rheb, rl, rpr, Sap-r, Sec61gamma, SH3PX1, shi, shrb, Snap29, SNF4Agamma, Sod1, Syx13, Syx17, Tango5, Trpml, Ubc6, Utx, Uvrag, Vamp7, Vps11, Vps15, Vps16A, Vps25, Vps28, Vps36, Vps39, zda

4.2. Physical Interactions Networks of Gene Products Upregulated in MGHs

Using the information of the Flybase database on the *D. melanogaster* orthologs, we created physical interaction networks of gene products significantly higher expressed in MGHs compared to either activated plasmatocytes or uninduced blood cells. The analysis resulted predicted functional clusters of gene products that may form stable complexes or associate transiently (**Fig. 25-27.**). These networks mirror the structural properties of MGHs,

as they depict clusters related to vesicles, lysosomes, transport along the microtubule, lipid metabolism, autophagy, components of vacuolar ATPase, Golgi apparatus, exocytosis, cytoskeletal organisation and cell adhesion. There is a striking overrepresentation of proteins associated with vesicular organelles, highlighting their importance in the biological functions of MGHs (**Fig. 25.**). Golgi-apparatus and exocytosis related gene products hint at the secretion of regulatory or toxic effector molecules (**Fig. 26.**). Proteins involved in cytoskeletal organization and adhesion proteins outline the molecular mechanisms involved in the impressive motility and encapsulation process of MGHs (**Fig. 27.**).

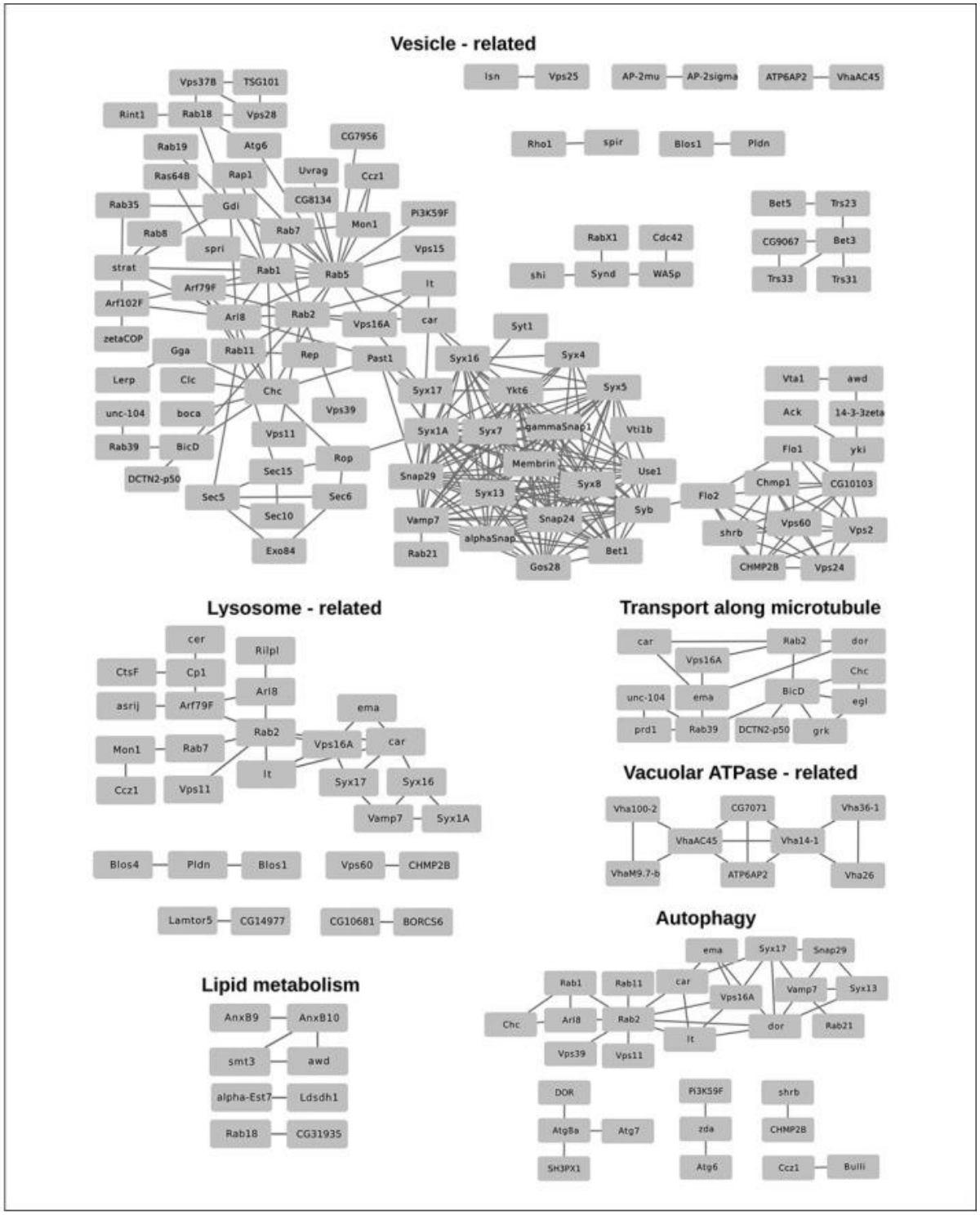

Figure 25. Predicted physical interaction networks of vesicle-, vacuole-, lysosome-, autophagy-, and lipid metabolism-related proteins encoded by genes upregulated in MGHs based on interactions of *D. melanogaster* orthologs. Their *D. ananassae* orthologs are listed in Suppl. Tables S2 and S3.

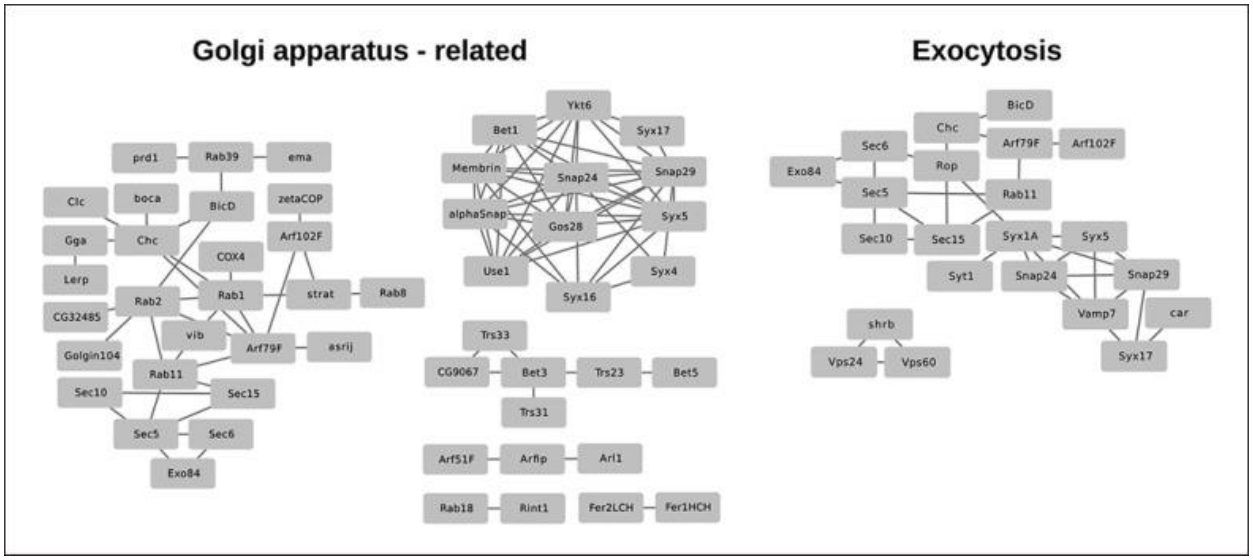

Figure 26. Predicted physical interaction networks of Golgi apparatus and exocytosis-related proteins encoded by genes upregulated in MGHs based on interactions of *D. melanogaster* orthologs. Their *D. ananassae* orthologs are listed in Suppl. Tables S2 and S3.

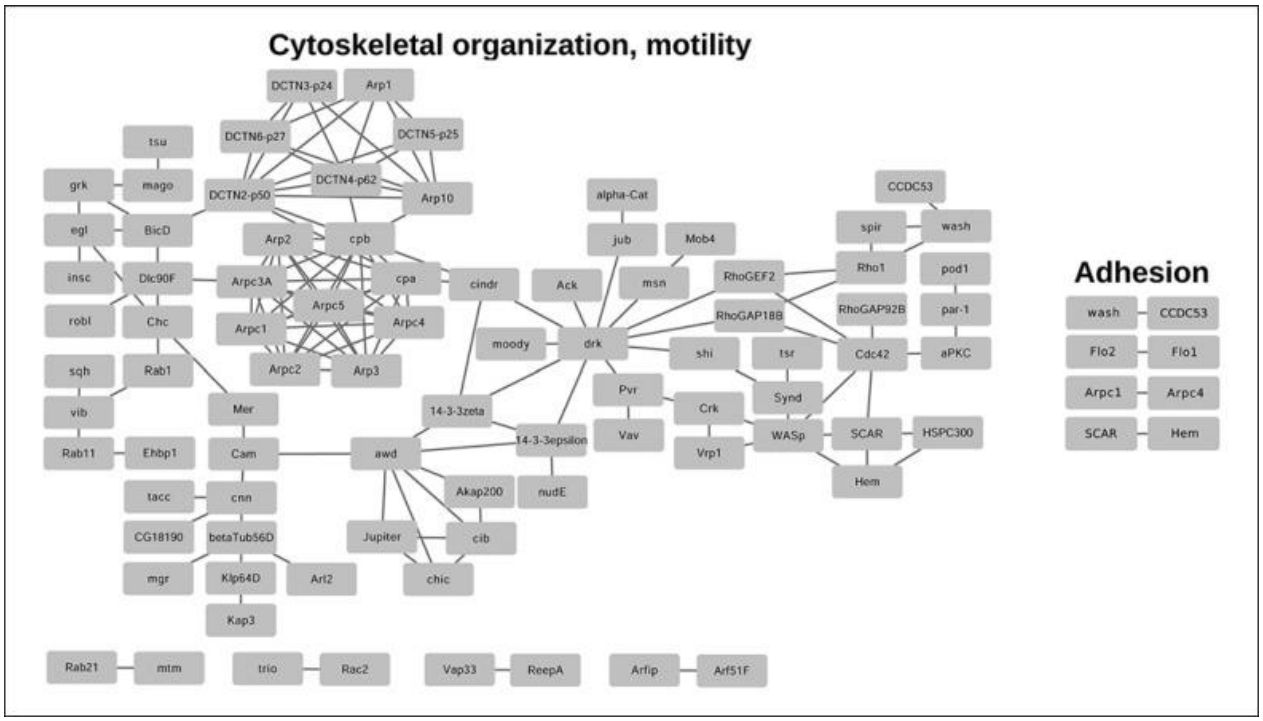

Figure 27. Predicted physical interaction networks of cytoskeleton and adhesion-related proteins encoded by genes upregulated in MGHs based on interactions of *D. melanogaster* orthologs. Their *D. ananassae* orthologs are listed in Suppl. Tables S2 and S3.

4.3. Signaling Pathways Expressed in MGHs

We have also investigated the activity of different signaling pathways in MGHs. We found that the immune pathways Toll, Imd, and JAK/STAT were inactive, as their components were not expressed in MGHs. However, genes encoding orthologs involved in JNK signaling had high expression, including bendless, Pvr, Alg-2, CYLD, cpa, and Cdc42 (Genova et al., 2000; Ishimaru et al., 2004; Tsuda et al., 2006; Xue et al., 2007; Jezowska et al., 2011; Ma et al., 2013; La Marca and Richardson, 2020). Furthermore, neither component of the PPO cascade was expressed in MGHs, confirming that the encapsulation reaction mediated by MGHs is devoid of melanisation.

4.4. Similarities between the Expression Profiles of MGHs and Lamellocytes

We compared the molecular makeup of MGHs to that of the lamellocyte, the encapsulating cell type of *D. melanogaster*. Sixty-one of the lamellocyte-specific genes (Cattenoz et al., 2020; Cho et al., 2020; Fu et al., 2020; Leitão et al., 2020; Tattikota et al., 2020; Wan et al., 2021) were also overexpressed in *D.ananassae* MGHs (**Suppl. Table S5**). The gene products include the glucose-producing Trehalase enzyme and the glucose transporter CG1208, emphasizing the high energy demand associated with immune activation, maturation, and encapsulation in both lamellocytes and MGHs. Several actin-interacting proteins (e.g., Actin 42A, Annexin B9, Jupiter, the filopodia/lamellipodia-associated Twinstar, Parvin, Actin-related protein 3, Pod1, Flare, Rho GTPase-activating protein at 18B, and the Myosin-7a binding protein CG43340) possibly involved in cytoskeletal rearrangements and encapsulation were also shared by the two cell types. Other shared molecules include integrin beta-nu subunit (itgbn), rhea, Rac2, taxi, FER tyrosine kinase, and bves, which are involved in cell-adhesion interactions and formation of cell-cell junctions, and thus they are likely important for parasitoid encapsulation. In addition, the ortholog of the lamellocyte-specific marker, *atilla*, was highly expressed by MGHs.

4.5. MGH-Specific Genes Lacking *D. melanogaster* Orthologs

Besides the evaluation of the similarities between *D. melanogaster* lamellocytes and *D. ananassae* MGHs, we also investigated the differences, which could uncover MGH-specific features. For this, we analysed the genes that lacked a *D. melanogaster* ortholog. Among the DEGs between MGHs and activated plasmatocytes there were 78 such genes (11% of DEGs), out of which 63 were expressed at significantly higher and 15 at significantly lower level in MGHs. Similarly, among the DEGs between MGHs and uninduced blood cells 612 had no *D. melanogaster* ortholog (13.6%), out of which 167 and

445 genes were expressed significantly higher in MGHs and uninduced blood cells, respectively.

Among the genes without *D. melanogaster* ortholog we identified two FREPs (Dana\GF22043 and Dana\GF12573) and a C-type lectin (Dana\GF15691) with MGH-specific expression. They all possess N-terminal signal peptides, thus hinting to their function as PRRs or even opsonins that could potentially recognize parasitoid eggs or larvae.

We have also come across an orphan gene family of 14 genes expressed by MGHs with homologs within several members of the *ananassae* subgroup and some other species of *Drosophilidae*, but absent in *D. melanogaster*. The gene products exhibited domain similarity to the Hemolysin E (also known as Cytolysin A) bacterial toxins, thus pointing to HGT. To assess their role in the immune response, we have further investigated them.

5. Analysis of *D. ananassae hemolysin E-like* Genes and their Encoded Proteins

The *in silico* analysis revealed that an impressive number of *hl* genes are encoded in the *D. ananassae* genome, in total 38 (**Table 2.**). Each of them contains at least one intron. The encoded proteins are 118 to 648 amino acids long. Out of the 38 predicted proteins, 14 possess a signal peptide, suggesting that some of them are either secreted or transmembrane proteins.

Table 2. List of *D. ananassae* hemolysin E-like genes and the predicted proteins. Data acquired from the NCBI database. The oligonucleotide primer sets used in the qRT-PCR did not amplify the specific fragments expected on *D. ananassae* cDNA for the genes highlighted in grey.

Gene	NCBI ID	Gene ID	Intron	Predicted Transcript	Predicted Protein		
					Amino Acid	kDa	Signal Peptide
hl1	Dana\GF19544	LOC6502300	1	1	356	39.14	-
hl2	Dana\GF19543	LOC6502299	1	1	325	36.56	-
hl3	Dana\GF19547	LOC6502303	1	1	318	36.09	-

hl4	Dana\GF19349	LOC6502109	3	1	319	36.28	-
hl5	Dana\GF20302	LOC6503013	2	1	355	39.03	-
hl6	Dana\GF22667	LOC6505322	1	1	370	41.92	-
hl7	Dana\GF19546	LOC6502302	1	1	311	35.52	-
hl8	Dana\GF19347	LOC6502107	1	1	228	25.46	-
hl9	Dana\GF19344	LOC6502104	1	1	327	36.51	-
hl10	Dana\GF19350	LOC6502110	1	1	348	38.46	-
hl11	Dana\GF19548	LOC6502304	1	1	363	39.85	-
hl12	Dana\GF19345	LOC6502105	1	1	351	38.79	-
hl13	LOC26515228	LOC26515228	2	3	295	33.46	-
hl14	Dana\GF27096	LOC26514505	2	1	296	33.61	-
hl15	Dana\GF26568	LOC26513977	1	2	282, 295	32.05, 33.4	-
hl16	Dana\GF21479	LOC6504161	1	1	305	35.03	+
hl17	Dana\GF20376	LOC6503084	1	2	308,398	34.01, 44.55	+
hl18	Dana\GF21478	LOC6504160	1	1	330	36.19	+
hl19	Dana\GF23175	LOC6505821	1	1	350	40.06	+
hl20	Dana\GF20382	LOC6503090	1	3	406	45.95	-

hl21	Dana\GF20379	LOC6503087	1	1	400	44.86	+
hl22	Dana\GF21656	LOC6504328	1	1	435	48.38	+
hl23	Dana\GF23208	LOC6505852	1	1	435	48.36	+
hl24	Dana\GF27432	LOC26514841	1	1	435	48.4	+
hl25	Dana\GF28180	LOC26515589	1	1	435	48.34	+
hl26	Dana\GF20390	EDV44498	5	1	648	75.36	-
hl27	Dana\GF20381	LOC6503089	1	1	286	32.58	+
hl28	Dana\GF19535	LOC6502292	1	1	305	34.92	-
hl29	Dana\GF26619	LOC26514028	1	1	323	36.82	-
hl30	Dana\GF20305	LOC6503016	1	1	368	41.28	+
hl31	Dana\GF26477	LOC26513886	1	1	389	43.25	+
hl32	Dana\GF26440	LOC26513849	1	1	409	46.45	+
hl33	Dana\GF26506	LOC26513915	1	1	419	47.71	+
hl34	LOC116655335	LOC116655335	1	1	398	44.7	+
hl35	LOC26515414	LOC26515414	1	1	297	34.46	-
hl36	LOC6503098	LOC6503098	1	1	589	63.73	-
hl37	LOC116655053	LOC116655053	1	1	325	36.94	-
hl38	LOC116655565	LOC116655565	1	1	118	12.99	-

5.1. Chromosomal Localization of *hl* Genes in *D. ananassae*

We have mapped the *hl* genes to the *D. ananassae* chromosomes (Assembly: ASM1763931v2), and found that with the exception of chromosome 4 and Y, each carry *hl* genes (**Fig. 28.**). Therefore, these genes are not limited to their chromosome of origin where they were transferred, if one HGT event occurred, but already duplicated and scattered across the genome. Most *hl* genes are localized on the left arm of the X chromosome. The *hl* genes that, according to the transcriptome analysis, were expressed in MGHs are *hl 1* to *14*, most of which are also localized on the L arm of the X chromosome.

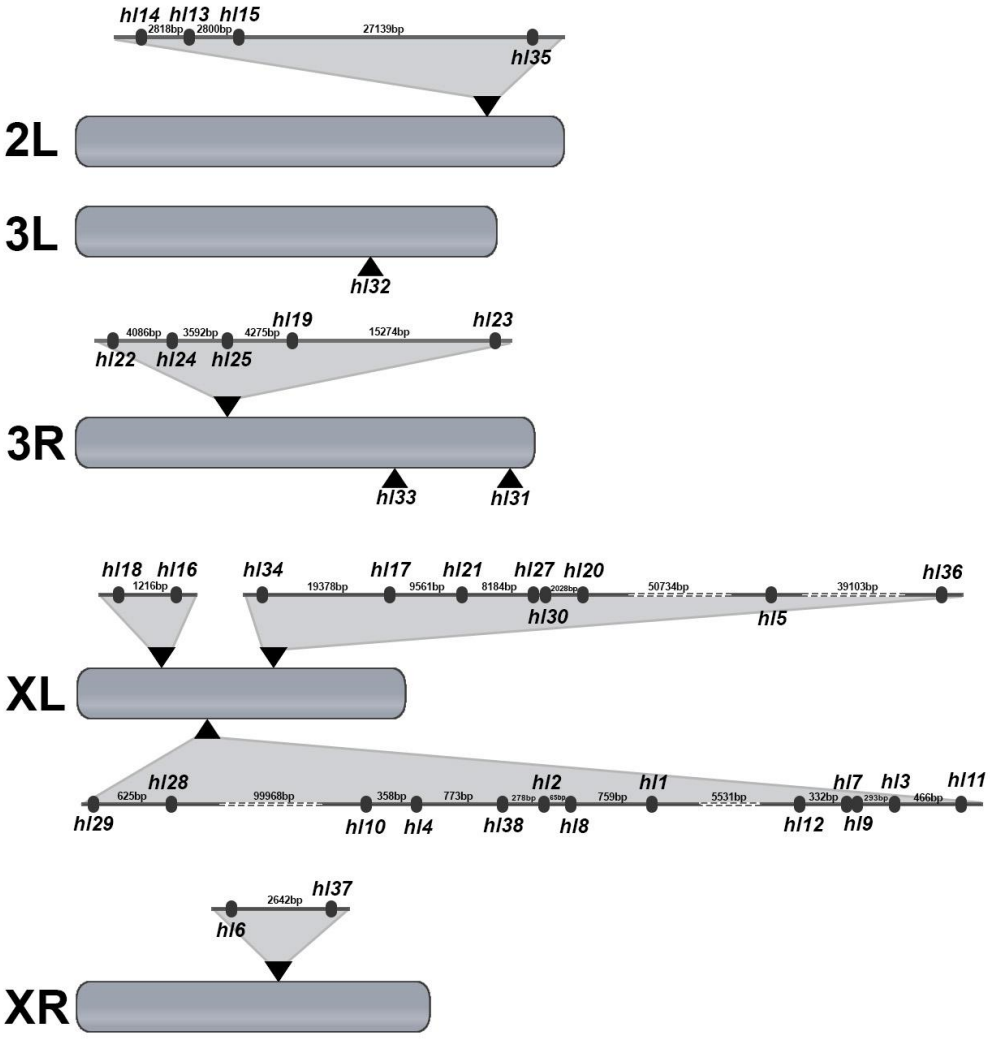

Figure 28. Localisation of the *hl* genes on the chromosomes of *D. ananassae*

5.2. Structural Prediction of *D. ananassae* HL Proteins

Multiple alignment of all *D. ananassae* HL protein sequences did not conclude a consensus sequence as there are no conserved sites, indicating high sequence variation among them (**Suppl. Fig. S6**).

HL amino acid sequences exhibit low sequence similarity to bacterial CytolysinA genes (<40% identity). Therefore, we looked into the AlphaFold predicted three dimensional structures of the *D. ananassae* HL proteins, and observed that the tertiary structure of the insect proteins are highly similar to that of the *E. coli* pore forming toxin, ClyA (**Fig. 29.**).

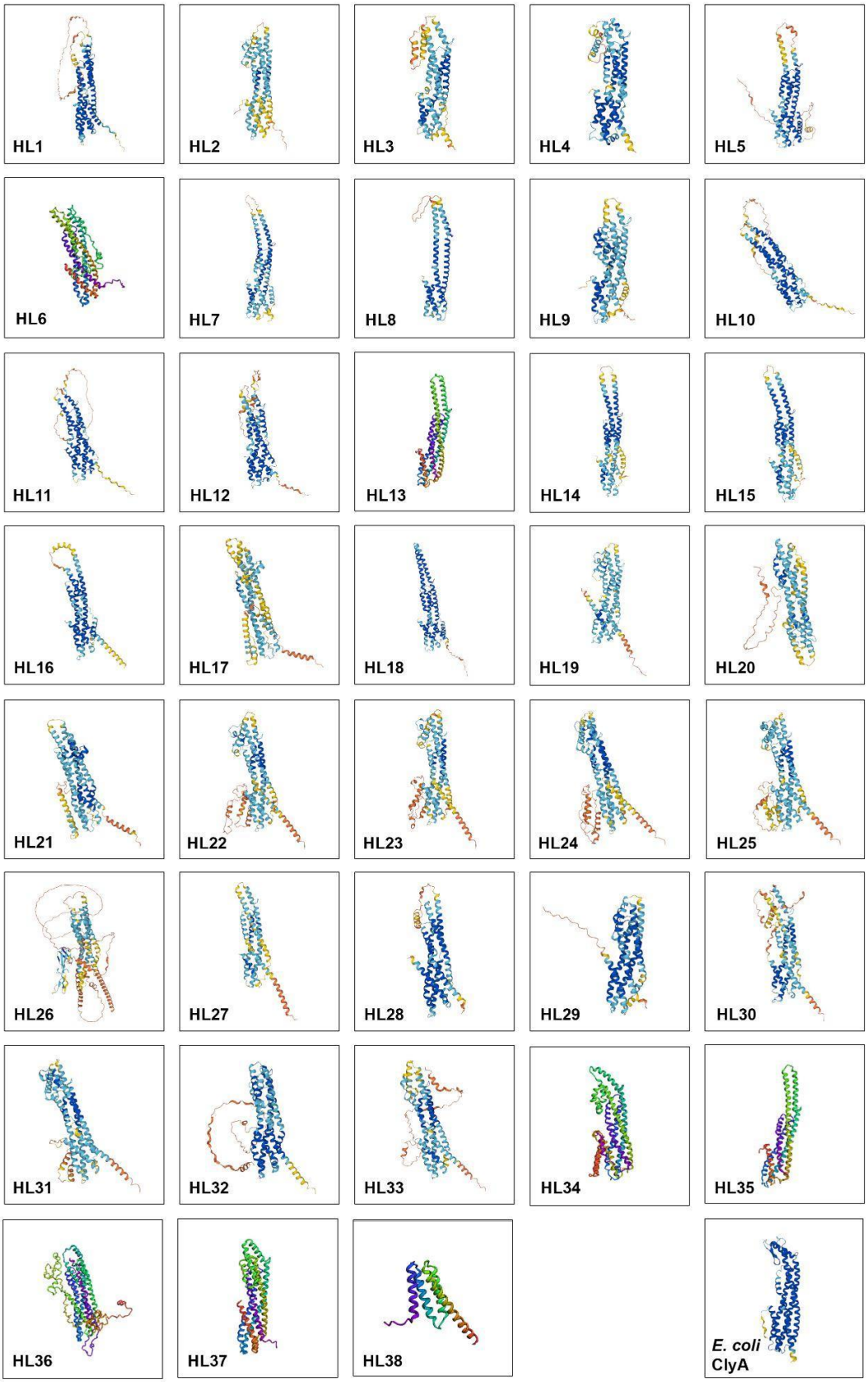

Figure 29. AlphaFold predicted tertiary structures of *D. ananassae* Hemolysin E-like proteins

5.3. Expresson of *D. ananassae hl* Genes Is Induced by Parasitoid Infection

We performed qRT-PCR analysis to assess whether the expression of *hl* genes is induced by parasitoid wasp infection. RNA was isolated from *L. boulardi* infected, and age matched naive larvae. Gene expression profiles of the infected samples were related to those of the naive animals. Some of the *hl* genes possessed high sequence similarity to each other, without unique amino acid sequence sections, thus no discriminative oligonucleotide primer sets could be used, and the expression of these genes could not be monitored individually (*hl13*, *hl14* and *hl22*, *hl24*, *hl25*). Although tested with multiple primer pairs, we could not detect the transcripts of *hl15*, *hl29*, *hl32*, *hl33* and *hl36*, as these genes possibly either had got pseudogenized or are absent from our *D. ananassae* strain. Most of the tested genes, except for *hl4*, *hl8*, *hl28*, *hl35* and *hl38*, significantly increased in parasitoid-infected individuals when compared to the naive samples (**Fig. 30.**), thus confirming that they are induced by parasitoids and must play a role in the immune response against them. The *hl16*, *hl27* and *hl34* genes displayed the highest fold change.

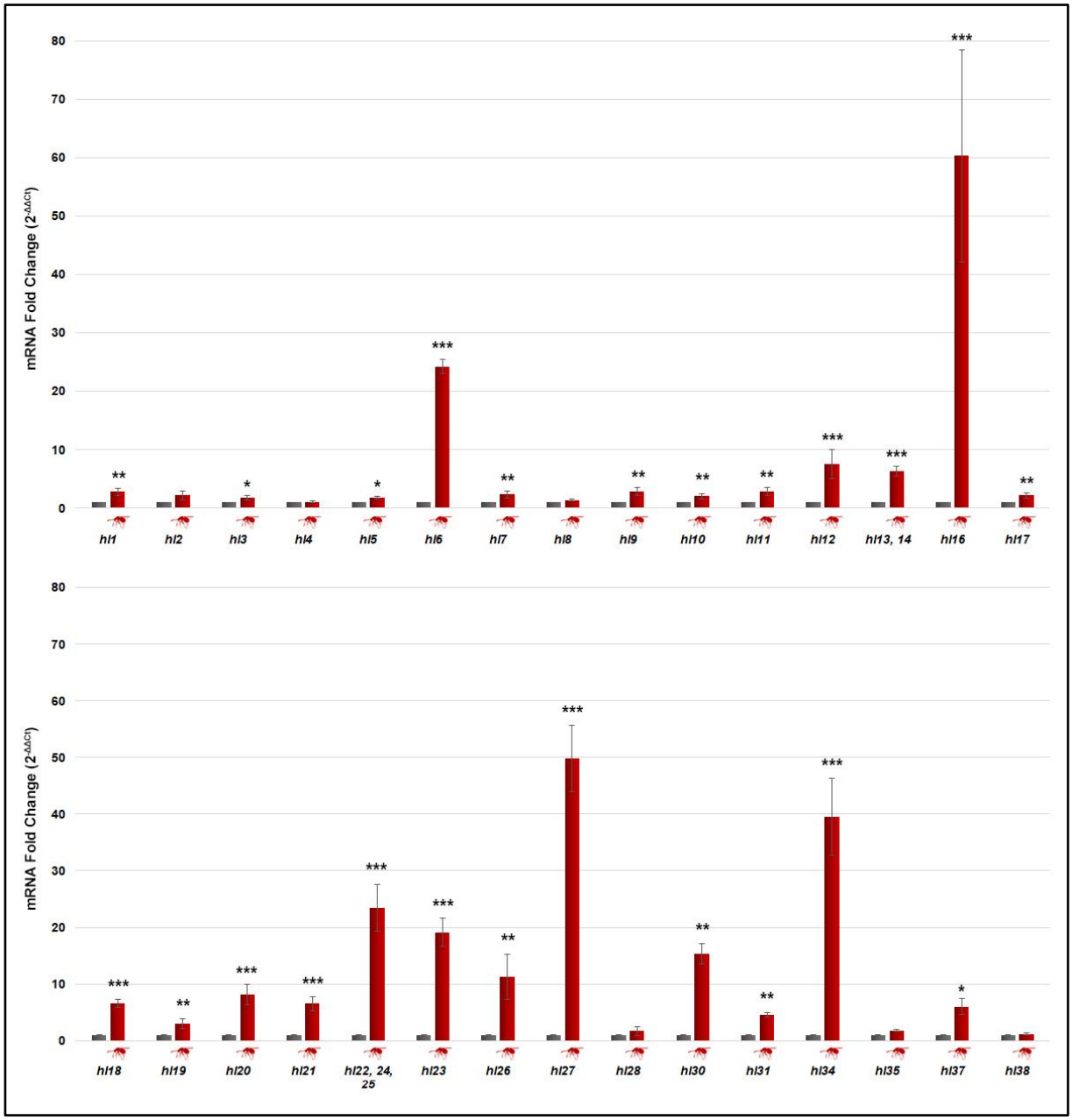

Figure 30. Expression of *hemolysin E*-like genes (*hl*) is induced by *L. boulardi* parasitoid wasp infection in *D. ananassae* larvae. Gene expression profiles of parasitoid-infected samples (red) were compared to that of naive animals (grey). The error bars indicate standard deviation of four data points. Only significant differences are indicated. *=$P \leq 0.05$; **=$P \leq 0.01$; ***=$P \leq 0.001$.

5.4. Tissue Specific Expression of *hemolysin E-like* Genes

We have investigated the expression of the *hl* genes in different tissues of *L. boulardi* infected larvae. Seventy-two hours after infection, blood cells, the fat body and the rest of the body were meticulously separated for RNA isolation. qRT-PCR analysis showed that the majority of the *hemolysin E-like* genes showed high expression in the fat body (*hl1, hl2, hl3, hl7, hl8, hl9, hl10, hl11, hl12, hl13, hl14, hl16, hl17, hl18, hl19, hl20, hl21, hl22, hl23, hl24, hl25, hl26, hl27, hl30, hl31, hl34, hl35, hl38)*, some *hl* genes presented the highest expression in blood cells (*hl5*, *hl6* and *hl37*), while the *hl4* and *hl28* genes presented higher expression in the rest of the organism (**Fig. 31.**).

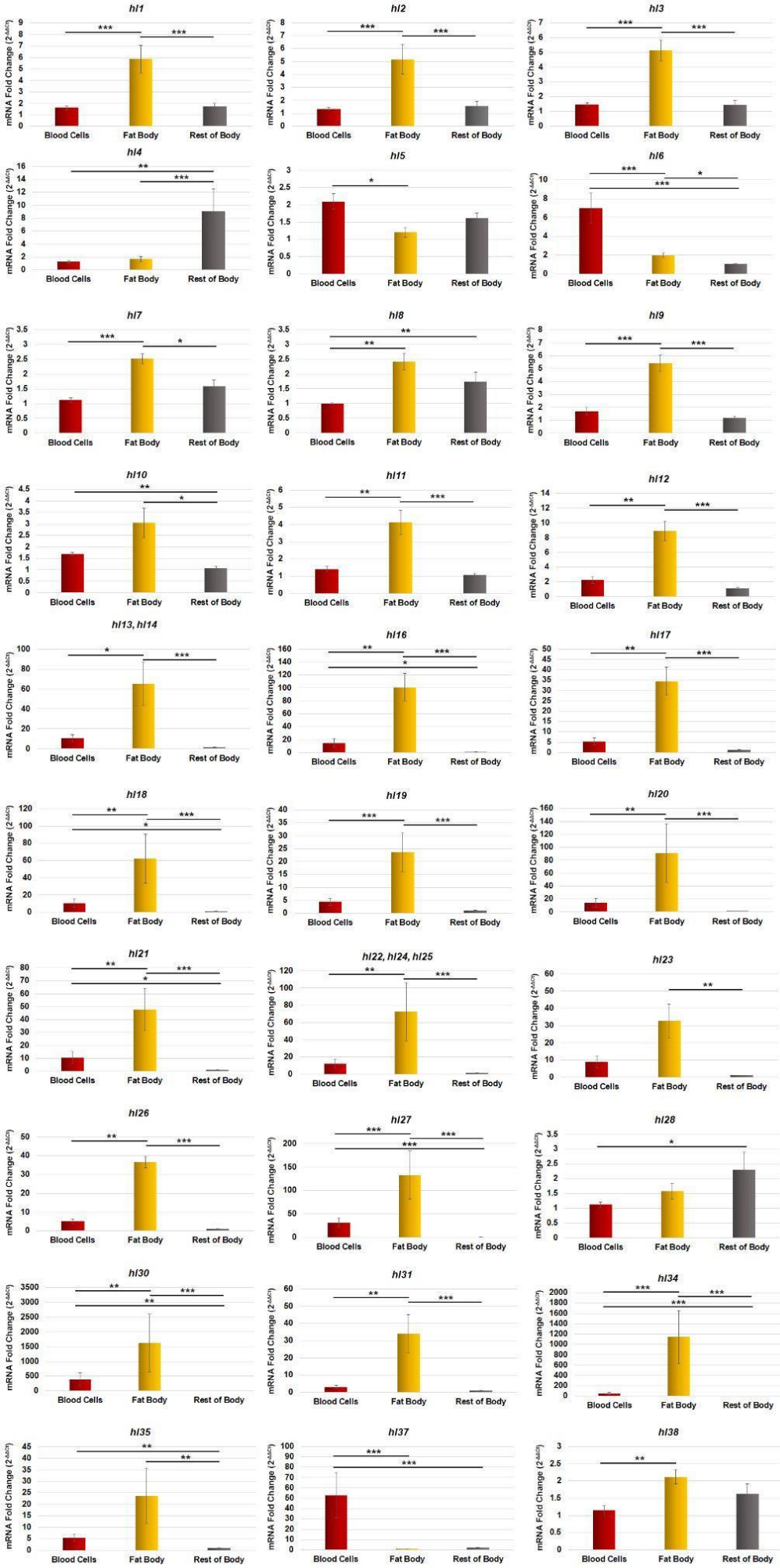
hl1
hl2
hl3
hl4
hl5
hl6
hl7
hl8
hl9
hl10
hl11
hl12
hl13, hl14
hl16
hl17
hl18
hl19
hl20
hl21
hl22, hl24, hl25
hl23
hl26
hl27
hl28
hl30
hl31
hl34
hl35
hl37
hl38
mRNA Fold Change (2-ΔΔCT)
Blood Cells
Fat Body
Rest of Body

Figure 31. Tissue specific expression of *hemolysin E-like* genes. Samples were generated from *L. boulardi* infected larvae 72 h after parasitization. ΔΔCt was calculated by normalizing ΔCt against that of the lowest sample for the respective gene. The fold change of the reference samples=1. The error bars indicate the standard deviation of six independent data points. Only significant differences are indicated. *=$P \leq 0.05$; **=$P \leq 0.01$; ***=$P \leq 0.001$.

5.5. Expression Analysis of the *hl6* and *hl16* Genes and Encoded Proteins

We have chosen two *hl* genes for further investigation: *hl6 (Dana\GF22667)*, which is expressed mostly in blood cells and *hl16 (Dana\GF21479)*, which shows high expression in the fat body. The *hl6* gene has one intron, encodes a 356 amino acid long protein (around 42kDa) that has no signal peptide. The *hl16 gene* also possesses one intron and the encoded protein is 305 amino acids long (about 35 kDa), including its signal peptide.

First, we tested whether other factors than parasitoid wasp infection can induce their expression. For this we pierced the larvae with either sterile minutien pins, pins dipped in a mix of Gram-positive (*Bacillus subtilis*) and Gram-negative (*E. coli*) bacteria or pins dipped in spores of *Beauveria bassiana* entomopathogenic fungus. We found no significant increase in either *hl6* or *hl16* expression following these treatments (**Fig. 32.**). These findings suggest that *hl* genes participate only in the immune response against parasitoid wasps, but not against bacteria or fungi.

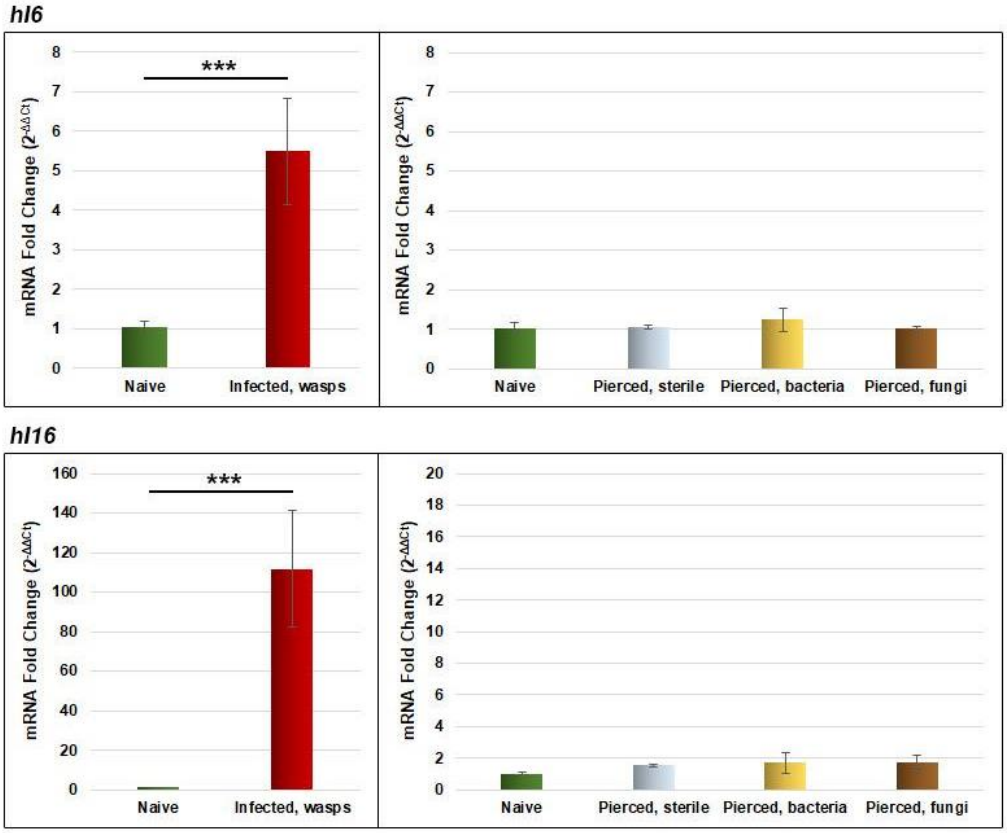

Figure 32. Wasp and injury-specific expression of the *hl6* and *hl16* genes. The error bars indicate the standard deviation of four independent data points. ΔΔCt was calculated by normalizing ΔCt against those of naive samples. Only significant differences are indicated. ***=$P \leq 0.001$.

We have analysed the expression of the two genes across developmental stages from early embryos to 10 days old adults. Second instar larvae (L2) were infected with *L. boulardi* parasitoid wasps and, in parallel, naive samples were also analysed. For both genes, naive animals exhibited expression variation of some degree during development (**Fig. 33.**). Parasitoid infection caused strong induction in the expression profile of both *hl6* and *hl16*, persisting up till the adult stage. To analyze protein expression patterns of HL6 and HL16 across development anti-HL sera were used. Western blot analysis revealed strong expression of both HL6 (42 kDa) and HL16 (35 kDa) proteins after parasitoid wasp attack in larval and pupal stages (**Fig. 33.**). Moreover, elevated expression of the HL16 protein could still be detected in infected adults.

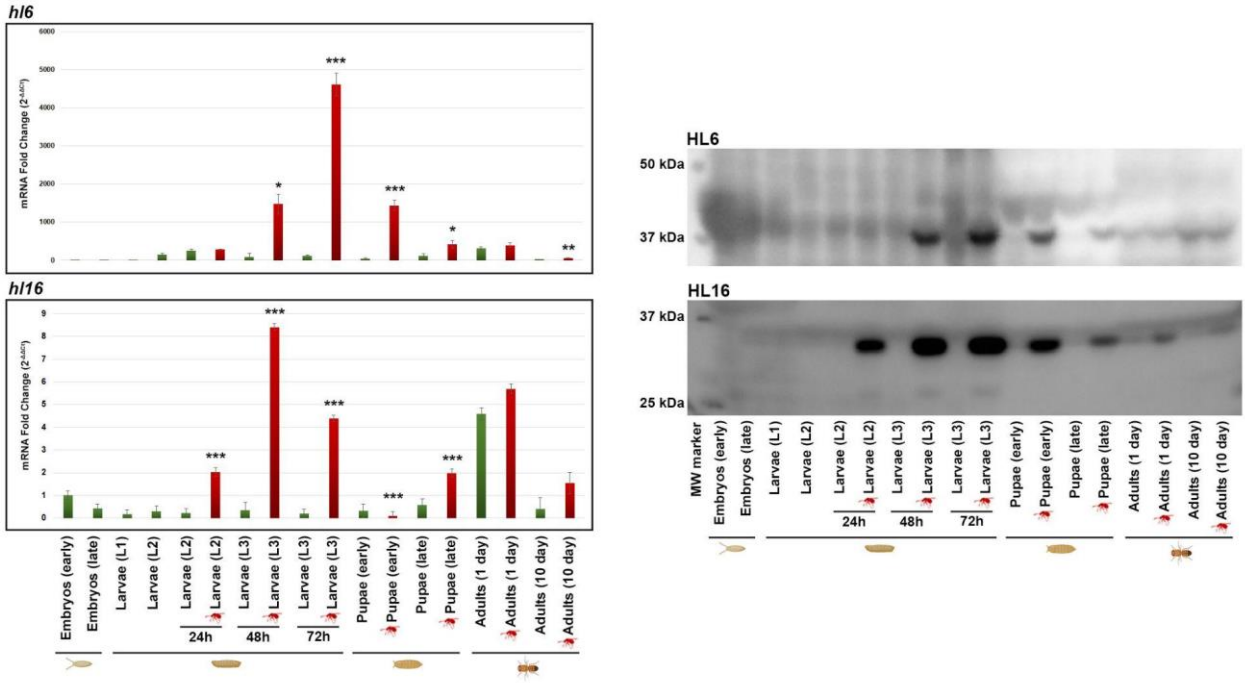

Figure 33. Expression of *hl6* and *hl16* genes is induced after *L. boulardi* infection across development and the same pattern is mirrored by the protein expression. Parasitoid infection took place at the second larval stage. Naive samples are labeled in green and wasp induced samples in red. ΔΔCt was calculated by normalizing ΔCt against the value of early embryos. The error bars indicate the standard deviation of four independent data points. Only significant differences between naive and infected samples are indicated. *=$P \leq 0.05$; ***=$P \leq 0.001$.

Next, using indirect immunofluorescence assays, we investigated the localization of HL6 and HL16 proteins in immunologically significant tissues: blood cells, the fat body, and the surface of parasitoid larvae (**Fig. 34.**). The HL6 protein was present both in MGHs and spherical cells. HL16 was detected mostly in vesicles found in the hemolymph, but was also present inside or on the surface of MGHs. It is not clear if the HL16 protein was taken up by MGHs or was produced by these cells and was packed in secretory vesicles to be released by exocytosis into the hemolymph. Both proteins were detected in the fat body of parasitoid infected samples.

Furthermore, both HL6 and HL16 proteins could be observed on the surface of *L. boulardi* parasitoid larvae isolated from infected *D. ananassae*, showing a direct contact with the parasitoids, which suggests their possible role in elimination of the invaders.

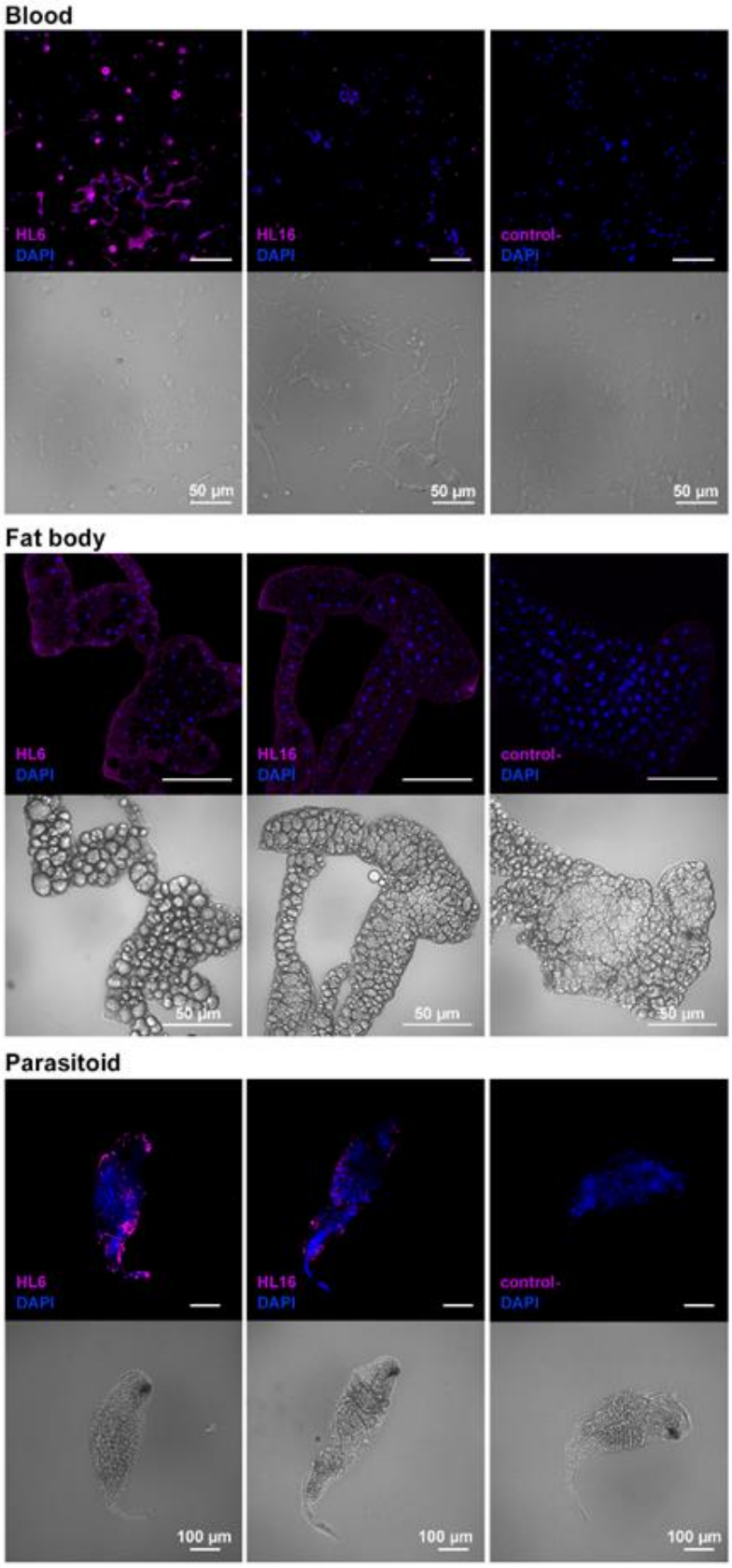

Figure 34. Detection of the HL6 and HL16 proteins in infected *D. ananassae* larvae using indirect immunofluorescence assay. Samples were harvested 72 h following *L. boulardi* parasitoid wasp infection and analyzed with an Olympus FV1000 confocal LSM microscope.

5.6. Toxicity Assay of Recombinant HL Proteins on U937 Cells

To assess the toxicity of the HLs, purified recombinant proteins were generated in both *E. coli* and D.Mel-2 cells, and added in a 3 μg/ml final concentration to plated U937 pro-monocytic cells, which are known targets of the bacterial Cytolysin A (Lai et al., 2000). Besides visual observations, toxicity was tested with a highly sensitive method, the Lactate Dehydrogenase (LDH) Cytotoxicity Assay, which detects the presence of the LDH, a cytoplasmic enzyme in the medium, hence, indicating damaged cellular membranes. The analysis was carried out at 2, 4, 6 and 24 h following incubation of the U937 cells with the HL proteins. We could not detect any toxic activity with neither of the HL proteins in the time period of 24 hours (data not shown). Furthermore, we observed that the recombinant *E. coli* Cytolysin A protein was toxic for the cells only when it was produced in *E. coli* cells, and showed no toxicity when generated in D.Mel-2 cells (**Fig. 35.**). The toxicity exhibited by the Cytolysin A produced in *E. coli* was already detected 2 h after the incubation.

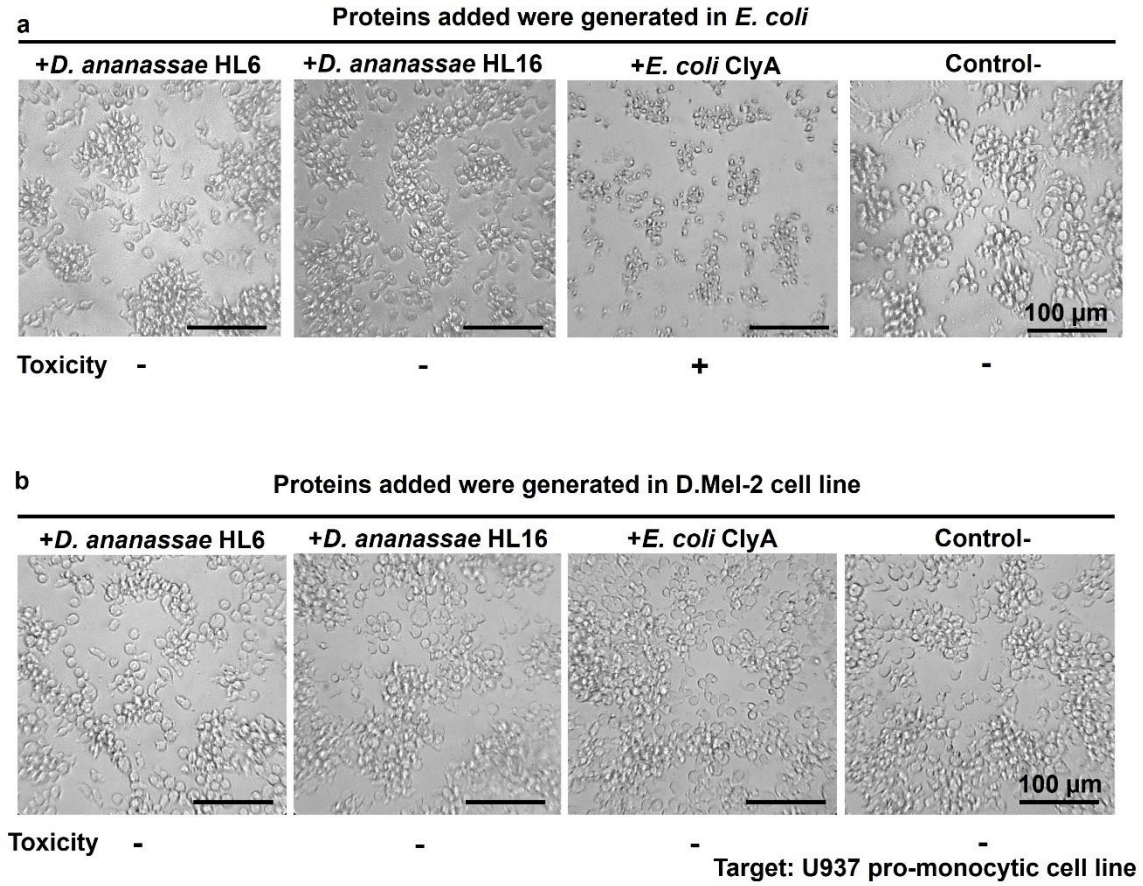

Figure 35. Toxicity of the recombinant proteins expressed in *E. coli* (a) and in the D.Mel-2 cell line (b).

5.7. Hemolysin E-like Genes in Other Insects and their Phylogenetic Analysis

We sought to determine whether insect-encoded *hemolysin E-like* genes arose from a horizontal gene transfer event from microbes to insects. The search recovered few hits to prokaryotic *hemolysin E* genes, but many hits to genes encoding uncharacterized or hypothetical proteins in other *Drosophila* and parasitoid wasp species (**Suppl. Fig. S7.**). But most importantly, none of the eukaryotic hits were bona fide eukaryotic genes. *Hemolysin E-like* genes were found besides the *ananassae* subgroup species, also in species of the *ficusphila*, *rhopaloa*, *willistoni*, *saltans* and *sturtevanti* subgroups of *Drosophilidae.* The genome of two distantly related hymenopteran parasitoids of flies also encode these genes, namely *Nasonia vitripennis* and *Trichomalopsis sarcophagae*.

A phylogenetic tree was generated. The final alignment used in tree generation contained 254 sites and 134 sequences, 17 of which were of prokaryotic origin. Notably, there are 0 conserved sites among all 134 sequences (no site has 100% conservation), indicating high sequence variation among this gene family. In all cases, insect homologs of Hemolysin E formed a monophyletic clade on a long branch with 100% bootstrap support. Relationships between insect homologs are poorly resolved, likely due to the sheer number of duplication events that happened within insect lineages (**Suppl. Fig. S7.**). The parasitoid Hemolysin E homologs interspersed among the drosophilid homologs suggests there may have been inter-insect HGT events that facilitated the incorporation of *hemolysin E* genes into diverse insect genomes or repeated donation of closely related *hemolysin E* genes from bacteria into these insects. Meanwhile, we could not determine the prokaryotic donor, from where these genes originated from. Therefore, we cannot entirely exclude convergent evolution.

6. *Z. indianus* MGH Maturation Exhibits Similarities to Mammalian Proplatelet Formation

The projection-formation of the *Z. indianus* MGH (**Suppl. Movie**) is reminiscent of megakaryocyte proplatelet formation, in which tubulin and actin rearrangement leads to the protrusion of pseudopodial projections that eventually dispatch and form mature platelets (Movie depicting proplatelet formation is included in the Supplementary for comparison (Italiano et al., 1999)). A major difference is that while in case of the megakaryocyte the process starts from an area of the cell and spreads out from there, in case of MGHs the whole cell starts to elongate and then create projections. Fully mature MGHs display the classical

components of proplatelets (Patel et al., 2005), including branch points, shafts, swellings, and tips (**Fig. 36.**). Towards the end of the movie, it is visible that the shafts start to thin and disappear, possibly resulting in the 4G7 positive anucleated fragments we had described previously. Note that while mammalian proplatelet formation takes place in the course of 4-10 hours, in *Z. indianus* this process is considerably faster as the movie presented covers a two-hour period.

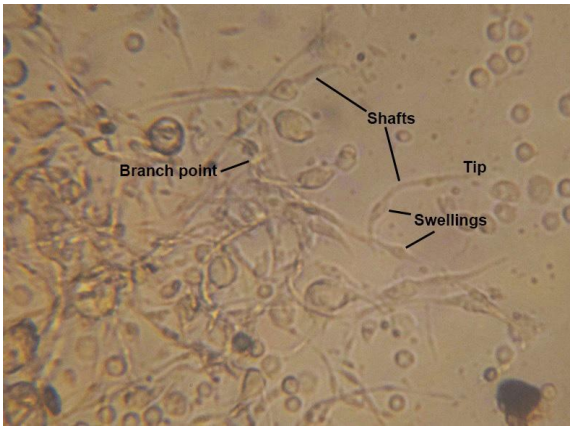

Figure 36. Structural components of MGHs. Screenshot of movie depicting MGH projection-formation (available in Supplementary Materials).

7. Anucleated Fragments Derived from MGHs Accumulate at Wound Sites in *Z. indianus*

We have previously described that the MGHs of *Z. indianus* are constitutively present in the hemolymph, and they release a large number of anucleated cytoplasmic fragments (Cinege et al., 2020). Formation of anucleated fragments and the morphological similarities to proplatelets led us to consider whether, by analogy, the anucleated fragments derived from *Z. indianus* MGHs could be involved in wound healing in larvae. To test this, we wounded early third instar naive and *L. victoriae*-infected larvae. The wound sites were investigated after 2 h by indirect immunofluorescence assay with the giant cell specific 4G7 antigen. We detected 4G7-positive fragments at wound sites in both naive and *L. victoriae*-infected animals (**Fig. 37.**), although the presence of nucleated giant hemocytes cannot be excluded. Accumulation of MGH-derived anucleated fragments at wound sites suggests a possible role in cuticle remediation.

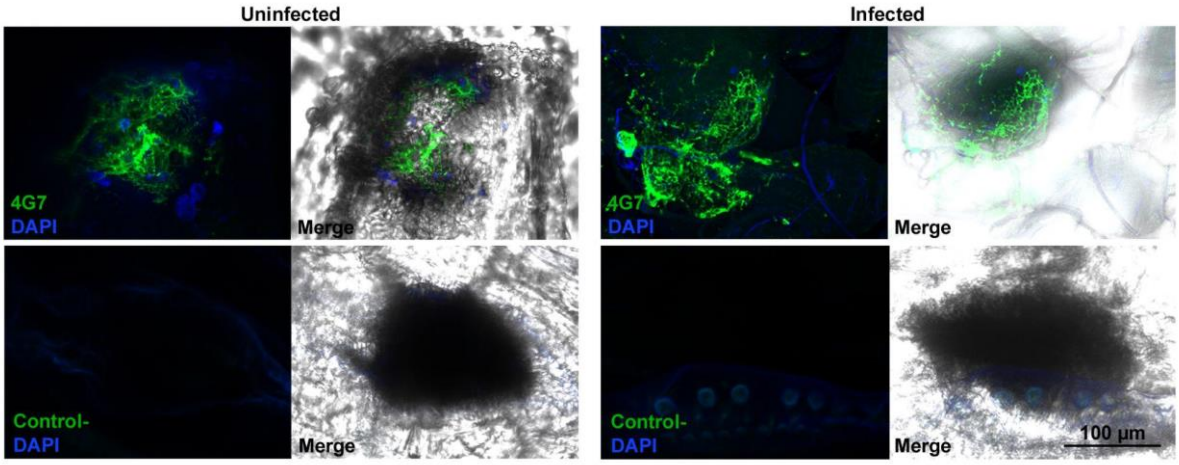

Figure 37. The accumulation of anucleated 4G7-positive fragments at wound sites in *Z. indianus* larvae

8. Transcriptome Analysis of Naive and Wasp Induced *Z. indianus* Blood Cells

To gain insights into the molecular mechanisms responsible for the effective immune response against parasitoids we performed the transcriptome analysis of hemocytes isolated from age-matched naive and *L. victoriae* infected *Z. indianus* larvae. In total, 7,052 different gene transcripts were detected. As there was no available information concerning the genes and proteins of *Z. indianus*, data was gathered about their *D. melanogaster* orthologs.

8.1. Differentially Expressed Genes Involved in the Response to Parasitoid Infection

After normalization, we identified 648 DEGs (**Suppl. Table S6.**), out of which 374 genes were expressed at significantly higher and 274 genes at significantly lower level in induced blood cells compared to naive hemocytes. This includes 37 genes with the exclusive expression in induced blood cells and 12 genes exclusively expressed in naive hemocytes. The performed GO enrichment analysis in the "cellular component" category shows that the enriched gene products are localized in the plasma membrane, junctions and in the cytoskeleton (**Suppl. Fig. S8.**). According to the "biological process" category gene products involved in immune response, junction formation, cytoskeletal organization, and defense response to Gram-positive bacteria are enriched (**Suppl. Fig. S9.**).

Therefore genes encoding proteins involved in encapsulation showed significantly higher expression in the infected samples, including cytoskeletal-related proteins and several integrin subunits: Strn-Mlck (ZIND16G_00004905) cytoskeletal dynamic regulation, Itgbn (ZIND16G_00009296), p130CAS (ZIND16G_00006792), if (ZIND16G_00005558), Dhc16F (ZIND16G_00008232), AdamTS-A (ZIND16G_00003414), trio (ZIND16G_00001152), cher (ZIND16G_00004253), ncd (ZIND16G_00005467), mew

(ZIND16G_00004434), scb (ZIND16G_00007892), trbd (ZIND16G_00008915), Rala (ZIND16G_00002638), Nrg (ZIND16G_00002077) and Eb1 (ZIND16G_00006903).

The peptidoglycan recognition proteins PGRP-SB1 (ZIND16G_00000431), PGRP-SC2 (ZIND16G_00004509) and PGRP-LB (ZIND16G_00003503) are significantly higher expressed in infected samples, while the main receptor of the Imd pathway, PGRP-LC (ZIND16G_00008135) was downregulated. There was an elevated expression of three AMPs: CecC (ZIND16G_00002978), DptB (ZIND16G_00002658) and AttD (ZIND16G_00001258). Proteins of other overexpressed genes participating in microbial elimination include Tep2 (ZIND16G_00008527), Tep3 (ZIND16G_00009332), IM33 (ZIND16G_00009971), Bbd (ZIND16G_00006553), slif (ZIND16G_00005220), and CG16799 (ZIND16G_00006321). Coinfection during parasitoid wasp oviposition might be the elicitor of these genes.

Genes encoding proteins of signaling pathways are not upregulated per se, but some of their components or regulators show elevated expression. These include Galphaf (ZIND16G_00000435), the transcriptional target of the JAK/STAT pathway, Pvf3 (ZIND16G_00008540), an activator of the JNK pathway, Mnr (ZIND16G_00002683), a positive regulator of Notch signaling, and Rala (ZIND16G_00002638), a GTPase that regulates Notch, Jak/Stat and JNK signaling pathways. But spz (ZIND16G_00008556), the activator of the Toll pathway is downregulated. Two SPs are also upregulated: Sp7 (ZIND16G_00001050) and grass (ZIND16G_00000143)

As immune responses are energetically costly processes, gene products involved in the biosynthesis or usage of sugars are elevated after parasitoid infection: CG5171 (ZIND16G_00007239), Treh (ZIND16G_00009882), beta-Man (ZIND16G_00007729), Ldh (ZIND16G_00008314) and Gnmt (ZIND16G_00004579).

Other notable upregulated gene products include two proteins involved in autophagy: Rab32 (ZIND16G_00008079) and S6k (ZIND16G_00001109) and Cathepsin L1 (Cp1) (ZIND16G_00005802), a lysosomal enzyme involved in the degradation of either microbes or parasites.

In this case, 74 of the 648 DEGs (11.42%) had no recognizable orthologs in *D. melanogaster*, which is a similar proportion as that seen in the transcriptome analysis of *D. ananassae* blood cells. Most of the genes having no orthologs in *D. melanogaster* belong to expanded and rapidly evolving gene families with uncertain orthology relationships: the serine proteases, the FREPs, and the C-type lectins.

8.2. Expression of *Z. indianus* Serine Proteases, FREPs, and C-type Lectins

The above-mentioned gene families, the serine proteases, the FREPs, and the C-type lectins, expressed either differentially or constitutively in blood cells, are of special interest. The serine proteases can act in complement-like cascades to activate Toll signaling, melanization, or coagulation. The FREPs and C-type lectins can act as PRRs or even opsonins. Taking in consideration both groups, the constitutively and differentially expressed genes, blood cells of *Z. indianus* express 90 serine proteases, 54 of which have specific *D. melanogaster* orthologs (**Supp. Table S7.**). The identified orthologs include genes with known roles, such as Hayan, Sp7 in melanization, and grass and modSP in Toll signaling. The remaining 36 genes that lack orthologs in *D. melanogaster* are specific to *Z. indianus*. Out of the 51 FREP genes expressed in blood cells of *Z. indianus*, only 22 possess *D. melanogaster* orthologs, but most of these genes have not been characterized so far (**Suppl. Table S7.**). We identified 18 *Z. indianus* lectin genes, with only five possessing *D. melanogaster* orthologs (**Supp. Table S7.**). The DEGs that belong to either serine proteases, FREPs, or C-type lectins are probably involved in parasitoid recognition or parasitoid-killing processes of *Z. indianus*.

8.3. Constitutively Expressed Genes Involved in Immunity

We identified constitutively expressed immune signaling pathways as we found components of the JNK pathway (Alg-2, bsk, CYLD, Cdc37, jra, msn, and Pvr) and elements of the JAK/STAT pathway (hop, Stat92E, dome, Ptp61F, and Socs36E) were expressed in both naive and induced blood cells. However, upd1 and upd3 genes, encoding the ligands of the JAK/STAT pathway, had no or very low expression, while the upd2 ortholog is not even encoded in the genome of *Z. indianus.*

As giant hemocytes, and the anucleated fragments derived from them are present in both naive and infected animals, we investigated the constitutively expressed genes to look for gene products involved in wound healing processes. We listed the genes with *D. melanogaster* orthologs known to be involved in blood coagulation, wound healing, and cuticle remediation (**Table 3.**).

Table 3. The set of constitutively expressed *Z. indianus* genes encoding for orthologs of *D. melanogaster* proteins involved in wound healing and hemolymph clotting.

***Z. indianus* gene ID**	***D. melanogaster* ortholog**	**Role in *D. melanogaster***
ZIND16G_00008476	fon	Fat body-secreted hemolymph clotting factor.
ZIND16G_00008262	Hml	Hemolymph clotting.
ZIND16G_00006641	PPO2	Melanization of wounds and capsules.
ZIND16G_00006889	PPO1	Melanization of wounds.
ZIND16G_00008507	CG42259	Involved in response to wounding.
ZIND16G_00003920	Glt	Cross-links blood clot.
ZIND16G_00001938	pbl	Wound healing.
ZIND16G_00006474	Tg	Cuticle development. Hemolymph coagulation, wound healing.
ZIND16G_00002297	Cht2	Cuticle development. Wound healing.
ZIND16G_00006825	Fhos	Plasmatocyte migration during immune response, autophagic programmed cell death.
ZIND16G_00007154	CG15170	Wound healing.
ZIND16G_00008356	TTLL4A	Wound healing.
ZIND16G_00007461	Mtl	Dorsal closure, wound healing, cell migration.
ZIND16G_00005073	Coq3	Wound healing.
ZIND16G_00008371	holn1	Wound healing.
ZIND16G_00004207	CG11089	Wound repair.
ZIND16G_00000950	CG6005	Wound healing.

Z. indianus gene ID	*D. melanogaster* ortholog	Role in *D. melanogaster*
ZIND16G_00009846	Mmp2	Cleaves proteins in the extracellular matrix. Wound healing.
ZIND16G_00001627	Idgf3	Component of hemolymph clot.
ZIND16G_00006536	CG3294	Splicing factor involved in wound healing.
ZIND16G_00001159	Cht7	Chitin-based cuticle development.
ZIND16G_00003151	Hmu	Wound healing.

Furthermore, we have also identified 143 genes that have mammalian orthologs that participate in megakaryocyte and blood platelet functions (**Suppl. Table S8**), however, those genes are most of interest which are involved in endoreplication or the polyploidization of megakaryocytes, as MGH nuclei in *Z. indianus* are also polyploid. The genes Plk1 (ZIND16G_00001174), Pak2 (ZIND16G_00004183), LRP6 (ZIND16G_00006596), RhoA (ZIND16G_00008071), CCNE1 (ZIND16G_00004255) are all indispensable for megakaryocyte maturation and polyploidy (Eliades et al., 2010; Macaulay et al., 2013; Suzuki et al., 2013; Kosoff et al., 2015; Trakala et al., 2015), and their orthologs are expressed in *Z. indianus* blood cells.

8.4. Comparison to Parasitoid Induced Genes of *D. melanogaster* and *D. ananassae* Hemocytes

We were curious whether the DEGs identified in the *Z. indianus* transcriptome include orthologs of lamellocyte-specific genes of *D. melanogaster*. We found that 21 lamellocyte marker genes were upregulated in *Z. indianus* blood cells after parasitoid infection, while three were downregulated (**Suppl. Table S9.**). The upregulated genes include orthologs of *atilla*, *cher*, and the integrins *Itgbn* and *mew*, as well as several genes involved in cytoskeletal organization and sugar import. In contrast, many plasmatocyte and crystal cell specific orthologs were downregulated in *Z. indianus* hemocytes after infection (**Suppl. Table S9.**), albeit modestly so. This may reflect a decreased relative proportion of the corresponding cell classes in the infected animal.

We have also compared the DEGs of *D. ananassae* MGHs and activated plasmatocytes with the DEGs of *Z. indianus*. We have found that six genes, which happen to be lamellocyte markers too, *atilla*, *Itgbn*, *Trehalase*, the sugar transporter *CG1208*, *Esyt2*, and *Gdap2*, were highly expressed in both parasitoid infected hemocytes of *Z. indianus* and *D. ananassae* MGHs. Three of the highly expressed *Z. indianus* genes, *Trehalase*, *Esyt2*, and *aru*, were also upregulated in the activated plasmatocytes of *D. ananassae*. This minor gene expression overlap probably occurs due to the analogous functions of the hemocytes in different species.

V. Discussion

Multinucleated giant hemocytes are involved in the encapsulation response against parasitoid wasps (Márkus et al., 2015). We have shown that the species differentiating MGHs have a higher resistance against parasitoids than the lamellocyte-differentiating *D. melanogaster* (Cinege et al., 2023). In contrast to *D. melanogaster*, where beside the parasitoid wasp infection, wounding of the cuticle is sufficient stimulus to induce lamellocyte differentiation (Márkus et al., 2005; Evans et al., 2022), we showed that in *D. ananassae* differentiation of fully mature MGHs is exclusively induced by parasitoid infection, as wounding or introduction of foreign objects resulted in formation of cells not reaching terminal differentiation. These results suggest that regulation of MGH differentiation is different from that of lamellocyte formation in *D. melanogaster*.

We aimed to get insights into the distinct features of MGHs through ultrastructural and transcriptomic approaches (Cinege et al., 2022). The transmission electron microscopic analysis revealed that *D. ananassae* MGHs possess a vesicle-rich cytoplasm with a large number of electron-dense vesicles forming multiform dense bodies (mdbs). While the contents of the electron-dense vesicles and mdbs remains unidentified, we determined that they possess an acidic feature, and we showed that they have role in parasitoid encapsulation as mdbs form a continuous layer on the parasitoid surface. It was described that lamellocytes also contain acidic, lysosomal vesicles (Shrestha and Gateff, 1982), but their function remains unexplored.

Furthermore, we have identified cell-in-cell internalizations for the first time in insect blood cells. The event is eerily similar to mammalian emperipolesis, as it involves the inclusion of a phagocytic cell by a giant cell type. Emperipolesis, an uncommon form of cell-cell interactions, is evolutionarily conserved in mammals (Cunin and Nigrovic, 2020). Several instances were described when megakaryocytes enclosed neutrophils, erythroblasts or myeloid cells (Rastogi et al., 2014). During the process, membrane transfer takes place from the guest cell to the host. However, the significance of emperipolesis remains mostly elusive. In this case interaction could also represent a step of a mechanism that ultimately leads to multinucleated cell formation.

Certain multinucleated enlarged cells containing lysosomes can sometimes point to senescence (Kloc et al., 2022). In case of *D. ananassae* and *Z. indianus* MGHs, TEM images support the integrity of their nuclei. Furthermore, the single cell-based transcriptome analysis of *D. ananassae* MGHs shows that the expression of senescence-associated beta-

galactosidase (González-Gualda et al., 2021) (Dana\GF14288) was even lower than in activated plasmatocytes, and several highly expressed genes suggest the increased energy demand of these cells. High energy demand and the expression of genes encoding sugar transporters was described in lamellocyte transcriptomes, too (Tattikota et al., 2020). Besides the upregulation of genes encoding sugar transporters and the Trehalase enzyme, MGHs had high expression of Lactate dehydrogenase (Ldh, Dana\GF10902), a key enzyme responsible for lactate production and NAD+ regeneration during aerobic glycolysis, known as the Warburg effect. This metabolic switch was described to take place in both mammalian and drosophilid hemocytes during immune responses against parasitoids and microbes (Delmastro-Greenwood and Piganelli, 2013; Bajgar et al., 2015; Krejčová et al., 2019). The advantage of glycolysis is that it is allows significantly faster macromolecule synthesis and proliferation than oxidative phosphorylation.

Non-melanotic encapsulation of parasitoids has been described in other insects, but is uncommon in the *Drosophila* genus (Kacsoh et al., 2014). Besides the lack of PPO3 in the *D. ananassae* genome, neither PPO1, PPO2, nor the serine proteases MP1, MP2 and Hayan, required for PPO activation are expressed in MGHs. Therefore, we can conclude that the melanization cascade is completely absent in MGHs. It is possible that deposition of melanin and the formation of a hard capsule would prevent toxic molecules from accessing the surface of the parasitoid.

We concluded that the only immune signaling pathway expressed in MGHs is the JNK, which is known to be involved in adhesion, cell migration and stress response, but it can also trigger autophagy (Deng et al., 2023). Numerous other genes associated with autophagy were also highly expressed in MGHs, while autophagosomes were visible in their cytoplasm (Cinege et al., 2022). Moreover, the cargo of multivesicular bodies can be destined for not just exocytosis, but recycling too (Fader and Colombo, 2009). Autophagy was described to induce membrane breakdown, facilitate cell fusion and thus promote giant cell formation (Kakanj et al., 2022). This self-degradation could be facilitated by the vacuolar-type ATPase, subunits of which are encoded by genes showing high expression in MGHs. This protein complex pumps protons into vesicles, thus acidifying them. Therefore, they could be the contributors to the acidity of the LysoTracker positive organelles. We noted that retention of the Lysotracker dye was much lower in the vesicles of MGHs than in those of activated plasmatocytes. This could be explained by a DEG, Dana\GF16603, an ortholog of the human ABCC4 gene, which was significantly higher expressed in MGHs compared to activated plasmatocytes. The gene encodes a P-glycoprotein, which has been shown to

extrude aromatic hydrophobic compounds, such as the LysoTracker fluorescent dye (Zhitomirsky et al., 2018). Thus, the extremely fast fading of fluorescence intensity of MGH acidic organelles could be due the ejection of the dye molecules by the P-glycoprotein. The higher rate of eviction of potentially toxic molecules evidentiates the increased stress-tolerance of MGHs possibly granted by genome duplication (Schoenfelder and Fox, 2015), and might grant greater immunity against the venom proteins employed by the parasitoids.

We have described GCEs and microvesicles that originate from MGHs. The exosomes and microvesicles might act as carriers of effector molecules to the target site at the parasitoid surface. But they might also be involved in cell-cell communications, as described in mammalian innate immunity (Ratajczak and Ratajczak, 2021).

The cargo molecules of these structures could likely be the members encoded by the gene family newly uncovered by us through the transcriptome analysis of *D. ananassae* hemocytes (Cinege et al., 2022). This family has 38 members in *D. ananassae*, showing domain similarity to the bacterial Hemolysin E (Cytolysin A) alpha-pore forming toxin. The prokaryote toxin acts as a virulence factor in several bacteria from the *Enterobacteriaceae* family, including *E. coli*, *Salmonella enterica* serovar Typhi or serovar Paratyphi A and *Shigella flexneri* (Hunt et al., 2010). Activity of Hemolysin E in bacteria is tightly controlled at a transcriptional level, but the encoded protein does not require any posttranslational modification. It also lacks a canonical signal sequence and is secreted instead through outer membrane vesicles, which have an average diameter of 20–300 nm (Murase, 2022). An analogy can be drawn between the bacterial extracellular vesicles, and the GCEs and microvesicles released by MGHs of *D. ananassae*, which could act as the carrier of these molecules to the target site.

In this work we investigated the *D. ananassae hemolysin E-like* genes and their encoded proteins, with particular interest to their structure, function and origin. Chromosomal localization of the *D. ananassae hl* genes are mostly restricted to the 2L, 3R and both arms of the X chromosome. We found that there is correlation between the chromosomal localization and the regulation of these genes. The *hl* genes that, according to their transcriptome analysis, were expressed in MGHs are *hl1* to *hl14*, most of which are localized on the XL chromosome in the vicinity of each other, thus they might be under the control of the same regulatory elements. Following their putative integration into the eukaryotic genome, they underwent a domestication process, and acquired introns and signal peptides.

We showed that the transcription and translation of *D. ananassae hl* genes and the encoded proteins are highly boosted after parasitoid wasp infection and that they are primarily expressed in the main immune tissues, the blood cells and the fat body, suggesting a role for HL proteins in immune responses against parasitoids. While most of HL proteins are secreted by the fat body, the scattered appearance of the HL16 protein on the MGHs suggests that blood cells can acquire HLs from the hemolymph through endocytosis, a process, which as could be concluded from the transcriptome data, takes place in MGHs. This mechanism might play a regulatory role, since the blood cells could serve as an assembly and activator site for the HL pore complexes, thus allowing the activation and employment of toxins during encapsulation, evading autotoxicity. As most of the *hl* genes are expressed by the fat body and the encoded HL proteins are present on the surface of the parasitoid surface, these molecules, beside the cytolethal distending toxin B (CdtB) and the apoptosis inducing protein of 56 kDa (AIP56) (Verster et al., 2023) could be among the first identified antiparasitoid humoral factors that act directly on the pathogen. Although the three-dimensional structure of *D. ananassae* HL proteins highly resemble to that of *E. coli* Hemolysin E, we could not detect toxicity of the recombinant *D. ananassae* HL proteins, generated in the eukaryotic D. Mel-2 cells, only the recombinant prokaryotic protein, produced in *E. coli*, was toxic for the U937 pro-monocytic cell line. This highlights the importance of the cell type or molecular environment where these molecules are produced in vivo. It is possible that only cells of *D. ananassae*, or only certain cell types of this species, as fat body cells or MGHs, could provide the proper intracellular conditions required to obtain an active form of the insect HL proteins. However, we have to take into consideration that the pore complexes assembled in vivo in insects might be built in fact by several different monomers, and various HL proteins could be essential for their correct assembly. We have made substantial progress on understanding the involvement of HL proteins in *D. ananassae* innate immunity, however, their exact mechanism of function still remains elusive.

We have found *hl* genes in species of the *ananassae, ficusphila*, *rhopaloa*, *willistoni*, *saltans* and *sturtevanti* subgroups of *Drosophilidae* (**Fig. 38.**). We hypothesize that the insect-encoded *hemolysin E-like* genes originate from an ancient horizontal gene transfer event from bacteria, followed by several duplication events in insects and possibly later inter-insect horizontal gene transfer events. However, the possibility of convergent evolution cannot be ruled out, as it is possible that insect proteins are annotated as Hemolysin E on the basis of structural similarity, rather than shared evolutionary relationships between the insect

and prokaryotic proteins. Furthermore, we could not find a clear insect-associated bacterial donor taxon lineage. The lack of a donor lineage could be the result of sampling bias or underrepresentation of these sequences in available databases.

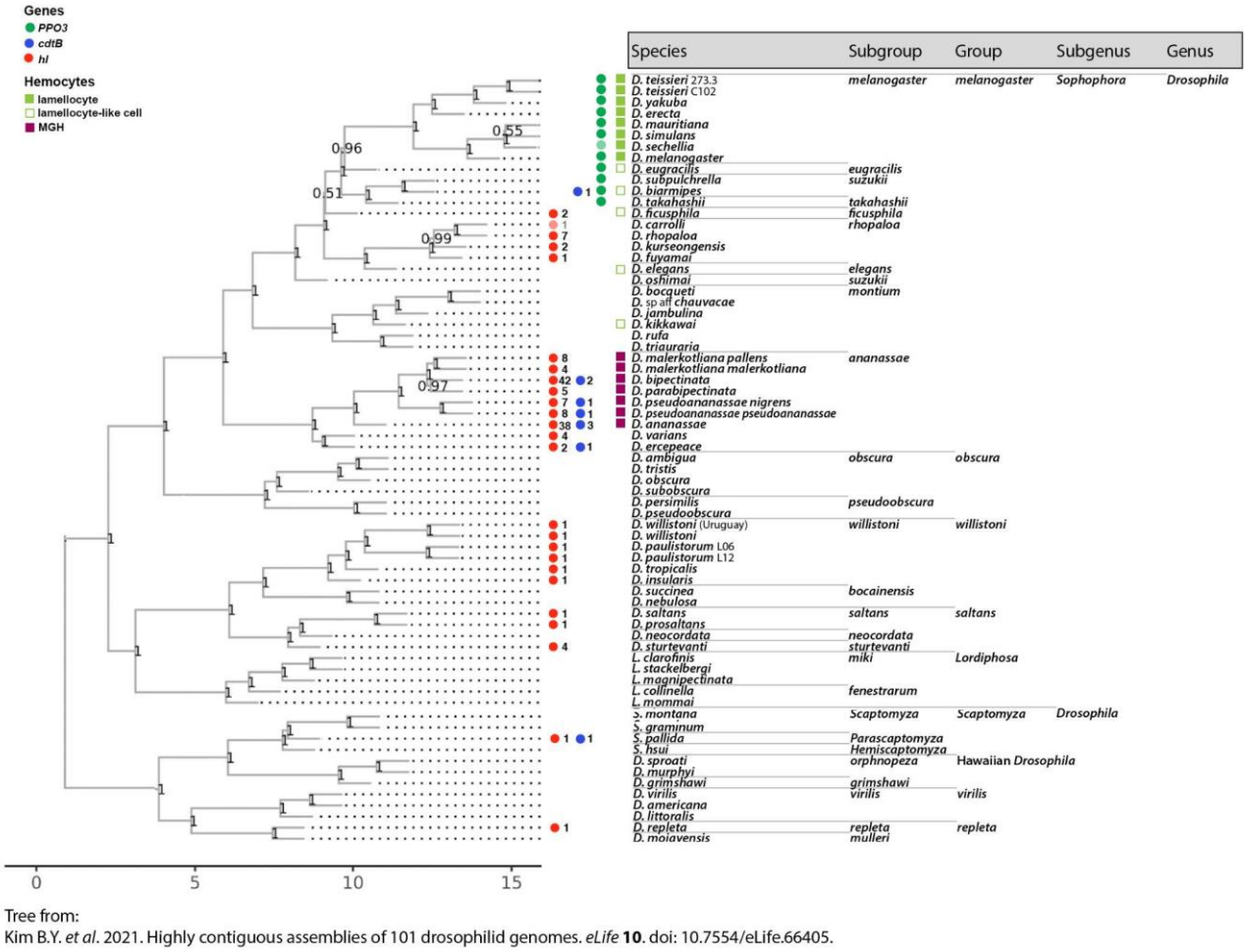

Figure 38. The occurrence of different anti-parasitoid immune strategies in drosophilids. Presence of *PPO3*, *cdtB* and *hl* genes, and of different encapsulating cells are indicated.

Horizontal gene transfer (HGT) to insects is more widespread than previously thought (Crisp et al., 2015). Moreover, the horizontal transfer of pore-forming toxin genes seems to be a recurring phenomenon across multiple kingdoms of life (Moran et al., 2012), as toxin families are more likely to be maintained because they alone can already confer a benefit in immune defense and therefore increase the fitness of the host. When looking at the broader picture, it is evident that several drosophilids that differentiate MGHs, beside the *hemolysin E-like* genes, also carry genes encoding for cytolethal distending toxin B (*cdtB*) (**Fig. 38.**). This further highlights the susceptibility to HGT of the species of the *ananassae* subgroup. The donor of the *hl* genes could be a Wolbachia-like endosymbiont, which is

present in the germline of drosophilids and can use parasitoid wasps as phoretic vectors (Ahmed et al., 2015), or even a symbiotic virus of a parasitic wasp (Di Lelio et al., 2019), as *hl* genes were detected in parasitoid species too. The evolutionary strategy to acquire genes quickly from prokaryotes might provide these species a powerful advantage in the coevolutionary race with parasites. Thus, the domesticated HL proteins might operate in a concerted action with the other components of the immune system, including the CdtB and the AIP56 proteins of prokaryotic origin, to establish an effective immune defense against parasitoid wasps.

MGHs share similar features with mammalian giant cells (GCs), probably as a result of convergent evolution. Some of these similarities could be the result of the adaptation to giant size. This size can be achieved only through whole-genome duplication (WGD) or polyploidy. Universal polyploidy-related transcriptomic changes include enrichment of genes related to ribosome biogenesis, transcription, adaptation to oxidative stress and the activation of aerobic glycolysis, while aerobic respiration is suppressed (Anatskaya and Vinogradov, 2022). Therefore, the switch to aerobic glycolysis could be the result of poliploidy, as the size growth requires fast anabolism.

The TEM analysis of MGHs uncovered emperipolesis-like phenomena identified along with several vesicles, dense bodies and autophagosomes and even multivesicular bodies, also typical for mammalian GCs and megakaryocytes (Cramer et al., 1997). Autophagy, involving several intracellular vesicles, is crucial in the proliferation, differentiation, migration, as well as the bone-resorption processes of osteoclasts (a type of GC) as it is required for the release of lysosomal proteolytic enzymes (Wang et al., 2023). Autophagy is also crucial in mammalian hematopoiesis, as it plays a role in both megakaryopoiesis and thrombopoiesis (You et al., 2016). Furthermore, the transcriptome analysis revealed that genes encoding for β integrin subunits were highly expressed in MGHs, genes which in mammals have essential role in macrophage-macrophage adhesions and subsequent fusions (Quinn and Schepetkin, 2009). The vacuolar type H+-ATPase is essential for foreign-body GCs in extracellular degradation (Harkel et al., 2015) and the genes encoding for the subunits of this enzyme were overexpressed in MGHs. Similarly, *Cysteine proteinase-1* was also one of the highly expressed genes in MGHs, and is homologous to mammalian cathepsin K, the main enzyme used by osteoclasts to degrade bone tissue (Janiszewski et al., 2023).

We have shown that *Z. indianus* MGHs are in some aspects analogous to mammalian megakaryocytes: they both possess a characteristic cytoplasm with an elaborate system of

canals that communicates with the extracellular space (Patel et al., 2005; Cinege et al., 2020), and both cell types release a large number of anucleated cytoplasmic fragments. Here we provide evidence for a novel function of the giant hemocytes, as we found that in both naive and parasitoid infected larvae, they were present at wound sites and hence could be involved in the wound healing process, similarly to megakaryocyte-originated platelets in mammals. We have also pointed out the structural similarities between proplatelets and MGH projections. However, projection formation of MGHs is significantly faster, which possibly correlates with the short lifespan and rapid immune responses of insects.

Transcriptomic analysis of *Z. indianus* blood cells revealed constitutive expression of several genes, which, based on their homology to *D. melanogaster* or mammalian genes, could be involved in wound healing and coagulation processes. We have also identified genes expressed in *Z. indianus* hemocytes that had homologs involved in the polyploidization and endoreplication of megakaryocytes. These genes were not upregulated in *D. ananassae* MGHs, further confirming that only the MGHs of *Z. indianus* form with both cell fusion and endoreplication, while *D. ananassae* MGHs do not employ cell fusion.

We have also identified rapidly evolving gene families expressed in *Z. indianus* blood cells, encoding a large number of FREPs and C-type lectins, which have been described to act as PRRs in other insect species. Therefore, they might recognize the different PAMPs of pathogens and trigger immune responses. In other species, C-type lectins with other functions have been identified, such as members of the RegIII family in humans, which can kill bacteria by pore formation (Mukherjee et al., 2014).

Genes encoding different JNK signaling pathway components were detected in the transcriptome of both *D. anananassae* and *Z. indianus*. JNK activation promotes the macrophage fusion during mammalian GC formation (Quinn and Schepetkin, 2009). Moreover, in certain conditions, JNK signaling can promote endoreplication and the formation of giant polyploid cells (Costa et al., 2022).

The lamellocyte-specific genes *atilla, itgbn, Treh, Esyt2,* and *CG1208,* were expressed at significantly higher levels in the MGHs of *D. ananassae* and the blood cells of parasitoid-infected *Z. indianus*; hence, they might constitute essential elements of anti-parasitoid defense. Itgbn participates in adhesion, Trehalase and the sugar transporter CG1208 supplies glucose and were discussed above. Esyt2, a member of the Synaptotagmin family, may be involved in coordinating intracellular calcium dynamics and constitutive membrane trafficking. This protein could be essential in evading the effects of the calcium

pump present in some wasp venoms (Mortimer et al., 2013). The role of atilla in immunity is unexplored and warrants further studies.

Giant cells that possess multiple polyploid nuclei represent a unique and understudied cell type (Peterson and Fox, 2021). Further studies of MGHs could elucidate the role of the redundant WGD in the form of both multinucleation and polyploidy in the same cell. *Drosophila* MGHs could also be investigated to discover the explicit functions of different unexplored aspects of mammalian GCs (emperipolesis, megakaryocyte autophagy etc.) as it would provide an easy and cost-effective alternative to mammalian study systems. Furthermore, as multinucleation can also result in the spatial specialisation of the individual nuclei (Peterson and Fox, 2021), it would be interesting to find out if nuclei closer to the parasitoid are differently regulated at the transcriptional level.

In conclusion, species differentiating MGHs have evolved a robust parasitoid defense mechanism distinct from that of the model organism *D. melanogaster*. These newfound complexities in drosophilid immune responses open novel, so far unexplored areas in the function, mechanisms, and evolution of the innate immune system.

VI. Summary

Insects possess an immune system that shares similarities in many aspects with vertebrate innate immunity. The innate immune system of drosophilids is comprised of humoral and cellular components, which act in concert to recognize and eliminate invaders. The main humoral organ, the fat body secretes into the hemolymph various molecules involved in pathogen recognition, immune regulation, and the elimination of microbes. The blood cells in the model organism *Drosophila melanogaster* are the phagocytic plasmatocytes, the crystal cells that participate in melanisation, and the lamellocytes responsible for the isolaton and elimination of large particles, like foreign objects and parasitoids. Infection by parasitoid wasps is a frequent danger encountered in nature by *Drosophila* species. The parasitoids use fly larvae or pupae for oviposition and as nutrient source during their development, therefore, the evolution of immune responses against these pathogens are essential for survival. One such immune strategy is the emergence of encapsulating blood cells with distinctive morphology and effector mechanisms.

We have shown that the drosophilids possessing multinucleated giant hemocytes (MGHs) exhibit higher resistance to parasitoid wasp infection than *D. melanogaster*. In *D. ananassae*, mature MGHs differentiate only after parasitoid infection, and their formation cannot be induced by cuticle wounding. The aim of this work was to characterize the morphological, genetic and functional features of MGHs. Transmission electron microscopic assays revealed that *D. ananassae* MGHs possess a vesicle-rich cytoplasm with a large number of electron-dense vesicles forming multiform dense bodies (mdbs). We found that the electron-dense vesicles are acidic, and that they form a continuous dense layer on the parasitoid surface. The MGHs release exosomes and microvesicles, which could act as carriers of effector molecules involved in isolation and elimination of the parasitoid. Transcriptome analysis of *D. ananassae* hemocytes revealed the high energy demand of the MGHs and showed that the JNK is the only signaling pathway expressed in these cells.

We have shown that the drosophilids differentiating MGHs, express horizontally acquired genes of microbial origin encoding for the cytolethal distending toxin B (*cdtB*), and a family of for pore-forming toxins, *hemolysin E-like* (*hl*). The expression of *hl* genes and the encoded proteins is increased after parasitoid wasp infection, with primary expression in the main immune tissues, the blood cells and the fat body. We also detected the presence of HL proteins on the surface of the parasitoid wasp larvae. These findings suggest the involvement of the HL proteins in the anti-parasitoid immune response. The evolutionary

strategy to acquire genes rapidly from prokaryotes might provide a powerful advantage to the species of the *ananassae* subgroup in the coevolutionary race with parasites. Especially the acquisition of toxins confers a benefit in immune defense reactions and therefore increases the fitness of the host.

MGHs share similar features with mammalian giant cells (GCs), which usually form with the fusion of macrophages. The ultrastructural analysis of MGHs uncovered the characteristic cytoplasm of MGHs with several vesicles, dense bodies, autophagosomes, and multivesicular bodies, all typical for mammalian GCs and megakaryocytes. We discovered an emperipolesis-like phenomena, when plasmatocytes are encased in the cytoplasm of MGHs, a process first described between neutrophils and megakaryocytes. Orthologs, crucial for mammalian GC function are expressed at high level in MGHs, such as genes encoding for β integrin subunits, vacuolar type H+-ATPase subunits and the enzyme Cysteine proteinase-1. We showed that several features of *Z. indianus* MGHs resemble those of mammalian megakaryocytes as they both possess a characteristic cytoplasm with an elaborate system of canals that communicates with the extracellular space, and both cell types release a large number of anucleated cytoplasmic fragments. We provided evidence for a novel function of the MGHs, as the anucleated fragments released by these cells accumulated at wound sites. Similarly to the platelets originated from the megakaryocytes, the anucleated fragments released by the giant hemocytes of *Z. indianus* could be involved in wound healing. Transcriptomic analysis of *Z. indianus* hemocytes revealed constitutive expression of several genes, which, based on their homology to *D. melanogaster* or mammalian genes, could be involved in wound healing and blood coagulation processes.

This work gives insights into structural, molecular and functional properties of multinucleated giant hemocytes, the cellular elements of a non-canonical and highly effective immune defense reaction in several *Drosophila* species. Furthermore, *Drosophila* MGHs could be investigated to discover the explicit functions of different unexplored areas of mammalian GC biology.

VII. Összefoglaló

A rovarok immunrendszere sok szempontból hasonló a gerinces veleszületett immunitáshoz. A *Drosophila* fajok veleszületett immunitása humorális és sejtközvetítette folyamatokból áll, amelyek együttműködnek a patogének felismerésében és kiiktatásában. A fő humorális szerv, a zsírtest különböző molekulákat választ ki, amelyek a kórokozók felismerésében, az immunfolyamatok szabályozásában és a mikrobák eliminációjában vesznek részt. A *Drosophila melanogaster* modellszervezetben három fő vérsejt típust különböztetünk meg: a fagocitózisban résztvevő plazmatocitákat, a melanizációban szerepet játszó kristálysejteket és a parazitoidok és idegen testek körül tokot képező lamellocitákat. A természetben a *Drosophila* fajokra a leggyakoribb veszélyt a parazitoid darazsak jelentik, melyek a fejlődő *Drosophila* lárvákba vagy bábokba helyezik petéjüket és tápanyagforrásként használják fel a légy szöveteit az egyedfejlődésükhöz. Ezért a parazitoidok elleni immunválaszok evolúciója elengedhetetlen a túléléshez. Egy ilyen evolúciós stratégia a jellegzetes morfológiájú és hatásmechanizmusú tokképző vérsejtek kifejlesztése.

Kimutattuk, hogy a sokmagvú óriás vérsejtekkel rendelkező fajok a *D. melanogaster*nél magasabb szintű rezisztenciát mutatnak parazitoid darázs-fertőzéssel szemben. Megfigyeltük, hogy a *D. melanogaster* tokképző lamellocitáival ellentétben, *D. ananassae*-ben terminálisan differenciálódott sokmagvú óriás vérsejtek csak parazitoid darázsfertőzés hatására jönnek létre, a kutikula sérülés nem indukálja képződésüket. Kísérleteink célja a sokmagvú óriás vérsejtek morfológiai, genetikai és funkcionális jellemzése volt. Transzmissziós elektronmikroszkópos vizsgálatokkal kimutattuk, hogy a *D. ananassae* sokmagvú óriás vérsejtek vezikulákban gazdag citoplazmával rendelkeznek, ahol nagyszámú, elektrondenz vezikula található. Megállapítottuk, hogy az elektrondenz vezikulák savas természetűek, multiform denz testeket képesek létrehozni, melyek elektrondenz összefüggő réteget alakítanak ki a parazitoidok felszínén. Megfigyeltük, hogy a sokmagvú óriás vérsejtek exoszómákat és mikrovezikulákat bocsátanak ki a hemolimfába, amelyeknek az effektor molekulák parazitoidhoz való szállításában lehet szerepük. A *D. ananassae* vérsejtek transzkriptomikai elemzése rámutatott a sokmagvú óriás vérsejtek magas energiaigényére, és kimutatta, hogy a JNK az egyetlen jelátviteli útvonal, amely ezekben a sejtekben expresszálódik.

Kimutattuk, hogy a sokmagvú óriás vérsejteket differenciáló *Drosophila* fajok a bakteriális eredetű citoletális duzzasztó toxin B (*cdtB*) alegységét kódoló gének mellett

Hemolysin E-szerű pórusképző toxinokat kódoló géneket (*hl*) is hordoznak. A *hl* gének és az általuk kódolt fehérjék kifejeződése parazitoid darázsfertőzést követően szignifikánsan megemelkedett, elsősorban a fő immunszövetekben: a vérsejtekben és a zsírtestben. Továbbá a HL fehérjék jelenlétét a parazitoidok felszínén is észleltük. Eredményeink arra utalnak, hogy a HL fehérjék résztvesznek a parazitoidok elleni immunválaszban. A prokariótáktól való azonnali génszerzés hatalmas evolúciós előnyt biztosíthat a parazitoidokkal folytatott koevolúciós harcban. Toxinok szerzése különösen hasznos az immunvédekezésben, így növelve a gazdaszervezet fitneszét.

A sokmagvú óriás vérsejtek nagyfokú hasonlóságot mutatnak az emlős óriássejtekkel, melyek makrofágok fúziójával jönnek létre. A sokmagvú óriás vérsejtek ultrastrukturális elemzése feltárta a számos vezikulával, denz testekkel, autofagoszómákkal és multivezikuláris testekkel rendelkező jellegzetes citoplazmájukat, amelyek mind az emlős óriássejtekre és megakariocitákra is jellemzőek. Felfedeztünk egy emperipolézisszerű jelenséget, amely során a plazmatociták az MGH-k citoplazmájába ágyazódnak. Ilyen folyamatot először a neutrofilek és megakariociták között írtak le. Az emlős óriássektek működéséhez elengedhetetlen ortológok magas szinten expresszálódnak a *Drosophila* sokmagvú óriás vérsejtekben, mint például a β integrin alegységek, a vakuoláris típusú H+-ATPáz alegységek és a cisztein-proteináz-1 enzim génjei. A *Z. indianus* sokmagvú óriás vérsejtek ultraszerkezete hasonló az emlős megakariocitákéhoz, mivel citoplazmájukban jellegzetes csatornahálózat található, amely kapcsolatban van az extracelluláris térrel, és mindkét sejttípus nagyszámú sejtmag nélküli fragmentumot képez és bocsát a hemolimfába. Továbbá azt találtuk, hogy a *Z. indianus* magnélküli fragmentumok felhalmozódtak a sebzések helyén, így hasonlóan az emlősök megakariocita eredetű vérlemezkéihez részt vesznek a sebgyógyulási folyamatokban. A *Z. indianus* vérsejtek transzkriptomikai elemzése számos olyan konstitutívan kifejeződő gént mutatott ki, amelyek homológjai *D. melanogaster*-ben vagy emlősökben sebgyógyulási és alvadási folyamatokban vesznek részt.

Eredményeink során a sokmagvú óriás vérsejtek szerkezeti, molekuláris és funkcionális tulajdonságaira derült fény. A sokmagvú óriás vérsejtek egy nem kanonikus, rendkívül hatékony immunválasz sejtes elemeinek alkotó részei számos *Drosophila* fajban. Továbbá a sokmagvú óriás vérsejtek vizsgálata hozzájárulhat az emlős óriássejtek eddig ismeretlen területeinek megismeréséhez.

VIII. Acknowledgements

First and foremost, I am profoundly grateful to my supervisor, Gyöngyi Cinege, for the opportunity to learn and practice a whole set of genetic and molecular techniques and for her guidance and tremendous help during the PhD study period and in writing the thesis. I am especially thankful to István Andó for the advice, guidance and help with my PhD work, thesis, and for the development of HL specific antibodies.

I would like to thank everyone who contributed to this work in any way. Many thanks to all my past and present colleagues from the Innate Immunity Group of the Biological Research Centre, for their support and help. I am grateful for the technical help and moral support to Olga Kovalcsik, Mónika Ilyés, Anita Balázs, and Henrietta Kovács.

I would like to thank all our collaborators, whose work helped me complete this work and I would like to highlight the contributions of: Attila Kovács, Zita Lerner, and Sarolta Pálfia (at the Department of Anatomy, Cell and Developmental Biology, Eötvös Loránd University, Budapest) for the generation and analysis of TEM samples; David Lukacsovich, Jochen Winterer, Tamás Lukacsovich and Csaba Földy (at the Laboratory of Neural Connectivity, Brain Research Institute, University of Zurich, Zurich, Switzerland) for the sequencing and technical help with the *D. ananassae* hemocyte transcriptome analysis; Nóra Zsindely, Gábor Nagy, and László Bodai (at the Department of Biochemistry and Molecular Biology, University of Szeged, Szeged) for the sequencing and technical help with the *Z. indianus* hemocyte transcriptome analysis; Zoltán Hegedűs (at the Laboratory of Bioinformatics, Biological Research Centre, Szeged) for the help with the transcriptome analyses; Dan Hultmark (at the Department of Molecular Biology, Umea University, Umea, Sweden) for the help with the interpretation of the transcriptome data; Zoltán Lipinszki and Edit Ábrahám (at the MTA SZBK Lendület Laboratory of Cell Cycle Regulation, Institute of Biochemistry, HUN-REN Biological Research Centre, Szeged) for the help in cloning, and for the expression and purification of the recombinant HL proteins; and Rebecca Tarnopol (at the Department of Plant and Microbial Biology, University of California, Berkeley, USA) for the phylogenetic analysis of the hemolysin E-like genes.

I express my appreciation to Dr. Vizler Csaba and Dr. Ferenc Jankovics for reading my thesis and for the constructive thoughts and comments they made.

Special thanks to my friends who made my time in Szeged more pleasant and bearable and encouraged me not to give up.

And last but not least, I convey my gratitude to my parents and grandparents for their moral and financial support filled with affection and encouragement throughout this difficult time.

Funding: This research was supported by the NKFI K128762 (G.C.) and the NKFI K135877 (I.A) grants from the Hungarian National Science Foundation and the HUN-REN Biological Research Centre, Institute of Genetics. I would also like to acknowledge my PhD funding from the University of Szeged.

IX. References

Adema, C.M., Hertel, L.A., Miller, R.D., Loker, E.S., 1997. A family of fibrinogen-related proteins that precipitates parasite-derived molecules is produced by an invertebrate after infection. Proc. Natl. Acad. Sci. 94, 8691–8696. https://doi.org/10.1073/pnas.94.16.8691

Agaisse, H., Petersen, U.M., Boutros, M., Mathey-Prevot, B., Perrimon, N., 2003. Signaling role of hemocytes in Drosophila JAK/STAT-dependent response to septic injury. Dev. Cell 5, 441–450. https://doi.org/10.1016/s1534-5807(03)00244-2

Ahmadzadeh, K., Vanoppen, M., Rose, C.D., Matthys, P., Wouters, C.H., 2022. Multinucleated Giant Cells: Current Insights in Phenotype, Biological Activities, and Mechanism of Formation. Front. Cell Dev. Biol. 10, 873226. https://doi.org/10.3389/fcell.2022.873226

Ahmed, M.Z., Li, S.-J., Xue, X., Yin, X.-J., Ren, S.-X., Jiggins, F.M., Greeff, J.M., Qiu, B.-L., 2015. The Intracellular Bacterium Wolbachia Uses Parasitoid Wasps as Phoretic Vectors for Efficient Horizontal Transmission. PLoS Pathog. 11, e1004672. https://doi.org/10.1371/journal.ppat.1004672

Altschul, S.F., Madden, T.L., Schäffer, A.A., Zhang, J., Zhang, Z., Miller, W., Lipman, D.J., 1997. Gapped BLAST and PSI-BLAST: a new generation of protein database search programs. Nucleic Acids Res. 25, 3389–3402. https://doi.org/10.1093/nar/25.17.3389

Amstrup, A.B., Bæk, I., Loeschcke, V., Givskov Sørensen, J., 2022. A functional study of the role of Turandot genes in Drosophila melanogaster: An emerging candidate mechanism for inducible heat tolerance. J. Insect Physiol. 143, 104456. https://doi.org/10.1016/j.jinsphys.2022.104456

Anatskaya, O.V., Vinogradov, A.E., 2022. Polyploidy as a Fundamental Phenomenon in Evolution, Development, Adaptation and Diseases. Int. J. Mol. Sci. 23. https://doi.org/10.3390/ijms23073542

Anderl, I., Vesala, L., Ihalainen, T.O., Vanha-aho, L.-M., Andó, I., Rämet, M., Hultmark, D., 2016. Transdifferentiation and Proliferation in Two Distinct Hemocyte Lineages in Drosophila melanogaster Larvae after Wasp Infection. PLOS Pathogens 12, e1005746. https://doi.org/10.1371/journal.ppat.1005746

Ao, J., Ling, E., Yu, X.-Q., 2007. Drosophila C-type Lectins Enhance Cellular Encapsulation. Mol. Immunol. 44, 2541–2548. https://doi.org/10.1016/j.molimm.2006.12.024

Arrese, E.L., Soulages, J.L., 2010. INSECT FAT BODY: ENERGY, METABOLISM, AND REGULATION. Annu. Rev. Entomol. 55, 207–225. https://doi.org/10.1146/annurev-ento-112408-085356

Babcock, D.T., Brock, A.R., Fish, G.S., Wang, Y., Perrin, L., Krasnow, M.A., Galko, M.J., 2008. Circulating blood cells function as a surveillance system for damaged tissue in Drosophila larvae. Proc. Natl. Acad. Sci. U. S. A. 105, 10017–10022. https://doi.org/10.1073/pnas.0709951105

Babišová, K., Mentelová, L., Geisseová, T.K., Beňová-Liszeková, D., Beňo, M., Chase, B.A., Farkaš, R., 2023. Apocrine secretion in the salivary glands of Drosophilidae

and other dipterans is evolutionarily conserved. Front. Cell Dev. Biol. 10, 1088055. https://doi.org/10.3389/fcell.2022.1088055

Bajgar, A., Kucerova, K., Jonatova, L., Tomcala, A., Schneedorferova, I., Okrouhlik, J., Dolezal, T., 2015. Extracellular Adenosine Mediates a Systemic Metabolic Switch during Immune Response. PLoS Biol. 13, e1002135. https://doi.org/10.1371/journal.pbio.1002135

Balog, J.Á., Honti, V., Kurucz, É., Kari, B., Puskás, L.G., Andó, I., Szebeni, G.J., 2021. Immunoprofiling of Drosophila Hemocytes by Single-cell Mass Cytometry. Genomics Proteomics Bioinformatics 19, 243–252. https://doi.org/10.1016/j.gpb.2020.06.022

Banerjee, U., Girard, J.R., Goins, L.M., Spratford, C.M., 2019. Drosophila as a Genetic Model for Hematopoiesis. Genetics 211, 367–417. https://doi.org/10.1534/genetics.118.300223

Bidla, G., Lindgren, M., Theopold, U., Dushay, M.S., 2005. Hemolymph coagulation and phenoloxidase in Drosophila larvae. Dev. Comp. Immunol. 29, 669–679. https://doi.org/10.1016/j.dci.2004.11.007

Bina, S., Zeidler, M., 2013. JAK/STAT Pathway Signalling in Drosophila Melanogaster, in: Madame Curie Bioscience Database [Internet]. Landes Bioscience.

Binari, R., Perrimon, N., 1994. Stripe-specific regulation of pair-rule genes by hopscotch, a putative Jak family tyrosine kinase in Drosophila. Genes Dev. 8, 300–312. https://doi.org/10.1101/gad.8.3.300

Boyle, E.I., Weng, S., Gollub, J., Jin, H., Botstein, D., Cherry, J.M., Sherlock, G., 2004. GO::TermFinder—open source software for accessing Gene Ontology information and finding significantly enriched Gene Ontology terms associated with a list of genes. Bioinforma. Oxf. Engl. 20, 3710–3715. https://doi.org/10.1093/bioinformatics/bth456

Bozler, J., Kacsoh, B.Z., Bosco, G., 2017. Nematocytes: Discovery and characterization of a novel anculeate hemocyte in Drosophila falleni and Drosophila phalerata. PLoS ONE 12, e0188133. https://doi.org/10.1371/journal.pone.0188133

Bragard, C., Baptista, P., Chatzivassiliou, E., Di Serio, F., Gonthier, P., Jaques Miret, J.A., Justesen, A.F., Magnusson, C.S., Milonas, P., Navas-Cortes, J.A., Parnell, S., Potting, R., Reignault, P.L., Stefani, E., Thulke, H., Van der Werf, W., Vicent Civera, A., Yuen, J., Zappalà, L., Grégoire, J., Malumphy, C., Kertesz, V., Maiorano, A., MacLeod, A., 2022. Pest categorisation of Zaprionus indianus. EFSA J. 20, e07144. https://doi.org/10.2903/j.efsa.2022.7144

Brodbeck, W.G., Anderson, J.M., 2009. GIANT CELL FORMATION AND FUNCTION. Curr. Opin. Hematol. 16, 53. https://doi.org/10.1097/MOH.0b013e32831ac52e

Brown, S., Hu, N., Hombría, J.C., 2001. Identification of the first invertebrate interleukin JAK/STAT receptor, the Drosophila gene domeless. Curr. Biol. CB 11, 1700–1705. https://doi.org/10.1016/s0960-9822(01)00524-3

Buchon, N., Poidevin, M., Kwon, H.-M., Guillou, A., Sottas, V., Lee, B.-L., Lemaitre, B., 2009. A single modular serine protease integrates signals from pattern-recognition receptors upstream of the Drosophila Toll pathway. Proc. Natl. Acad. Sci. U. S. A. 106, 12442–12447. https://doi.org/10.1073/pnas.0901924106

Canon, J., Banerjee, U., 2000. Runt and Lozenge function in Drosophila development. Semin. Cell Dev. Biol. 11, 327–336. https://doi.org/10.1006/scdb.2000.0185

Carareto, C.M., 2011. Tropical Africa as a cradle for horizontal transfers of transposable elements between species of the genera Drosophila and Zaprionus. Mob. Genet. Elem. 1, 179–186. https://doi.org/10.4161/mge.1.3.18052

Carton, Y., Bouletreau, M., Alphen, J., van Lenteren, J., 1986. The Drosophila parasitic wasps, in: The Genetics and Biology of Drosophila. pp. 347-394.

Cattenoz, P.B., Sakr, R., Pavlidaki, A., Delaporte, C., Riba, A., Molina, N., Hariharan, N., Mukherjee, T., Giangrande, A., 2020. Temporal specificity and heterogeneity of Drosophila immune cells. EMBO J. 39, e104486. https://doi.org/10.15252/embj.2020104486

Chambers, T.J., 1977. Fusion of macrophages following simultaneous attempted phagocytosis of glutaraldehyde-fixed red cells. J. Pathol. 122, 71–80. https://doi.org/10.1002/path.1711220204

Charrière, G.M., Ip, W.E., Dejardin, S., Boyer, L., Sokolovska, A., Cappillino, M.P., Cherayil, B.J., Podolsky, D.K., Kobayashi, K.S., Silverman, N., Lacy-Hulbert, A., Stuart, L.M., 2010. Identification of Drosophila Yin and PEPT2 as Evolutionarily Conserved Phagosome-associated Muramyl Dipeptide Transporters. J. Biol. Chem. 285, 20147–20154. https://doi.org/10.1074/jbc.M110.115584

Cho, B., Yoon, S.-H., Lee, Daewon, Koranteng, F., Tattikota, S.G., Cha, N., Shin, M., Do, H., Hu, Y., Oh, S.Y., Lee, Daehan, Vipin Menon, A., Moon, S.J., Perrimon, N., Nam, J.-W., Shim, J., 2020. Single-cell transcriptome maps of myeloid blood cell lineages in Drosophila. Nat. Commun. 11, 4483. https://doi.org/10.1038/s41467-020-18135-y

Choi, J.Y., Bubnell, J.E., Aquadro, C.F., 2015. Population Genomics of Infectious and Integrated Wolbachia pipientis Genomes in Drosophila ananassae. Genome Biol. Evol. 7, 2362–2382. https://doi.org/10.1093/gbe/evv158

Cinege, G., Lerner, Z., Magyar, L.B., Soós, B., Tóth, R., Kristó, I., Vilmos, P., Juhász, G., A.L., K., Hegedűs, Z., 2020. Cellular immune response involving multinucleated giant hemocytes with two-step genome amplification in the drosophilid Zaprionus indianus. J Innate Immun 25, 1–16. https://doi.org/10/gth4pw

Cinege, G., Magyar, L.B., Kovács, A.L., Lerner, Z., Juhász, G., Lukacsovich, D., Winterer, J., Lukacsovich, T., Hegedűs, Z., Kurucz, E., Hultmark, D., Földy, C., Andó, I., 2022. Broad ultrastructural and transcriptomic changes underlie the multinucleated giant hemocyte mediated innate immune response against parasitoids. J Innate Immun 14, 335–354. https://doi.org/10.1159/000520110

Cinege, G., Magyar, L.B., Kovacs, H., Varga, V., Bodai, L., Zsindely, N., Nagy, G., Hegedűs, Z., Hultmark, D., Andó, I., 2023. Distinctive features of Zaprionus indianus hemocyte differentiation and function revealed by transcriptomic analysis. Front Immunol 14. https://doi.org/10.3389/fimmu.2023.1322381

Coates, J.A., Brooks, E., Brittle, A.L., Armitage, E.L., Zeidler, M.P., Evans, I.R., 2021. Identification of functionally distinct macrophage subpopulations in Drosophila. eLife 10, e58686. https://doi.org/10.7554/eLife.58686

Colinet, D., Cazes, D., Belghazi, M., Gatti, J.-L., Poirié, M., 2011. Extracellular

Superoxide Dismutase in Insects. J. Biol. Chem. 286, 40110–40121. https://doi.org/10.1074/jbc.M111.288845

Colinet, D., Dubuffet, A., Cazes, D., Moreau, S., Drezen, J.-M., Poirié, M., 2009. A serpin from the parasitoid wasp Leptopilina boulardi targets the Drosophila phenoloxidase cascade. Dev. Comp. Immunol. 33, 681–689. https://doi.org/10.1016/j.dci.2008.11.013

Colinet, D., Schmitz, A., Depoix, D., Crochard, D., Poirié, M., 2007. Convergent Use of RhoGAP Toxins by Eukaryotic Parasites and Bacterial Pathogens. PLoS Pathog. 3, e203. https://doi.org/10.1371/journal.ppat.0030203

Comeault, A.A., Wang, J., Tittes, S., Isbell, K., Ingley, S., Hurlbert, A.H., Matute, D.R., 2020. Genetic Diversity and Thermal Performance in Invasive and Native Populations of African Fig Flies. Mol. Biol. Evol. 37, 1893–1906. https://doi.org/10.1093/molbev/msaa050

Cooper, D., Eleftherianos, I., 2017. Memory and Specificity in the Insect Immune System: Current Perspectives and Future Challenges. Front. Immunol. 8, 539. https://doi.org/10.3389/fimmu.2017.00539

Costa, C.A.M., Wang, X.-F., Ellsworth, C., Deng, W.-M., 2022. Polyploidy in development and tumor models in Drosophila. Semin. Cancer Biol. 81, 106–118. https://doi.org/10.1016/j.semcancer.2021.09.011

Cramer, E.M., Norol, F., Guichard, J., Breton-Gorius, J., Vainchenker, W., Massé, J.-M., Debili, N., 1997. Ultrastructure of Platelet Formation by Human Megakaryocytes Cultured With the Mpl Ligand. Blood 89, 2336–2346. https://doi.org/10.1182/blood.V89.7.2336

Crisp, A., Boschetti, C., Perry, M., Tunnacliffe, A., Micklem, G., 2015. Expression of multiple horizontally acquired genes is a hallmark of both vertebrate and invertebrate genomes. Genome Biol. 16, 50. https://doi.org/10.1186/s13059-015-0607-3

Csordás, G., Gábor, E., Honti, V., 2021. There and back again: The mechanisms of differentiation and transdifferentiation in Drosophila blood cells. Dev. Biol. 469, 135–143. https://doi.org/10.1016/j.ydbio.2020.10.006

Cunin, P., Nigrovic, P.A., 2020. Megakaryocyte emperipolesis: a new frontier in cell-in-cell interaction. Platelets 31, 700–706. https://doi.org/10.1080/09537104.2019.1693035

Dayan, D., Buchner, A., Garlick, J., 1989. Touton-like giant cells in periapical granulomas. J. Endod. 15, 210–211. https://doi.org/10.1016/S0099-2399(89)80237-7

De Gregorio, E., Spellman, P.T., Tzou, P., Rubin, G.M., Lemaitre, B., 2002. The Toll and Imd pathways are the major regulators of the immune response in Drosophila. EMBO J. 21, 2568–2579. https://doi.org/10.1093/emboj/21.11.2568

Delmastro-Greenwood, M.M., Piganelli, J.D., 2013. Changing the energy of an immune response. Am. J. Clin. Exp. Immunol. 2, 30–54.

Deng, Y., Adam, V., Nepovimova, E., Heger, Z., Valko, M., Wu, Q., Wei, W., Kuca, K., 2023. c-Jun N-terminal kinase signaling in cellular senescence. Arch. Toxicol. 97, 2089–2109. https://doi.org/10.1007/s00204-023-03540-1

Deprá, M., Panzera, Y., Ludwig, A., Valente, V.L.S., Loreto, E.L.S., 2010. Hosimary: a

new hAT transposon group involved in horizontal transfer. Mol. Genet. Genomics MGG 283, 451–459. https://doi.org/10.1007/s00438-010-0531-x

Di Lelio, I., Illiano, A., Astarita, F., Gianfranceschi, L., Horner, D., Varricchio, P., Amoresano, A., Pucci, P., Pennacchio, F., Caccia, S., 2019. Evolution of an insect immune barrier through horizontal gene transfer mediated by a parasitic wasp. PLoS Genet. 15, e1007998. https://doi.org/10.1371/journal.pgen.1007998

Di Tommaso, P., Moretti, S., Xenarios, I., Orobitg, M., Montanyola, A., Chang, J.-M., Taly, J.-F., Notredame, C., 2011. T-Coffee: a web server for the multiple sequence alignment of protein and RNA sequences using structural information and homology extension. Nucleic Acids Res. 39, W13–W17. https://doi.org/10.1093/nar/gkr245

DiAngelo, J.R., Bland, M.L., Bambina, S., Cherry, S., Birnbaum, M.J., 2009. The immune response attenuates growth and nutrient storage in Drosophila by reducing insulin signaling. Proc. Natl. Acad. Sci. U. S. A. 106, 20853–20858. https://doi.org/10.1073/pnas.0906749106

Dostálová, A., Rommelaere, S., Poidevin, M., Lemaitre, B., 2017. Thioester-containing proteins regulate the Toll pathway and play a role in Drosophila defence against microbial pathogens and parasitoid wasps. BMC Biol. 15, 79. https://doi.org/10.1186/s12915-017-0408-0

Dudzic, J.P., Kondo, S., Ueda, R., Bergman, C.M., Lemaitre, B., 2015. Drosophila innate immunity: regional and functional specialization of prophenoloxidases. BMC Biol. 13, 81. https://doi.org/10.1186/s12915-015-0193-6

Dunning Hotopp, J.C., Clark, M.E., Oliveira, D.C.S.G., Foster, J.M., Fischer, P., Muñoz Torres, M.C., Giebel, J.D., Kumar, N., Ishmael, N., Wang, S., Ingram, J., Nene, R.V., Shepard, J., Tomkins, J., Richards, S., Spiro, D.J., Ghedin, E., Slatko, B.E., Tettelin, H., Werren, J.H., 2007. Widespread lateral gene transfer from intracellular bacteria to multicellular eukaryotes. Science 317, 1753–1756. https://doi.org/10.1126/science.1142490

Dushay, M.S., 2009. Insect hemolymph clotting. Cell. Mol. Life Sci. 66, 2643–2650. https://doi.org/10.1007/s00018-009-0036-0

Duvic, B., Hoffmann, J.A., Meister, M., Royet, J., 2002. Notch signaling controls lineage specification during Drosophila larval hematopoiesis. Curr. Biol. CB 12, 1923–1927. https://doi.org/10.1016/s0960-9822(02)01297-6

Dziedziech, A., Theopold, U., 2022. Proto-pyroptosis: An Ancestral Origin for Mammalian Inflammatory Cell Death Mechanism in Drosophila melanogaster. J. Mol. Biol. 434, 167333. https://doi.org/10.1016/j.jmb.2021.167333

Edgar, R.C., 2004. MUSCLE: a multiple sequence alignment method with reduced time and space complexity. BMC Bioinformatics 5, 113. https://doi.org/10.1186/1471-2105-5-113

Ekengren, S., Hultmark, D., 2001. A family of Turandot-related genes in the humoral stress response of Drosophila. Biochem. Biophys. Res. Commun. 284, 998–1003. https://doi.org/10.1006/bbrc.2001.5067

Ekengren, S., Tryselius, Y., Dushay, M.S., Liu, G., Steiner, H., Hultmark, D., 2001. A humoral stress response in Drosophila. Curr. Biol. 11, 714–718.

https://doi.org/10.1016/S0960-9822(01)00203-2
Eleftherianos, I., Heryanto, C., Bassal, T., Zhang, W., Tettamanti, G., Mohamed, A., 2021. Haemocyte-mediated immunity in insects: Cells, processes and associated components in the fight against pathogens and parasites. Immunology 164, 401–432. https://doi.org/10.1111/imm.13390
Eliades, A., Papadantonakis, N., Ravid, K., 2010. New Roles for Cyclin E in Megakaryocytic Polyploidization. J. Biol. Chem. 285, 18909–18917. https://doi.org/10.1074/jbc.M110.102145
Evans, C.J., Hartenstein, V., Banerjee, U., 2003. Thicker Than Blood: Conserved Mechanisms in Drosophila and Vertebrate Hematopoiesis. Dev. Cell 5, 673–690. https://doi.org/10.1016/S1534-5807(03)00335-6
Evans, C.J., Liu, T., Girard, J.R., Banerjee, U., 2022. Injury-induced inflammatory signaling and hematopoiesis in Drosophila. Proceedings of the National Academy of Sciences 119, e2119109119. https://doi.org/10.1073/pnas.2119109119
Fader, C.M., Colombo, M.I., 2009. Autophagy and multivesicular bodies: two closely related partners. Cell Death Differ. 16, 70–78. https://doi.org/10.1038/cdd.2008.168
Fessler, L.I., Nelson, R.E., Fessler, J.H., 1994. Drosophila extracellular matrix. Methods Enzymol. 245, 271–294. https://doi.org/10.1016/0076-6879(94)45016-1
Franz, A., Wood, W., Martin, P., 2018. Fat Body Cells Are Motile and Actively Migrate to Wounds to Drive Repair and Prevent Infection. Dev. Cell 44, 460-470.e3. https://doi.org/10.1016/j.devcel.2018.01.026
Fu, Y., Huang, X., Zhang, P., van de Leemput, J., Han, Z., 2020. Single-cell RNA sequencing identifies novel cell types in Drosophila blood. J. Genet. Genomics 47, 175–186. https://doi.org/10.1016/j.jgg.2020.02.004
Galko, M.J., Krasnow, M.A., 2004. Cellular and Genetic Analysis of Wound Healing in Drosophila Larvae. PLoS Biol. 2, e239. https://doi.org/10.1371/journal.pbio.0020239
Garg, A., Wu, L.P., 2014. Drosophila Rab14 mediates phagocytosis in the immune response to Staphylococcus aureus. Cell. Microbiol. 16, 296–310. https://doi.org/10.1111/cmi.12220
Genova, J.L., Jong, S., Camp, J.T., Fehon, R.G., 2000. Functional analysis of Cdc42 in actin filament assembly, epithelial morphogenesis, and cell signaling during Drosophila development. Dev. Biol. 221, 181–194. https://doi.org/10.1006/dbio.2000.9671
González-Gualda, E., Baker, A.G., Fruk, L., Muñoz-Espín, D., 2021. A guide to assessing cellular senescence in vitro and in vivo. FEBS J. 288, 56–80. https://doi.org/10.1111/febs.15570
Govind, S., 2008. Innate immunity in Drosophila: Pathogens and pathways. Insect Sci. Online 15, 29–43. https://doi.org/10.1111/j.1744-7917.2008.00185.x
Gregory, G.D., Miccio, A., Bersenev, A., Wang, Y., Hong, W., Zhang, Z., Poncz, M., Tong, W., Blobel, G.A., 2010. FOG1 requires NuRD to promote hematopoiesis and maintain lineage fidelity within the megakaryocytic-erythroid compartment. Blood 115, 2156–2166. https://doi.org/10.1182/blood-2009-10-251280
Gupta, G., Athanikar, S.B., Pai, V.V., Naveen, K.N., 2014. Giant Cells in Dermatology.

Indian J. Dermatol. 59, 481–484. https://doi.org/10.4103/0019-5154.139887
Gupta, V., Frank, A.M., Matolka, N., Lazzaro, B.P., 2022. Inherent constraints on a polyfunctional tissue lead to a reproduction-immunity tradeoff. BMC Biol. 20, 127. https://doi.org/10.1186/s12915-022-01328-w
Haller, S., Franchet, A., Hakkim, A., Chen, J., Drenkard, E., Yu, S., Schirmeier, S., Li, Z., Martins, N., Ausubel, F.M., Liégeois, S., Ferrandon, D., 2018. Quorum-sensing regulator RhlR but not its autoinducer RhlI enables Pseudomonas to evade opsonization. EMBO Rep. 19, e44880. https://doi.org/10.15252/embr.201744880
Hanson, M.A., Lemaitre, B., 2020. New insights on Drosophila antimicrobial peptide function in host defense and beyond. Curr. Opin. Immunol. 62, 22–30. https://doi.org/10.1016/j.coi.2019.11.008
Harkel, B. ten, Schoenmaker, T., Picavet, D.I., Davison, N.L., Vries, T.J. de, Everts, V., 2015. The Foreign Body Giant Cell Cannot Resorb Bone, But Dissolves Hydroxyapatite Like Osteoclasts. PLoS ONE 10. https://doi.org/10.1371/journal.pone.0139564
Harnish, J.M., Link, N., Yamamoto, S., 2021. Drosophila as a Model for Infectious Diseases. Int. J. Mol. Sci. 22, 2724. https://doi.org/10.3390/ijms22052724
Herrera, S.C., Bach, E.A., 2021. The Emerging Roles of JNK Signaling in Drosophila Stem Cell Homeostasis. Int. J. Mol. Sci. 22, 5519. https://doi.org/10.3390/ijms22115519
Hoffmann, J.A., Kafatos, F.C., Janeway, C.A., Ezekowitz, R.A.B., 1999. Phylogenetic Perspectives in Innate Immunity. Science 284, 1313–1318. https://doi.org/10.1126/science.284.5418.1313
Honti, V., Csordás, G., Márkus, R., Kurucz, É., Jankovics, F., Andó, I., 2010. Cell lineage tracing reveals the plasticity of the hemocyte lineages and of the hematopoietic compartments in Drosophila melanogaster. Mol. Immunol. 47, 1997–2004. https://doi.org/10.1016/j.molimm.2010.04.017
Hultmark, D., Andó, I., 2022. Hematopoietic plasticity mapped in Drosophila and other insects. eLife 11, e78906. https://doi.org/10.7554/eLife.78906
Hunt, S., Green, J., Artymiuk, P.J., 2010. Hemolysin E (HlyE, ClyA, SheA) and related toxins. Adv. Exp. Med. Biol. 677, 116–126. https://doi.org/10.1007/978-1-4419-6327-7_10
Ishimaru, S., Ueda, R., Hinohara, Y., Ohtani, M., Hanafusa, H., 2004. PVR plays a critical role via JNK activation in thorax closure during Drosophila metamorphosis. EMBO J. 23, 3984–3994. https://doi.org/10.1038/sj.emboj.7600417
Italiano, J.E., Lecine, P., Shivdasani, R.A., Hartwig, J.H., 1999. Blood Platelets Are Assembled Principally at the Ends of Proplatelet Processes Produced by Differentiated Megakaryocytes. J. Cell Biol. 147, 1299–1312.
Janeway, C.A., Medzhitov, R., 2002. Innate Immune Recognition. Annu. Rev. Immunol. 20, 197–216. https://doi.org/10.1146/annurev.immunol.20.083001.084359
Janiszewski, T., Kołt, S., Ciastoń, I., Vizovisek, M., Poręba, M., Turk, B., Drąg, M., Kozieł, J., Kasperkiewicz, P., 2023. Investigation of osteoclast cathepsin K activity in osteoclastogenesis and bone loss using a set of chemical reagents. Cell Chem. Biol. 30, 159-174.e8. https://doi.org/10.1016/j.chembiol.2023.01.001

Jezowska, B., Fernández, B.G., Amândio, A.R., Duarte, P., Mendes, C., Brás-Pereira, C., Janody, F., 2011. A dual function of Drosophila capping protein on DE-cadherin maintains epithelial integrity and prevents JNK-mediated apoptosis. Dev. Biol. 360, 143–159. https://doi.org/10.1016/j.ydbio.2011.09.016

Jiravanichpaisal, P., Lee, B.L., Söderhäll, K., 2006. Cell-mediated immunity in arthropods: Hematopoiesis, coagulation, melanization and opsonization. Immunobiology 211, 213–236. https://doi.org/10.1016/j.imbio.2005.10.015

Jumper, J., Evans, R., Pritzel, A., Green, T., Figurnov, M., Ronneberger, O., Tunyasuvunakool, K., Bates, R., Žídek, A., Potapenko, A., Bridgland, A., Meyer, C., Kohl, S.A.A., Ballard, A.J., Cowie, A., Romera-Paredes, B., Nikolov, S., Jain, R., Adler, J., Back, T., Petersen, S., Reiman, D., Clancy, E., Zielinski, M., Steinegger, M., Pacholska, M., Berghammer, T., Bodenstein, S., Silver, D., Vinyals, O., Senior, A.W., Kavukcuoglu, K., Kohli, P., Hassabis, D., 2021. Highly accurate protein structure prediction with AlphaFold. Nature 596, 583–589. https://doi.org/10.1038/s41586-021-03819-2

Kacsoh, B.Z., Bozler, J., Schlenke, T.A., 2014. A role for nematocytes in the cellular immune response of the Drosophilid Zaprionus indianus. Parasitology 141, 697–715. https://doi.org/10.1017/S0031182013001431

Kacsoh, B.Z., Schlenke, T.A., 2012. High Hemocyte Load Is Associated with Increased Resistance against Parasitoids in Drosophila suzukii, a Relative of D. melanogaster. PLoS ONE 7, e34721. https://doi.org/10.1371/journal.pone.0034721

Kakanj, P., Bhide, S., Moussian, B., Leptin, M., 2022. Autophagy–mediated plasma membrane removal promotes the formation of epithelial syncytia. EMBO J. 41, e109992. https://doi.org/10.15252/embj.2021109992

Kambris, Z., Brun, S., Jang, I.-H., Nam, H.-J., Romeo, Y., Takahashi, K., Lee, W.-J., Ueda, R., Lemaitre, B., 2006. Drosophila immunity: a large-scale in vivo RNAi screen identifies five serine proteases required for Toll activation. Curr. Biol. CB 16, 808–813. https://doi.org/10.1016/j.cub.2006.03.020

Kaneko, T., Silverman, N., 2005. Bacterial recognition and signalling by the Drosophila IMD pathway. Cell. Microbiol. 7, 461–469. https://doi.org/10.1111/j.1462-5822.2005.00504.x

Kinoshita, Y., Shiratsuchi, N., Araki, M., Inoue, Y.H., 2023. Anti-Tumor Effect of Turandot Proteins Induced via the JAK/STAT Pathway in the mxc Hematopoietic Tumor Mutant in Drosophila. Cells 12, 2047. https://doi.org/10.3390/cells12162047

Klasson, L., Kumar, N., Bromley, R., Sieber, K., Flowers, M., Ott, S.H., Tallon, L.J., Andersson, S.G.E., Dunning Hotopp, J.C., 2014. Extensive duplication of the Wolbachia DNA in chromosome four of Drosophila ananassae. BMC Genomics 15, 1097. https://doi.org/10.1186/1471-2164-15-1097

Kleino, A., Valanne, S., Ulvila, J., Kallio, J., Myllymäki, H., Enwald, H., Stöven, S., Poidevin, M., Ueda, R., Hultmark, D., Lemaitre, B., Rämet, M., 2005. Inhibitor of apoptosis 2 and TAK1-binding protein are components of the Drosophila Imd pathway. EMBO J. 24, 3423–3434. https://doi.org/10.1038/sj.emboj.7600807

Kloc, M., Uosef, A., Subuddhi, A., Kubiak, J.Z., Piprek, R.P., Ghobrial, R.M., 2022. Giant

Multinucleated Cells in Aging and Senescence—An Abridgement. Biology 11, 1121. https://doi.org/10.3390/biology11081121

Kosoff, R.E., Aslan, J.E., Kostyak, J.C., Dulaimi, E., Chow, H.Y., Prudnikova, T.Y., Radu, M., Kunapuli, S.P., McCarty, O.J.T., Chernoff, J., 2015. Pak2 restrains endomitosis during megakaryopoiesis and alters cytoskeleton organization. Blood 125, 2995–3005. https://doi.org/10.1182/blood-2014-10-604504

Kraaijeveld, A.R., Elrayes, N.P., Schuppe, H., Newland, P.L., 2011. L-arginine enhances immunity to parasitoids in Drosophila melanogaster and increases NO production in lamellocytes. Dev. Comp. Immunol. 35, 857–864. https://doi.org/10.1016/j.dci.2011.03.019

Krejčová, G., Danielová, A., Nedbalová, P., Kazek, M., Strych, L., Chawla, G., Tennessen, J.M., Lieskovská, J., Jindra, M., Doležal, T., Bajgar, A., 2019. Drosophila macrophages switch to aerobic glycolysis to mount effective antibacterial defense. eLife 8, e50414. https://doi.org/10.7554/eLife.50414

Kurtz, J., 2005. Specific memory within innate immune systems. Trends Immunol. 26, 186–192. https://doi.org/10.1016/j.it.2005.02.001Kurucz, E., Váczi, B., Márkus, R., Laurinyecz, B., Vilmos, P., Zsámboki, J., Csorba, K., Gateff, E., Hultmark, D., Andó, I., 2007a. Definition of Drosophila hemocyte subsets by cell-type specific antigens. Acta Biol. Hung. 58 Suppl, 95–111. https://doi.org/10.1556/ABiol.58.2007.Suppl.8

Kurucz, É., Márkus, R., Zsámboki, J., Folkl-Medzihradszky, K., Darula, Z., Vilmos, P., Udvardy, A., Krausz, I., Lukacsovich, T., Gateff, E., Zettervall, C.-J., Hultmark, D., Andó, I., 2007b. Nimrod, a Putative Phagocytosis Receptor with EGF Repeats in Drosophila Plasmatocytes. Current Biology 17, 649–654. https://doi.org/10.1016/j.cub.2007.02.041

Kúthy-Sutus, E., Kharrat, B., Gábor, E., Csordás, G., Sinka, R., Honti, V., 2022. A Novel Method for Primary Blood Cell Culturing and Selection in Drosophila melanogaster. Cells 12, 24. https://doi.org/10.3390/cells12010024

Kvell, K., Cooper, EL., Engelmann, P., Bovari, J., Nemeth, P., 2007. Blurring Borders: Innate Immunity with Adaptive Features. Clin. Dev. Immunol. 2007, 83671. https://doi.org/10.1155/2007/83671

La Marca, J.E., Richardson, H.E., 2020. Two-Faced: Roles of JNK Signalling During Tumourigenesis in the Drosophila Model. Front. Cell Dev. Biol. 8, 42. https://doi.org/10.3389/fcell.2020.00042

Lai, X.-H., Arencibia, I., Johansson, A., Wai, S.N., Oscarsson, J., Kalfas, S., Sundqvist, K.-G., Mizunoe, Y., Sjöstedt, A., Uhlin, B.E., 2000. Cytocidal and Apoptotic Effects of the ClyA Protein from Escherichia coli on Primary and Cultured Monocytes and Macrophages. Infect. Immun. 68, 4363–4367.

Langhans, Th., 1868. Ueber Riesenzellen mit wandständigen Kernen in Tuberkeln und die fibröse Form des Tuberkels. Arch. Für Pathol. Anat. Physiol. Für Klin. Med. 42, 382–404. https://doi.org/10.1007/BF02006420

Lanot, R., Zachary, D., Holder, F., Meister, M., 2001. Postembryonic hematopoiesis in Drosophila. Dev. Biol. 230, 243–257. https://doi.org/10.1006/dbio.2000.0123

Lavine, M.D., Strand, M.R., 2002. Insect hemocytes and their role in immunity. Insect

Biochem. Mol. Biol., Recent Progress in Insect Molecular Biology 32, 1295–1309. https://doi.org/10.1016/S0965-1748(02)00092-9

Lebestky, T., Chang, T., Hartenstein, V., Banerjee, U., 2000. Specification of Drosophila Hematopoietic Lineage by Conserved Transcription Factors. Science 288, 146–149. https://doi.org/10.1126/science.288.5463.146

Leitão, A.B., Arunkumar, R., Day, J.P., Geldman, E.M., Morin-Poulard, I., Crozatier, M., Jiggins, F.M., 2020. Constitutive activation of cellular immunity underlies the evolution of resistance to infection in Drosophila. eLife 9, e59095. https://doi.org/10.7554/eLife.59095

Lerner, Z., 2020. Egy új vérsejt típus, a sokmagvú óriássejt szerepe a Drosophila sejt-közvetítette immunválaszában (PhD diss.). University of Szeged, Szeged.

Letourneau, M., Lapraz, F., Sharma, A., Vanzo, N., Waltzer, L., Crozatier, M., 2016. Drosophila hematopoiesis under normal conditions and in response to immune stress. FEBS Lett. 590, 4034–4051. https://doi.org/10.1002/1873-3468.12327

Li, J.L., Zarbock, A., Hidalgo, A., 2017. Platelets as autonomous drones for hemostatic and immune surveillance. J. Exp. Med. 214, 2193–2204. https://doi.org/10.1084/jem.20170879

Li, S., Yu, X., Feng, Q., 2019. Fat Body Biology in the Last Decade. Annu. Rev. Entomol. 64, 315–333. https://doi.org/10.1146/annurev-ento-011118-112007

Li, W., 2021. Dscam in arthropod immune priming: What is known and what remains unknown. Dev. Comp. Immunol. 125, 104231. https://doi.org/10.1016/j.dci.2021.104231

Li, W., Godzik, A., 2006. Cd-hit: a fast program for clustering and comparing large sets of protein or nucleotide sequences. Bioinformatics 22, 1658–1659. https://doi.org/10.1093/bioinformatics/btl158

Lipinszki, Z., Vernyik, V., Farago, N., Sari, T., Puskas, L.G., Blattner, F.R., Posfai, G., Gyorfy, Z., 2018. Enhancing the Translational Capacity of E. coli by Resolving the Codon Bias. ACS Synth. Biol. 7, 2656–2664. https://doi.org/10.1021/acssynbio.8b00332

Loof, T.G., Schmidt, O., Herwald, H., Theopold, U., 2011. Coagulation Systems of Invertebrates and Vertebrates and Their Roles in Innate Immunity: The Same Side of Two Coins? J. Innate Immun. 3, 34–40. https://doi.org/10.1159/000321641

Losick, V.P., Fox, D.T., Spradling, A.C., 2013. Polyploidization and cell fusion contribute to wound healing in the adult Drosophila epithelium. Curr. Biol. CB 23, 2224–2232. https://doi.org/10.1016/j.cub.2013.09.029

Lu, Y., Su, F., Li, Q., Zhang, J., Li, Y., Tang, T., Hu, Q., Yu, X.-Q., 2020. Pattern recognition receptors in Drosophila immune responses. Dev. Comp. Immunol. 102, 103468. https://doi.org/10.1016/j.dci.2019.103468

Ma, X., Shao, Y., Zheng, H., Li, M., Li, W., Xue, L., 2013. Src42A modulates tumor invasion and cell death via Ben/dUev1a-mediated JNK activation in Drosophila. Cell Death Dis. 4, e864. https://doi.org/10.1038/cddis.2013.392

Macaulay, I.C., Thon, J.N., Tijssen, M.R., Steele, B.M., MacDonald, B.T., Meade, G., Burns, P., Rendon, A., Salunkhe, V., Murphy, R.P., Bennett, C., Watkins, N.A., He, X., Fitzgerald, D.J., Italiano, J.E., Maguire, P.B., 2013. Canonical Wnt signaling in

megakaryocytes regulates proplatelet formation. Blood 121, 188–196. https://doi.org/10.1182/blood-2012-03-416875
Machlus, K.R., Italiano, J.E., 2013. The incredible journey: From megakaryocyte development to platelet formation. J. Cell Biol. 201, 785–796. https://doi.org/10.1083/jcb.201304054
Makhijani, K., Alexander, B., Rao, D., Petraki, S., Herboso, L., Kukar, K., Batool, I., Wachner, S., Gold, K.S., Wong, C., O'Connor, M.B., Brückner, K., 2017. Regulation of Drosophila hematopoietic sites by Activin-β from active sensory neurons. Nat. Commun. 8, 15990. https://doi.org/10.1038/ncomms15990
Makhijani, K., Alexander, B., Tanaka, T., Rulifson, E., Brückner, K., 2011. The peripheral nervous system supports blood cell homing and survival in the Drosophila larva. Development 138, 5379–5391. https://doi.org/10.1242/dev.067322
Márkus, R., Kurucz, É., Rus, F., Andó, I., 2005. Sterile wounding is a minimal and sufficient trigger for a cellular immune response in Drosophila melanogaster. Immunology Letters 101, 108–111. https://doi.org/10.1016/j.imlet.2005.03.021
Márkus, R., Laurinyecz, B., Kurucz, É., Honti, V., Bajusz, I., Sipos, B., Somogyi, K., Kronhamn, J., Hultmark, D., Andó, I., 2009. Sessile hemocytes as a hematopoietic compartment in Drosophila melanogaster. Proc. Natl. Acad. Sci. 106, 4805–4809. https://doi.org/10.1073/pnas.0801766106
Márkus, R., Lerner, Z., Honti, V., Csordás, G., Zsámboki, J., Cinege, G., Párducz, Á., Lukacsovich, T., Kurucz, É., Andó, I., 2015. Multinucleated Giant Hemocytes Are Effector Cells in Cell-Mediated Immune Responses of Drosophila. J. Innate Immun. 7, 340–353. https://doi.org/10.1159/000369618
McDonald, M.M., Kim, A.S., Mulholland, B.S., Rauner, M., 2021. New Insights Into Osteoclast Biology. JBMR Plus 5, e10539. https://doi.org/10.1002/jbm4.10539
McKean, K.A., Yourth, C.P., Lazzaro, B.P., Clark, A.G., 2008. The evolutionary costs of immunological maintenance and deployment. BMC Evol. Biol. 8, 76. https://doi.org/10.1186/1471-2148-8-76
Meister, M., 2004. Blood cells of Drosophila: cell lineages and role in host defence. Curr. Opin. Immunol. 16, 10–15. https://doi.org/10.1016/j.coi.2003.11.002
Melcarne, C., Lemaitre, B., Kurant, E., 2019. Phagocytosis in Drosophila: From molecules and cellular machinery to physiology. Insect Biochem. Mol. Biol. 109, 1–12. https://doi.org/10.1016/j.ibmb.2019.04.002
Melillo, D., Marino, R., Italiani, P., Boraschi, D., 2018. Innate Immune Memory in Invertebrate Metazoans: A Critical Appraisal. Front. Immunol. 9, 1915. https://doi.org/10.3389/fimmu.2018.01915
Meschi, E., Delanoue, R., 2021. Adipokine and fat body in flies: Connecting organs. Mol. Cell. Endocrinol. 533, 111339. https://doi.org/10.1016/j.mce.2021.111339
Miller, M.A., Pfeiffer, W., Schwartz, T., 2010. Creating the CIPRES Science Gateway for inference of large phylogenetic trees, in: 2010 Gateway Computing Environments Workshop (GCE). Presented at the 2010 Gateway Computing Environments Workshop (GCE), pp. 1–8. https://doi.org/10.1109/GCE.2010.5676129
Moran, Y., Fredman, D., Szczesny, P., Grynberg, M., Technau, U., 2012. Recurrent Horizontal Transfer of Bacterial Toxin Genes to Eukaryotes. Mol. Biol. Evol. 29,

2223–2230. https://doi.org/10.1093/molbev/mss089
Mortimer, N.T., Goecks, J., Kacsoh, B.Z., Mobley, J.A., Bowersock, G.J., Taylor, J., Schlenke, T.A., 2013. Parasitoid wasp venom SERCA regulates Drosophila calcium levels and inhibits cellular immunity. Proc. Natl. Acad. Sci. U. S. A. 110, 9427–9432. https://doi.org/10.1073/pnas.1222351110
Mukherjee, S., Zheng, H., Derebe, M., Callenberg, K., Partch, C.L., Rollins, D., Propheter, D.C., Rizo, J., Grabe, M., Jiang, Q.-X., Hooper, L.V., 2014. Antibacterial membrane attack by a pore-forming intestinal C-type lectin. Nature 505, 103–107. https://doi.org/10.1038/nature12729
Murase, K., 2022. Cytolysin A (ClyA): A Bacterial Virulence Factor with Potential Applications in Nanopore Technology, Vaccine Development, and Tumor Therapy. Toxins 14, 78. https://doi.org/10.3390/toxins14020078
Murray, P.J., Allen, J.E., Biswas, S.K., Fisher, E.A., Gilroy, D.W., Goerdt, S., Gordon, S., Hamilton, J.A., Ivashkiv, L.B., Lawrence, T., Locati, M., Mantovani, A., Martinez, F.O., Mege, J.-L., Mosser, D.M., Natoli, G., Saeij, J.P., Schultze, J.L., Shirey, K.A., Sica, A., Suttles, J., Udalova, I., van Ginderachter, J.A., Vogel, S.N., Wynn, T.A., 2014. Macrophage Activation and Polarization: Nomenclature and Experimental Guidelines. Immunity 41, 14–20. https://doi.org/10.1016/j.immuni.2014.06.008
Nagaosa, K., Okada, R., Nonaka, S., Takeuchi, K., Fujita, Y., Miyasaka, T., Manaka, J., Ando, I., Nakanishi, Y., 2011. Integrin βv-mediated Phagocytosis of Apoptotic Cells in Drosophila Embryos*. J. Biol. Chem. 286, 25770–25777. https://doi.org/10.1074/jbc.M110.204503
Nam, H.-J., Jang, I.-H., Asano, T., Lee, W.-J., 2008. Involvement of pro-phenoloxidase 3 in lamellocyte-mediated spontaneous melanization in Drosophila. Mol. Cells 26, 606–610.
Nam, H.-J., Jang, I.-H., You, H., Lee, K.-A., Lee, W.-J., 2012. Genetic evidence of a redox-dependent systemic wound response via Hayan Protease-Phenoloxidase system in Drosophila. EMBO J. 31, 1253–1265. https://doi.org/10.1038/emboj.2011.476
Nászai, M., Carroll, L.R., Cordero, J.B., 2015. Intestinal stem cell proliferation and epithelial homeostasis in the adult Drosophila midgut. Insect Biochem. Mol. Biol. 67, 9–14. https://doi.org/10.1016/j.ibmb.2015.05.016
Nguyen, L.-T., Schmidt, H.A., von Haeseler, A., Minh, B.Q., 2015. IQ-TREE: A Fast and Effective Stochastic Algorithm for Estimating Maximum-Likelihood Phylogenies. Mol. Biol. Evol. 32, 268–274. https://doi.org/10.1093/molbev/msu300
Nickerson, D.P., Brett, C.L., Merz, A.J., 2009. Vps-C complexes: gatekeepers of endolysosomal traffic. Curr. Opin. Cell Biol. 21, 543–551. https://doi.org/10.1016/j.ceb.2009.05.007
Nonaka, S., Nagaosa, K., Mori, T., Shiratsuchi, A., Nakanishi, Y., 2013. Integrin αPS3/βv-mediated Phagocytosis of Apoptotic Cells and Bacteria in Drosophila*. J. Biol. Chem. 288, 10374–10380. https://doi.org/10.1074/jbc.M113.451427
Nordman, J., Li, S., Eng, T., MacAlpine, D., Orr-Weaver, T.L., 2011. Developmental control of the DNA replication and transcription programs. Genome Res. 21, 175–181. https://doi.org/10.1101/gr.114611.110

Orr-Weaver, T.L., 2015. When Bigger Is Better: The Role of Polyploidy in Organogenesis. Trends Genet. TIG 31, 307–315. https://doi.org/10.1016/j.tig.2015.03.011

Paradis, E., Schliep, K., 2019. ape 5.0: an environment for modern phylogenetics and evolutionary analyses in R. Bioinformatics 35, 526–528. https://doi.org/10.1093/bioinformatics/bty633

Pastor-Pareja, J.C., Wu, M., Xu, T., 2008. An innate immune response of blood cells to tumors and tissue damage in Drosophila. Dis. Model. Mech. 1, 144–154. https://doi.org/10.1242/dmm.000950

Patel, S.R., Hartwig, J.H., Italiano, J.E., 2005. The biogenesis of platelets from megakaryocyte proplatelets. J. Clin. Invest. 115, 3348–3354. https://doi.org/10.1172/JCI26891

Pearson, A.M., Baksa, K., Rämet, M., Protas, M., McKee, M., Brown, D., Ezekowitz, R.A.B., 2003. Identification of cytoskeletal regulatory proteins required for efficient phagocytosis in Drosophila. Microbes Infect. 5, 815–824. https://doi.org/10.1016/S1286-4579(03)00157-6

Peterson, N.G., Fox, D.T., 2021. Communal living: the role of polyploidy and syncytia in tissue biology. Chromosome Res. 29, 245. https://doi.org/10.1007/s10577-021-09664-3

Poteryaev, D., Datta, S., Ackema, K., Zerial, M., Spang, A., 2010. Identification of the Switch in Early-to-Late Endosome Transition. Cell 141, 497–508. https://doi.org/10.1016/j.cell.2010.03.011

Qi, X., Sun, Y., Xiong, S., 2015. A single freeze-thawing cycle for highly efficient solubilization of inclusion body proteins and its refolding into bioactive form. Microb. Cell Factories 14, 24. https://doi.org/10.1186/s12934-015-0208-6

Quinn, M.T., Schepetkin, I.A., 2009. Role of NADPH Oxidase in Formation and Function of Multinucleated Giant Cells. J. Innate Immun. 1, 509–526. https://doi.org/10.1159/000228158

Ramond, E., Petrignani, B., Dudzic, J.P., Boquete, J.-P., Poidevin, M., Kondo, S., Lemaitre, B., 2020. The adipokine NimrodB5 regulates peripheral hematopoiesis in Drosophila. FEBS J. 287, 3399–3426. https://doi.org/10.1111/febs.15237

Rastogi, V., Sharma, R., Misra, S.R., Yadav, L., Sharma, V., 2014. Emperipolesis – A Review. J. Clin. Diagn. Res. JCDR 8, ZM01–ZM02. https://doi.org/10.7860/JCDR/2014/10361.5299

Ratajczak, M.Z., Ratajczak, J., 2021. Innate Immunity Communicates Using the Language of Extracellular Microvesicles. Stem Cell Rev. Rep. 17, 502–510. https://doi.org/10.1007/s12015-021-10138-6

Ribeiro, C., Brehélin, M., 2006. Insect haemocytes: What type of cell is that? J. Insect Physiol. 52, 417–429. https://doi.org/10.1016/j.jinsphys.2006.01.005

Rizki, M.T.M., 1957. Alterations in the haemocyte population of Drosophila melanogaster. J. Morphol. 100, 437–458. https://doi.org/10.1002/jmor.1051000303

Rizki, M.T.M., 1953. The larval blood cells of Drosophila willistoni. J. Exp. Zool. 123, 397–411. https://doi.org/10.1002/jez.1401230302

Rizki, R.M., Rizki, T.M., 1990. Parasitoid virus-like particles destroy Drosophila cellular immunity. Proc. Natl. Acad. Sci. U. S. A. 87, 8388–8392.

Rizki, T.M., Rizki, R.M., Grell, E.H., 1980. A mutant affecting the crystal cells inDrosophila melanogaster. Wilhelm Rouxs Arch. Dev. Biol. 188, 91–99. https://doi.org/10.1007/BF00848799

Robertson, C.W., 1936. The metamorphosis of Drosophila melanogaster, including an accurately timed account of the principal morphological changes. J. Morphol. 59, 351–399. https://doi.org/10.1002/jmor.1050590207

Roth, S.W., Bitterman, M.D., Birnbaum, M.J., Bland, M.L., 2018. Innate Immune Signaling in Drosophila Blocks Insulin Signaling by Uncoupling PI(3,4,5)P3 Production and Akt Activation. Cell Rep. 22, 2550–2556. https://doi.org/10.1016/j.celrep.2018.02.033

Royet, J., Reichhart, J.-M., Hoffmann, J.A., 2005. Sensing and signaling during infection in Drosophila. Curr. Opin. Immunol. 17, 11–17. https://doi.org/10.1016/j.coi.2004.12.002

Russo, J., Dupas, S., Frey, F., Carton, Y., Brehelin, M., 1996. Insect immunity: early events in the encapsulation process of parasitoid (Leptopilina boulardi) eggs in resistant and susceptible strains of Drosophila. Parasitology 112, 135–142. https://doi.org/10.1017/S0031182000065173

Sampson, C.J., Williams, M.J., 2012. Real-Time Analysis of Drosophila Post-Embryonic Haemocyte Behaviour. PLOS ONE 7, e28783. https://doi.org/10.1371/journal.pone.0028783

Schmucker, D., Clemens, J.C., Shu, H., Worby, C.A., Xiao, J., Muda, M., Dixon, J.E., Zipursky, S.L., 2000. Drosophila Dscam is an axon guidance receptor exhibiting extraordinary molecular diversity. Cell 101, 671–684. https://doi.org/10.1016/s0092-8674(00)80878-8

Schoenfelder, K.P., Fox, D.T., 2015. The expanding implications of polyploidy. J. Cell Biol. 209, 485. https://doi.org/10.1083/jcb.201502016

Shannon, P., Markiel, A., Ozier, O., Baliga, N.S., Wang, J.T., Ramage, D., Amin, N., Schwikowski, B., Ideker, T., 2003. Cytoscape: A Software Environment for Integrated Models of Biomolecular Interaction Networks. Genome Res. 13, 2498–2504. https://doi.org/10.1101/gr.1239303

Sheikh, Z., Brooks, P.J., Barzilay, O., Fine, N., Glogauer, M., 2015. Macrophages, Foreign Body Giant Cells and Their Response to Implantable Biomaterials. Materials 8, 5671–5701. https://doi.org/10.3390/ma8095269

Shin, M., Cha, N., Koranteng, F., Cho, B., Shim, J., 2020. Subpopulation of Macrophage-Like Plasmatocytes Attenuates Systemic Growth via JAK/STAT in the Drosophila Fat Body. Front. Immunol. 11, 63. https://doi.org/10.3389/fimmu.2020.00063

Shrestha, R., Gateff, E., 1982. Ultrastructure and Cytochemistry of the Cell Types in the Larval Hematopoietic Organs and Hemolymph of Drosophila Melanogaster. (drosophila/hematopoiesis/blool cells/ultrastructure/cytochemistry). Dev. Growth Differ. 24, 65–82. https://doi.org/10.1111/j.1440-169X.1982.00065.x

Singh, B.N., 2020. Drosophila ananassae: a species characterized by spontaneous male recombination in appreciable frequency. J. Genet. 99, 12. https://doi.org/10.1007/s12041-019-1169-z

Singh, B.N., 2000. Drosophila ananassae: A species characterized by several unusual

genetic features. Curr. Sci. 78, 391–398.
Singh, P., Singh, B.N., 2008. Population genetics of Drosophila ananassae. Genet. Res. 90, 409–419. https://doi.org/10.1017/S0016672308009737
Stamatakis, A., 2014. RAxML version 8: a tool for phylogenetic analysis and post-analysis of large phylogenies. Bioinformatics 30, 1312–1313. https://doi.org/10.1093/bioinformatics/btu033
Stanley, D., Haas, E., Kim, Y., 2023. Beyond Cellular Immunity: On the Biological Significance of Insect Hemocytes. Cells 12, 599. https://doi.org/10.3390/cells12040599
Steenwyk, J.L., Iii, T.J.B., Li, Y., Shen, X.-X., Rokas, A., 2020. ClipKIT: A multiple sequence alignment trimming software for accurate phylogenomic inference. PLOS Biol. 18, e3001007. https://doi.org/10.1371/journal.pbio.3001007
Stothard, P., 2000. The sequence manipulation suite: JavaScript programs for analyzing and formatting protein and DNA sequences. BioTechniques 28, 1102, 1104. https://doi.org/10.2144/00286ir01
Stöven, S., Silverman, N., Junell, A., Hedengren-Olcott, M., Erturk, D., Engström, Y., Maniatis, T., Hultmark, D., 2003. Caspase-mediated processing of the Drosophila NF-κB factor Relish. Proc. Natl. Acad. Sci. U. S. A. 100, 5991–5996. https://doi.org/10.1073/pnas.1035902100
Stroschein-Stevenson, S.L., Foley, E., O'Farrell, P.H., Johnson, A.D., 2005. Identification of Drosophila Gene Products Required for Phagocytosis of Candida albicans. PLOS Biol. 4, e4. https://doi.org/10.1371/journal.pbio.0040004
Supek, F., Bošnjak, M., Škunca, N., Šmuc, T., 2011. REVIGO Summarizes and Visualizes Long Lists of Gene Ontology Terms. PLoS ONE 6, e21800. https://doi.org/10.1371/journal.pone.0021800
Suzuki, A., Shin, J.-W., Wang, Yuhuan, Min, S.H., Poncz, M., Choi, J.K., Discher, D.E., Carpenter, C.L., Lian, L., Zhao, L., Wang, Yangfeng, Abrams, C.S., 2013. RhoA Is Essential for Maintaining Normal Megakaryocyte Ploidy and Platelet Generation. PLOS ONE 8, e69315. https://doi.org/10.1371/journal.pone.0069315
Szkalisity, A., Piccinini, F., Beleon, A., Balassa, T., Varga, I.G., Migh, E., Molnar, C., Paavolainen, L., Timonen, S., Banerjee, I., Ikonen, E., Yamauchi, Y., Ando, I., Peltonen, J., Pietiäinen, V., Honti, V., Horvath, P., 2021. Regression plane concept for analysing continuous cellular processes with machine learning. Nat. Commun. 12, 2532. https://doi.org/10.1038/s41467-021-22866-x
Tang, H., 2009. Regulation and function of the melanization reaction in Drosophila. Fly (Austin) 3, 105–111. https://doi.org/10.4161/fly.3.1.7747
Tang, H., Kambris, Z., Lemaitre, B., Hashimoto, C., 2006. Two proteases defining a melanization cascade in the immune system of Drosophila. J. Biol. Chem. 281, 28097–28104. https://doi.org/10.1074/jbc.M601642200
Tanji, T., Ohashi-Kobayashi, A., Natori, S., 2006. Participation of a galactose-specific C-type lectin in Drosophila immunity. Biochem. J. 396, 127–138. https://doi.org/10.1042/BJ20051921
Tattikota, S.G., Cho, B., Liu, Y., Hu, Y., Barrera, V., Steinbaugh, M.J., Yoon, S.-H., Comjean, A., Li, F., Dervis, F., Hung, R.-J., Nam, J.-W., Ho Sui, S., Shim, J.,

Perrimon, N., 2020. A single-cell survey of Drosophila blood. eLife 9, e54818. https://doi.org/10.7554/eLife.54818

Tetreau, G., Dhinaut, J., Gourbal, B., Moret, Y., 2019. Trans-generational Immune Priming in Invertebrates: Current Knowledge and Future Prospects. Front. Immunol. 10, 1938. https://doi.org/10.3389/fimmu.2019.01938

Teufel, F., Almagro Armenteros, J.J., Johansen, A.R., Gíslason, M.H., Pihl, S.I., Tsirigos, K.D., Winther, O., Brunak, S., von Heijne, G., Nielsen, H., 2022. SignalP 6.0 predicts all five types of signal peptides using protein language models. Nat. Biotechnol. 40, 1023–1025. https://doi.org/10.1038/s41587-021-01156-3

Theopold, U., Krautz, R., Dushay, M.S., 2014. The Drosophila clotting system and its messages for mammals. Dev. Comp. Immunol., Drosophila Immunity 42, 42–46. https://doi.org/10.1016/j.dci.2013.03.014

Trakala, M., Partida, D., Salazar-Roa, M., Maroto, M., Wachowicz, P., de Cárcer, G., Malumbres, M., 2015. Activation of the endomitotic spindle assembly checkpoint and thrombocytopenia in Plk1-deficient mice. Blood 126, 1707–1714. https://doi.org/10.1182/blood-2015-03-634402

Tsuda, M., Seong, K.-H., Aigaki, T., 2006. POSH, a scaffold protein for JNK signaling, binds to ALG-2 and ALIX in Drosophila. FEBS Lett. 580, 3296–3300. https://doi.org/10.1016/j.febslet.2006.05.005

Ulvila, J., Vanha-Aho, L.-M., Rämet, M., 2011. Drosophila phagocytosis - still many unknowns under the surface. APMIS Acta Pathol. Microbiol. Immunol. Scand. 119, 651–662. https://doi.org/10.1111/j.1600-0463.2011.02792.x

Valanne, S., Vesala, L., Maasdorp, M.K., Salminen, T.S., Rämet, M., 2022. The Drosophila Toll Pathway in Innate Immunity: from the Core Pathway toward Effector Functions. J. Immunol. Baltim. Md 1950 209, 1817–1825. https://doi.org/10.4049/jimmunol.2200476

Valanne, S., Wang, J.-H., Rämet, M., 2011. The Drosophila Toll signaling pathway. J. Immunol. Baltim. Md 1950 186, 649–656. https://doi.org/10.4049/jimmunol.1002302

Vanha-aho, L.-M., Anderl, I., Vesala, L., Hultmark, D., Valanne, S., Rämet, M., 2015. Edin Expression in the Fat Body Is Required in the Defense Against Parasitic Wasps in Drosophila melanogaster. PLOS Pathog. 11, e1004895. https://doi.org/10.1371/journal.ppat.1004895

Verster, K.I., Cinege, G., Lipinszki, Z., Magyar, L.B., Kurucz, É., Tarnopol, R.L., Ábrahám, E., Darula, Z., Karageorgi, M., Tamsil, J.A., Akalu, S.M., Andó, I., Whiteman, N.K., 2023. Evolution of insect innate immunity through domestication of bacterial toxins. Proc. Natl. Acad. Sci. U. S. A. 120, e2218334120. https://doi.org/10.1073/pnas.2218334120

Verster, K.I., Wisecaver, J.H., Karageorgi, M., Duncan, R.P., Gloss, A.D., Armstrong, E.E., Price, D.K., Menon, A.R., Ali, Z.M., Whiteman, N.K., 2019. Horizontal Transfer of Bacterial Cytolethal Distending Toxin B Genes to Insects. Mol. Biol. Evol. 36, 2105–2110. https://doi.org/10.1093/molbev/msz146

Wan, B., Belghazi, M., Lemauf, S., Poirié, M., Gatti, J.-L., 2021. Proteomics of purified lamellocytes from Drosophila melanogaster HopTum-l identifies new membrane

proteins and networks involved in their functions. Insect Biochem. Mol. Biol. 134, 103584. https://doi.org/10.1016/j.ibmb.2021.103584

Wang, H., Zhou, J., Li, J., Geng, Y., Meng, P., Ma, C., Zhu, Z., Zhang, W., Hong, L., Quan, Y., Wei, J., Huang, Q., Zhou, Y., Su, Z., Zhu, X., Chen, C., Chen, S., Gu, J., 2021. A study of multinucleated giant cells in esophageal cancer. Clin. Immunol. 222, 108600. https://doi.org/10.1016/j.clim.2020.108600

Wang, J., Zhang, Y., Cao, J., Wang, Y., Anwar, N., Zhang, Z., Zhang, D., Ma, Y., Xiao, Y., Xiao, L., Wang, X., 2023. The role of autophagy in bone metabolism and clinical significance. Autophagy 19, 2409–2427. https://doi.org/10.1080/15548627.2023.2186112

Watson, F.L., Püttmann-Holgado, R., Thomas, F., Lamar, D.L., Hughes, M., Kondo, M., Rebel, V.I., Schmucker, D., 2005. Extensive diversity of Ig-superfamily proteins in the immune system of insects. Science 309, 1874–1878. https://doi.org/10.1126/science.1116887

Whitten, J.M., 1964. Haemocytes and the metamorphosing tissues in Sarcophaga bullata, Drosophila melanogaster, and other cyclorrhaphous Diptera. J. Insect Physiol. 10, 447–469. https://doi.org/10.1016/0022-1910(64)90070-8

Wood, W., Martin, P., 2017. Macrophage Functions in Tissue Patterning and Disease: New Insights from the Fly. Dev. Cell 40, 221–233. https://doi.org/10.1016/j.devcel.2017.01.001

Wright, A.E., Douglas, S.R., 1903. An experimental investigation of the rôle of the blood fluids in connection with phagocytosis. 1903. Rev. Infect. Dis. 11, 827–834. https://doi.org/10.1093/clinids/11.5.827

Xavier, M.J., Williams, M.J., 2011. The Rho-Family GTPase Rac1 Regulates Integrin Localization in Drosophila Immunosurveillance Cells. PLoS ONE 6, e19504. https://doi.org/10.1371/journal.pone.0019504

Xia, X., You, M., Rao, X.-J., Yu, X.-Q., 2018. Insect C-type lectins in innate immunity. Dev. Comp. Immunol. 83, 70–79. https://doi.org/10.1016/j.dci.2017.11.020

Xue, L., Igaki, T., Kuranaga, E., Kanda, H., Miura, M., Xu, T., 2007. Tumor suppressor CYLD regulates JNK-induced cell death in Drosophila. Dev. Cell 13, 446–454. https://doi.org/10.1016/j.devcel.2007.07.012

Yang, H., Hultmark, D., 2016. Tissue communication in a systemic immune response of Drosophila. Fly (Austin) 10, 115–122. https://doi.org/10.1080/19336934.2016.1182269

Yang, L., Qiu, L.-M., Fang, Q., Stanley, D.W., Ye, G.-Y., 2021. Cellular and humoral immune interactions between Drosophila and its parasitoids. Insect Sci. 28, 1208–1227. https://doi.org/10.1111/1744-7917.12863

You, T., Wang, Q., Zhu, L., 2016. Role of autophagy in megakaryocyte differentiation and platelet formation. Int. J. Physiol. Pathophysiol. Pharmacol. 8, 28–34.

Younes, S., Al-Sulaiti, A., Nasser, E.A.A., Najjar, H., Kamareddine, L., 2020. Drosophila as a Model Organism in Host–Pathogen Interaction Studies. Front. Cell. Infect. Microbiol. 10, 214. https://doi.org/10.3389/fcimb.2020.00214

Yu, G., Smith, D.K., Zhu, H., Guan, Y., Lam, T.T.-Y., 2017. ggtree: an r package for visualization and annotation of phylogenetic trees with their covariates and other

associated data. Methods Ecol. Evol. 8, 28–36. https://doi.org/10.1111/2041-210X.12628

Yu, S., Luo, F., Xu, Y., Zhang, Y., Jin, L.H., 2022. Drosophila Innate Immunity Involves Multiple Signaling Pathways and Coordinated Communication Between Different Tissues. Front. Immunol. 13, 905370. https://doi.org/10.3389/fimmu.2022.905370

Zettervall, C.-J., Anderl, I., Williams, M.J., Palmer, R., Kurucz, E., Ando, I., Hultmark, D., 2004. A directed screen for genes involved in Drosophila blood cell activation. Proc. Natl. Acad. Sci. U. S. A. 101, 14192–14197. https://doi.org/10.1073/pnas.0403789101

Zhang, S.-M., Adema, C.M., Kepler, T.B., Loker, E.S., 2004. Diversification of Ig Superfamily Genes in an Invertebrate. Science 305, 251–254. https://doi.org/10.1126/science.1088069

Zheng, H., Yang, X., Xi, Y., 2016. Fat body remodeling and homeostasis control in Drosophila. Life Sci. 167, 22–31. https://doi.org/10.1016/j.lfs.2016.10.019

Zhitomirsky, B., Farber, H., Assaraf, Y.G., 2018. LysoTracker and MitoTracker Red are transport substrates of P-glycoprotein: implications for anticancer drug design evading multidrug resistance. J. Cell. Mol. Med. 22, 2131–2141. https://doi.org/10.1111/jcmm.13485

Zhong, W., McClure, C.D., Evans, C.R., Mlynski, D.T., Immonen, E., Ritchie, M.G., Priest, N.K., 2013. Immune anticipation of mating in Drosophila: Turandot M promotes immunity against sexually transmitted fungal infections. Proc. R. Soc. B Biol. Sci. 280, 20132018. https://doi.org/10.1098/rspb.2013.2018

List of Publications

MTMT ID: 10069445

Peer-reviewed international publications required for the fulfilment of the doctoral process

Cinege, G.*, **Magyar, L.B.***, Kovács, A.L., Lerner, Z., Juhász, G., Lukacsovich, D., Winterer, J., Lukacsovich, T., Hegedűs, Z., Kurucz, É., Hultmark, D., Földy, C., Andó, I., 2021. Broad Ultrastructural and Transcriptomic Changes Underlie the Multinucleated Giant Hemocyte Mediated Innate Immune Response against Parasitoids. Journal of Innate Immunity 14, 335–354. **IF 7.111** https://doi.org/10.1159/000520110

* - authors contributed equally to this work

Verster, K.I., Cinege, G., Lipinszki, Z., **Magyar, L.B.**, Kurucz, É., Tarnopol, R.L., Ábrahám, E., Darula, Z., Karageorgi, M., Tamsil, J.A., Akalu, S.M., Andó, I., Whiteman, N.K., 2023. Evolution of insect innate immunity through domestication of bacterial toxins. Proceedings of the National Academy of Sciences 120, e2218334120. **IF 11.1** https://doi.org/10.1073/pnas.2218334120

Other peer-reviewed international publications

Cinege, G., Lerner, Z., **Magyar, L.B.**, Soós, B., Tóth, R., Kristó, I., Vilmos, P., Juhász, G., Kovács, A.L., Hegedűs, Z., Sensen, C.W., Kurucz, É., Andó, I., 2019. Cellular Immune Response Involving Multinucleated Giant Hemocytes with Two-Step Genome Amplification in the *Drosophilid Zaprionus indianus*. Journal of Innate Immunity 12, 257–272. **IF 4.932** https://doi.org/10.1159/000502646

Cinege, G., **Magyar, L.B.**, Kovács, H., Varga, V., Bodai, L., Zsindely, N., Nagy, G., Hegedűs, Z., Hultmark, D., Andó, I., 2023. Distinctive features of *Zaprionus indianus* hemocyte differentiation and function revealed by transcriptomic analysis. Front Immunol 14, 1322381. **IF 7.3** https://doi.org/10.3389/fimmu.2023.1322381

Cinege, G., Fodor, K., **Magyar, L.B.**, Lipinszki, Z., Hultmark, D., Andó, I. Cellular immunity of *Drosophila willistoni* reveals novel complexity of the insect anti parasitoid defense. In press, Cells.

Tarnopol, R,, Tamsil, J., Cinege, G., Ha, J., Verster, K.I., Ábrahám, E., **Magyar, L.B**, Kim, B.Y., Bernstein, S.L., Lipinszki, Z., Andó, I., Whiteman, N.K. Retracing the horizontal transfer of a novel innate immune factor in *Drosophila*. Manuscript submitted, Nature.

Magyar, L.B., Ábrahám, E., Lipinszki, Z., Tarnopol, L.R. Whiteman, N.K., Varga, V., Hultmark, D., Andó, I., Cinege, G., Pore forming prokaryotic toxin-like proteins in the anti-parasitoid immune response in *Drosophila*. Manuscript in preparation

Conference contributions

European Phagocyte Workshop, March 29-April 1, 2023, Budapest, presentation

51st Conference of the Hungarian Society for Immunology, 19-21 October 2022, Kecskemét, poster

XXI. Genetikai Műhelyek Magyarországon Minikonferencia, 9th September 2022, BRC, Szeged, poster

50th Conference of the Hungarian Society for Immunology, 20-22 October 2021, Kecskemét, presentation

A Magyar Tudomány Ünnepe, 19th November 2020, Online, presentation

49th Conference of the Hungarian Society for Immunology, 7-8 October 2020, Online, poster

Straub Days Conference, 30-31 May 2019, BRC, Szeged, poster

48th Conference of the Hungarian Society for Immunology, 16-18 October 2019, Bükfürdő, poster

Supplementary Materials

Suppl. Movie 1. Projection formation of a Z. indianus MGH 72h after *L. victoriae* parasitoid infection. Shooting duration 2h.

Suppl. Figure S1. Map and sequence of the pMT-CoHygro-DEST-3×Flag Gateway destination expression plasmid. pMT: copper-inducible metallothionein promoter (REF: https://www.ncbi.nlm.nih.gov/pmc/articles/PMC334736/), CoHygro: Hygromycin B phosphotransferase selection marker, DEST: destination Gatewy cassette, 3×Flag: immunoaffinity tag.

Suppl. Figure S2. Gene Ontology (GO) enrichment analysis in the "cellular component" category for genes that were significantly (p<0.05) upregulated (red) or downregulated (green) in MGHs compared to activated plasmatocytes. GO terms are plotted according to the significance of their enrichment ($-\log_{10}$ p-value).

Suppl. Figure S3. Gene Ontology (GO) enrichment analysis in "biological process" category for genes that were significantly (p<0.05) upregulated (red) or downregulated (green) in MGHs compared to activated plasmatocytes. GO terms are plotted according to the significance of their enrichment ($-\log_{10}$ p-value).

Suppl. Figure S4. Gene Ontology (GO) enrichment analysis in the "cellular component" category for genes that were significantly (p<0.05) upregulated (red) or downregulated (blue) in MGHs compared to uninduced blood cells. GO terms are plotted according to the significance of their enrichment ($-\log_{10}$ p-value).

Suppl. Figure S5. Gene Ontology (GO) enrichment analysis in "biological process" categoryfor genes that were significantly (p<0.05) upregulated (red) or downregulated (blue) in MGHs compared to uninduced blood cells. GO terms are plotted according to the significance of their enrichment ($-\log_{10}$ p-value).

Suppl. Figure S6. Multiple alignment of *D. ananassae*-encoded Hemolysin E-like proteins

Suppl. Figure S7. HemolysinE gene tree. The maximum likelihood tree (log likelihood -32790.294571) computed with RAxML using the JTT+gamma. A Hemolysin E homolog from *E. coli* (WP_248417656.1) was selected as the root. Nodes with <50% bootstrap

support are collapsed. The insect clade of Hemolysin E homologs is poorly resolved, likely due to several lineage-specific duplication events. Taxonomy of each accession is indicated with the heatmap. Scale bar = substitutions per site.

Suppl. Fig. S8. Gene Ontology (GO) enrichment analysis in the "cellular component" category for the DEGs between the infected and naive samples. Genes that were significantly upregulated in the infected samples are labeled in green and those that were significantly downregulated are labeled in red. GO terms are plotted according to the significance of their enrichment ($-\log_{10}$ p-value).

Suppl. Fig. S9. Gene Ontology (GO) enrichment analysis in the "biological process" category for the DEGs between the infected and naive samples. Genes that were significantly upregulated in the infected samples are labeled in green and those that were significantly downregulated are labeled in red. GO terms are plotted according to the significance of their enrichment ($-\log_{10}$ p-value).

Suppl. Table S1. Oligonucleotide primers used in the study. Restriction sites on the adapter sequences are marked in bold and underlined.

Suppl. Table S2. The set of genes significantly differentially expressed between MGHs and activated plasmatocytes. Positive and negative fold-change values indicate higher and lower gene expression levels in MGHs compared to plasmatocytes. Genes expressed exclusively in MGHs are indicated with light grey background. Genes expressed exclusively in activated plasmatocytes are indicated with dark grey background.

Suppl. Table S3. The set of genes significantly differentially expressed between MGHs and uninduced blood cell pools. Positive and negative fold-change values indicate higher and lower gene expression levels in MGHs compared to uninduced blood cells. Genes expressed exclusively in MGHs are indicated with light grey background. Genes expressed exclusively in uninduced blood cells are indicated with dark grey background.

Suppl. Table S4. The set of genes significantly differentially expressed between activated plasmatocytes and uninduced blood cell pools. Positive and negative fold-change values indicate higher and lower gene expression levels in activated plasmatocytes compared to uninduced blood cells. Genes expressed exclusively in activated plasmatocytes are indicated with light grey background. Genes expressed exclusively in uninduced blood cells are indicated with dark grey background.

Suppl. Table S5. List of *D. melanogaster* lamellocyte-specific genes, which were also highly expressed in *D. ananassae* MGHs. Genes that were found to be enriched in lamellocytes in at least two of the previous studies were included.

Suppl. Table S6. Set of genes differentially expressed in naive and *L. victoriae* infected *Z. indianus* blood cells. Positive and negative log2FoldChange values indicate higher and lower gene expression levels, respectively, in infected compared to naive samples. Genes expressed exclusively in naive samples are indicated with a light grey background and those expressed exclusively in infected samples are indicated with a dark grey background.

Suppl. Table S7. Set of putative serine protease, FREP, and C-type lectin genes expressed either differentially (grey) or constitutively in *Z. indianus* blood cells.

Suppl. Table S8. List of the mammalian megakaryocyte and platelet associated genes possessing constitutively expressed orthologs in *Z. indianus* blood cells. Genes involved in poliploidysation are indicated with yellow.

Suppl. Table S9. *D. melanogaster* blood cell specific markers expressed differentially in *Z. indianus*. Data originating from single cell RNA sequencing of lamellocytes (LC), crystal cells (CC), and plasmatocytes (PC).